颗粒物质研究
Granular Matter Physics

厚美瑛
mayhou@iphy.ac.cn

提 纲

- 颗粒物质简介与特性
- 颗粒气体
  - 颗粒气体速度分布律研究
  - 颗粒气体团簇

Lecture 1

- 颗粒流体及稀疏-密集流转变
  - 颗粒流的激波波前的密度与温度分布结构
  - 颗粒经典非平衡系统涨落耗散关系
- 颗粒固体
  - 颗粒固体的声波探测

Lecture 2

References

- "生物物理学：能量、信息、生命" by Phillip Nelson (黎明 戴陆如 译)
- "颗粒物质物理与力学" 孙其诚 厚美瑛 金峰等著
- "颗粒物质力学导论" 孙其诚 王光谦 著

颗粒物质

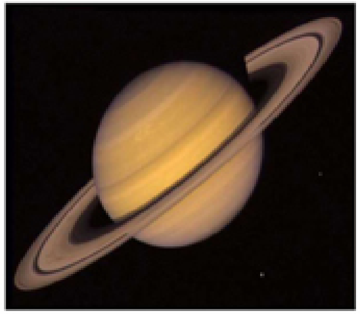

颗粒体系：大量宏观颗粒的集合体（宏观颗粒：大于微米量级）

- 0.001 – 0.1mm　粉末
- 0.1 – 5mm　颗粒
- 5mm以上　块状物

颗粒势能

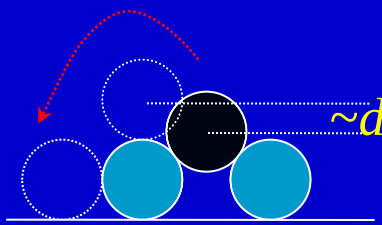

~ mgd with m~ 10^{-3} g, g=10m/s^2, d~1mm

~ 10^{-8} J

热能

~ kT with k=1.38 x 10^{-21} J/K, T~300K

~ 4 x 10^{-21} J

<u>Dynamic Temperature</u> ~ 0 as compared to granular energy

能量耗散体系

外力作用:
振动,
重力,
剪切力
撞击

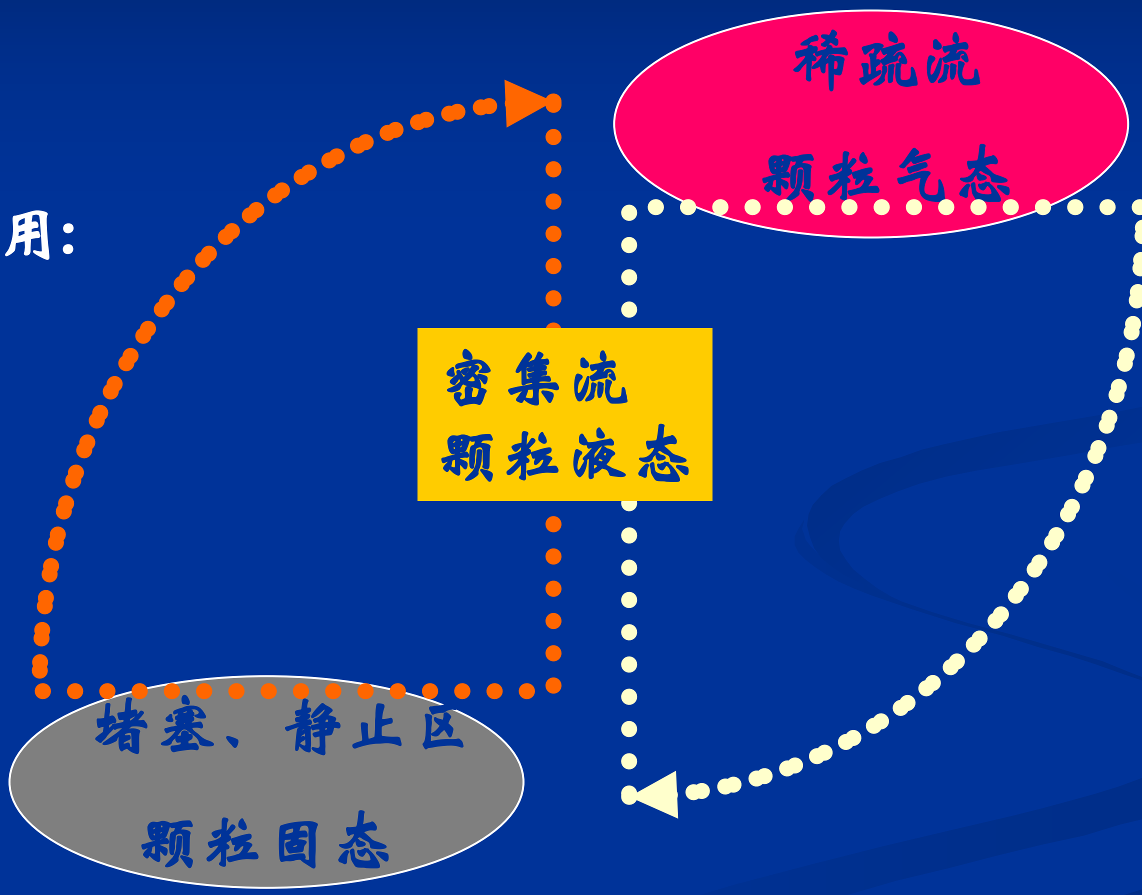

摩擦耗散
非弹性碰撞

颗粒物质

普通物质

固体　　液体　　气体

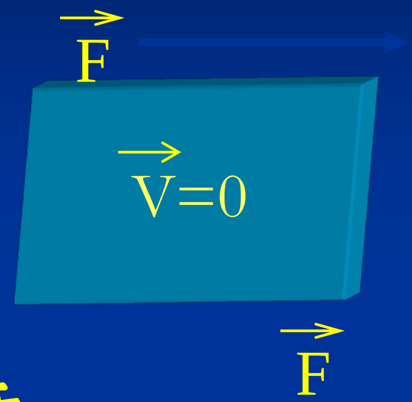

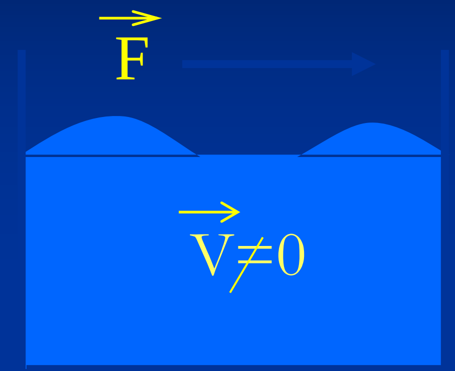

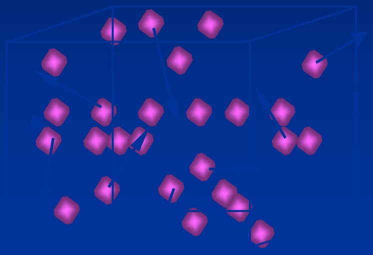

颗粒物质

固-液态

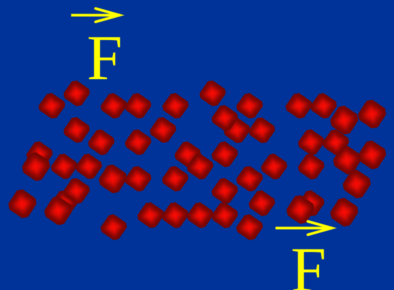

加压膨胀

屈服应力

凝-气态

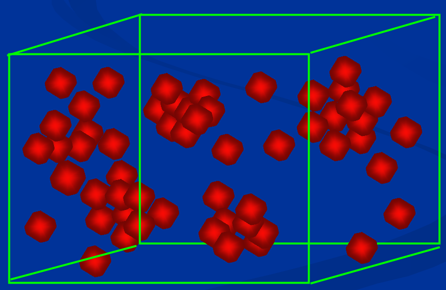

Clustering

Patterns in the sand

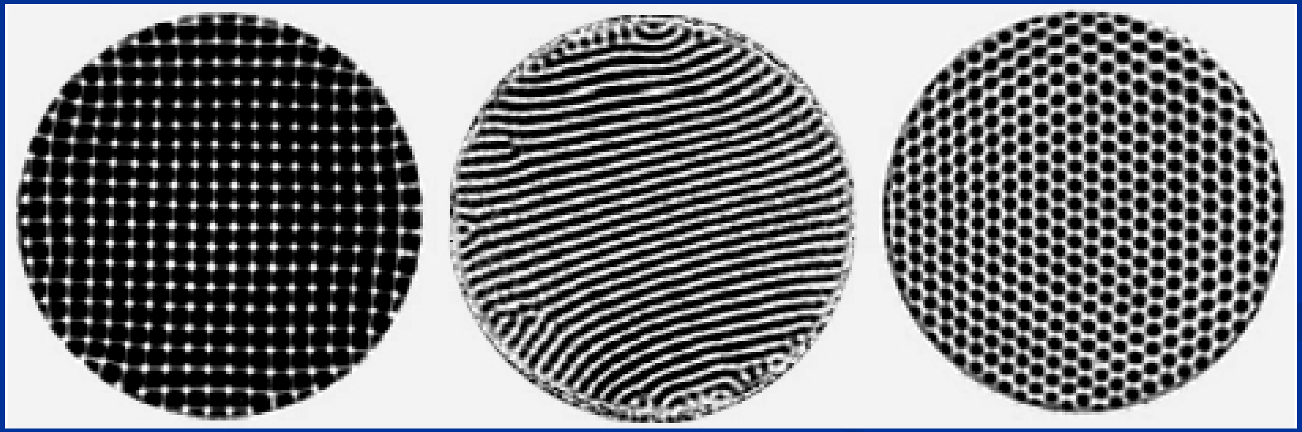

颗粒流体

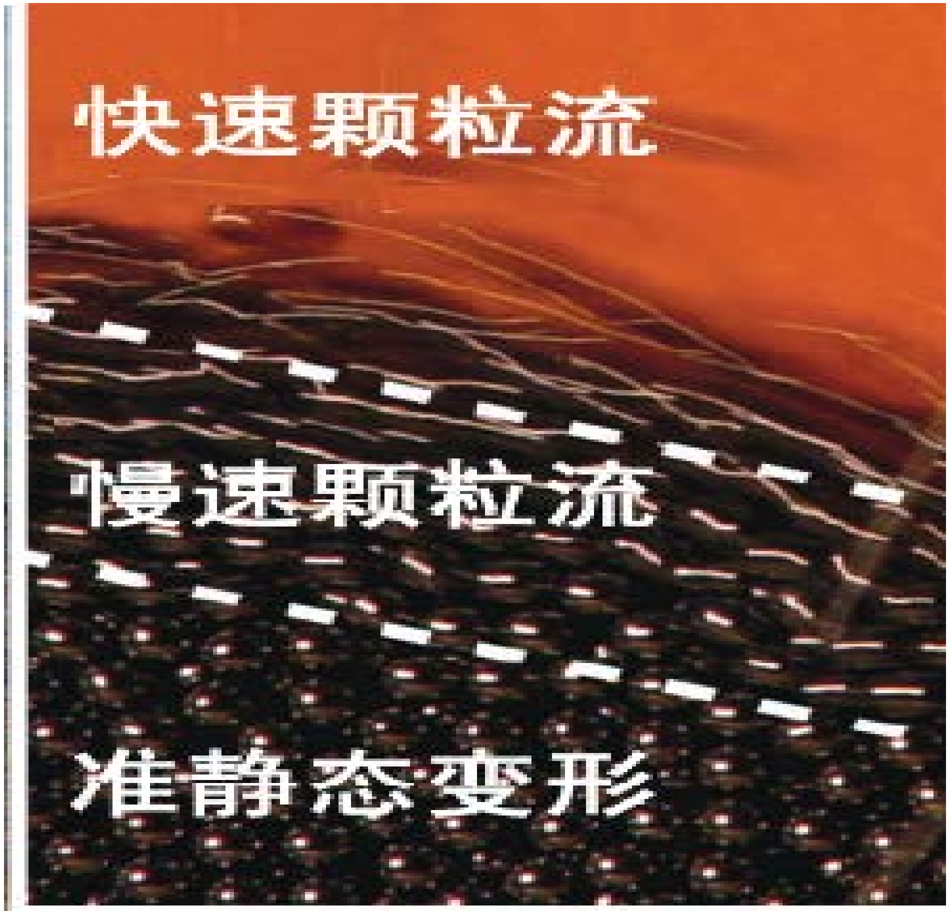

颗粒体系简介与特性

“自推进”颗粒

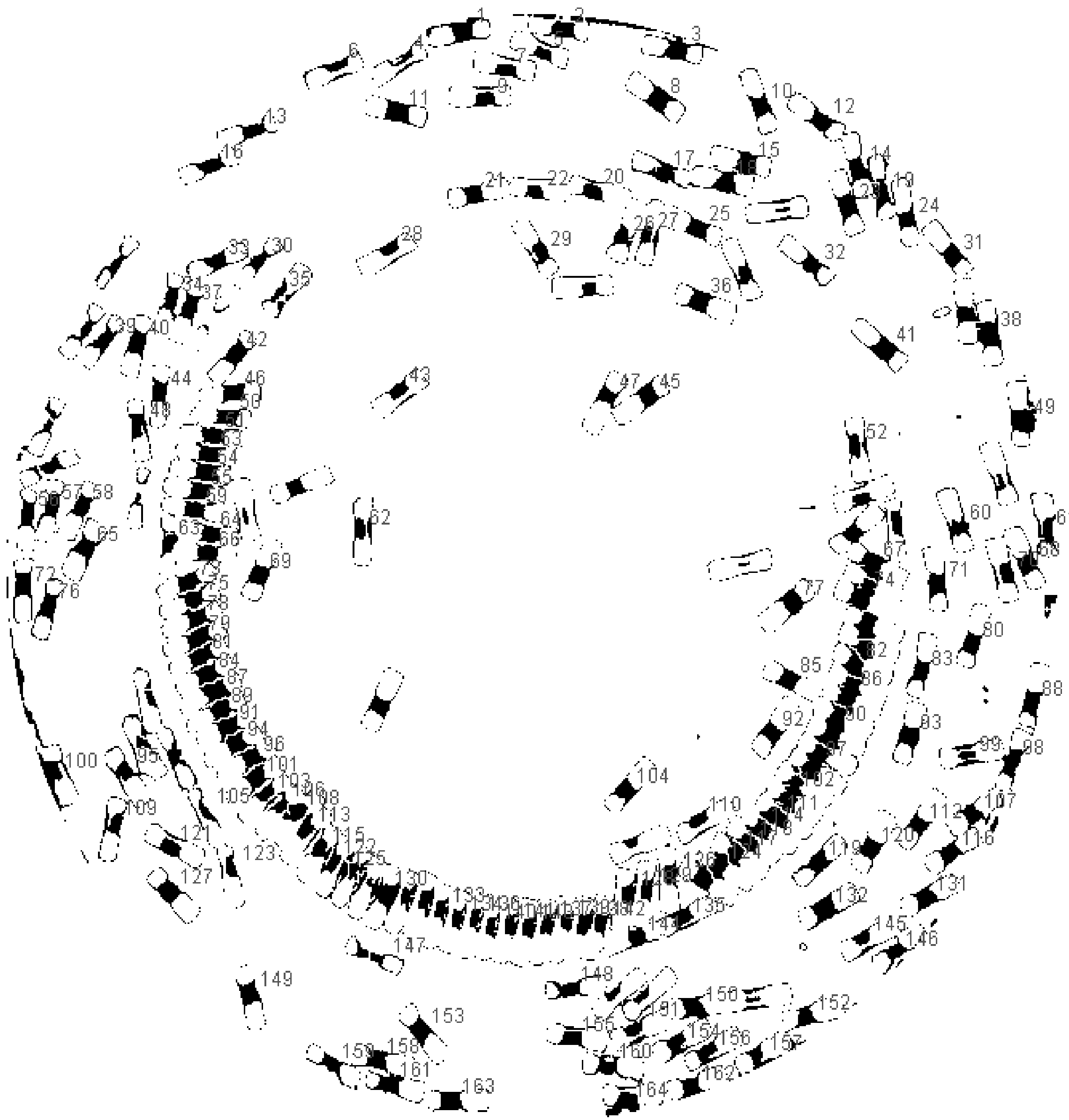

颗粒体系简介与特性

颗粒固体

颗粒流体

颗粒气体

颗 粒 气 体

颗粒气体体系

颗粒气体体系

宏观尺寸，分子尺度热扰动可以忽略 → 远离热力学平衡的非平衡态体系

相互作用简单：非弹性碰撞 → 能量耗散

振动，剪切等能量输入方式处理起来相对简单 → 与外界能量交换

颗粒气体可以作为一个很好的研究非平衡态体系的典型范例

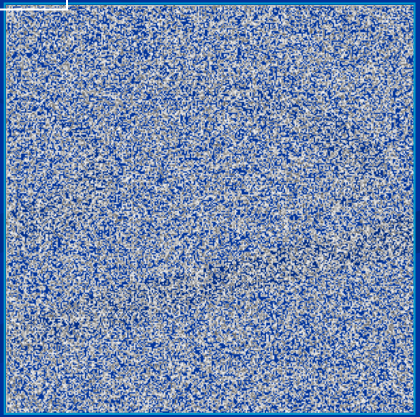

- Velocity distribution
- Energy dissipation along flow direction during condensation
- Clustering in granular gas
- Cluster in compartmentalized granular system

颗粒气体　　团聚现象 (Clustering)

Molecular gas system

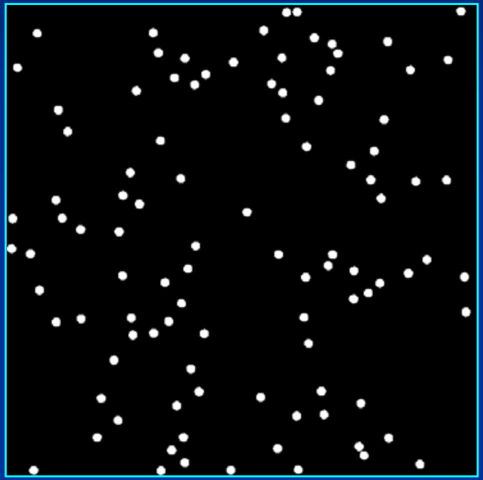

granular gas system

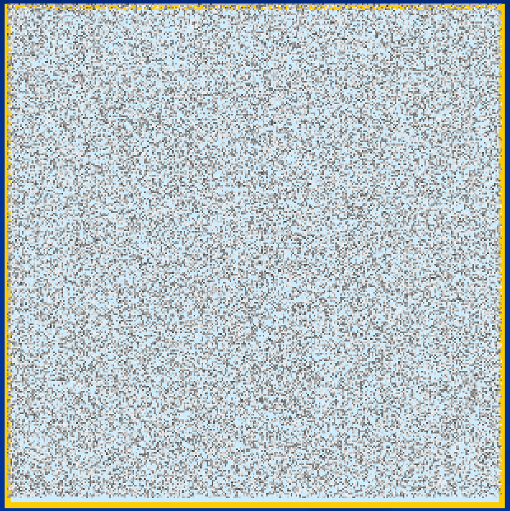

Goldhirsch I and Zanetti G, Phys.Rev.Lett.1993

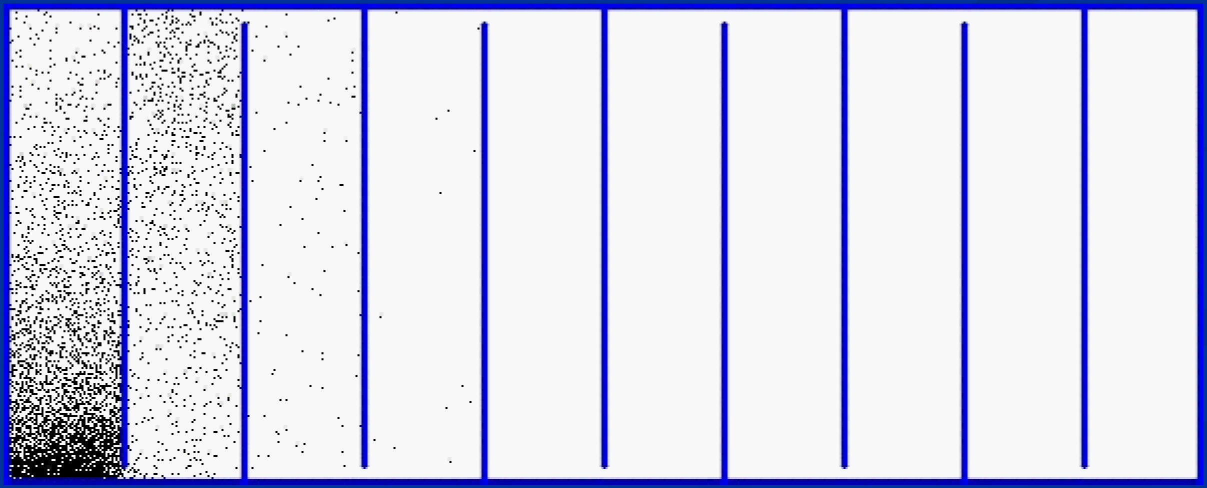

单种颗粒分聚现象：Maxwell's Demon

理想气体

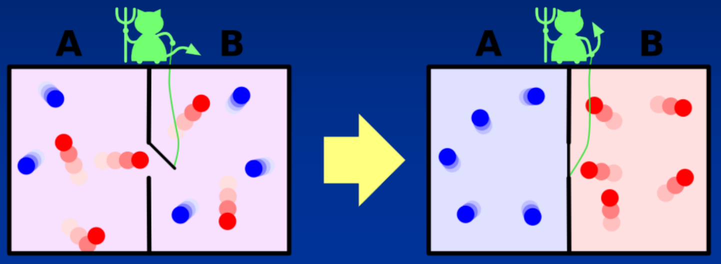

颗粒气体

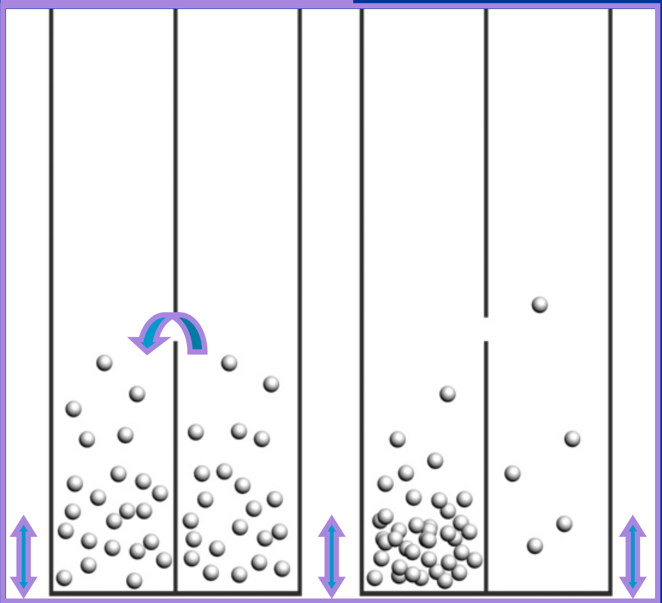

Maxwell妖

仅当运动速度较快的分子靠近开口时，Maxwell妖才允许其通过。从而使得两仓中一边是运动速度较快的分子，一边是较慢的分子。而在颗粒气体中，颗粒本身就扮演着Maxwell妖的角色，颗粒自发地聚集在一个仓中。

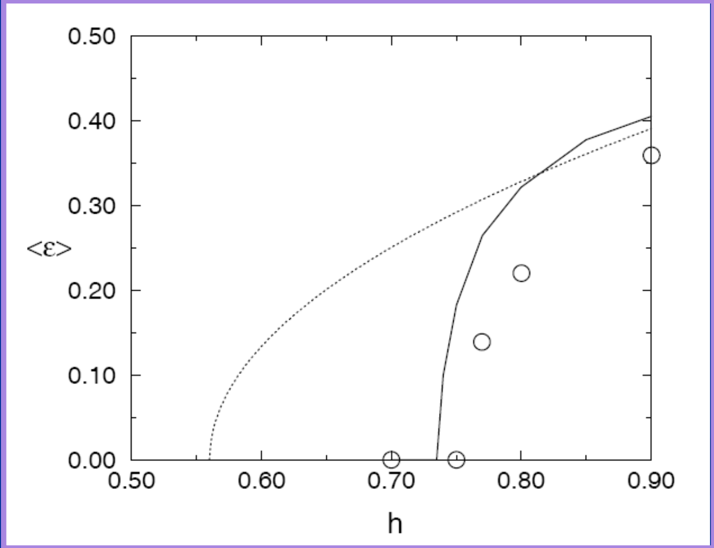

控制参量发生变化时，体系由均匀态变为分聚态，对应于叉形分岔(**pitchfork**)。

J. Eggers Phys. Rev. Lett. **83** (1999) 5322

两种颗粒时空布局振荡现象：颗粒时钟

颗粒时钟

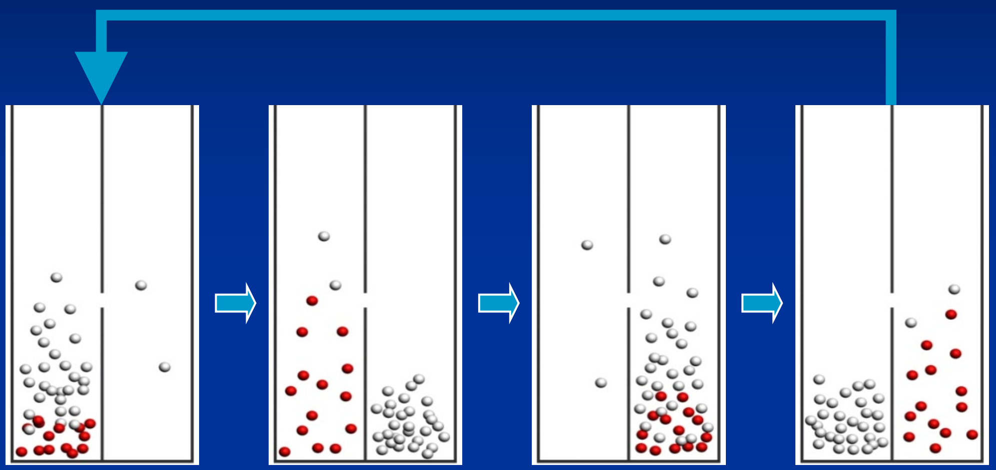

不同的颗粒配比和驱动速度下，体系呈现出不同的布局状态，均匀态，振荡态及分聚态。

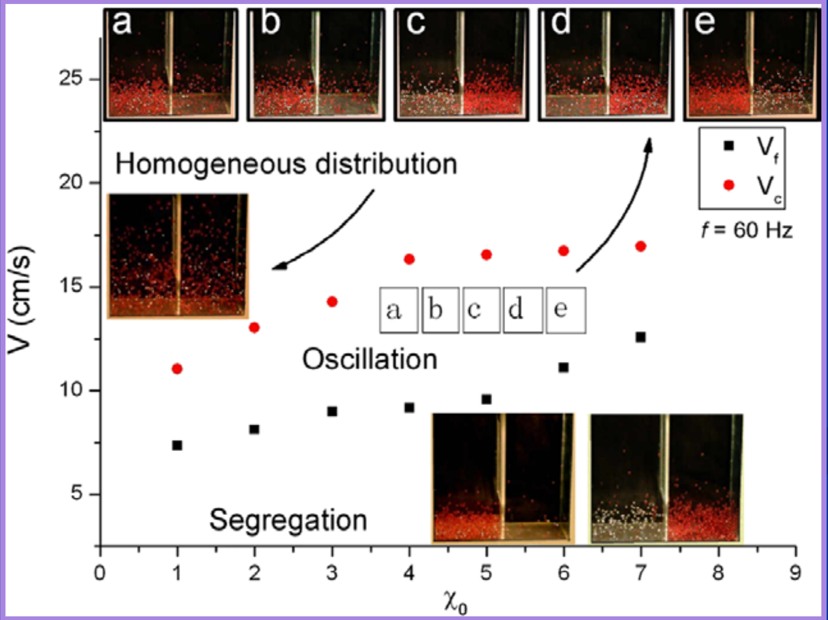

两种相同大小不同质量的颗粒在合适的驱动速度下会在两仓中来回布局振荡，有着较为稳定的振荡周期，称为颗粒时钟。

Hou *et. al* Phys. Rev. Lett. **100** (2008) 068001

颗 粒 流 体

颗粒液体 激波在颗粒流经常可见

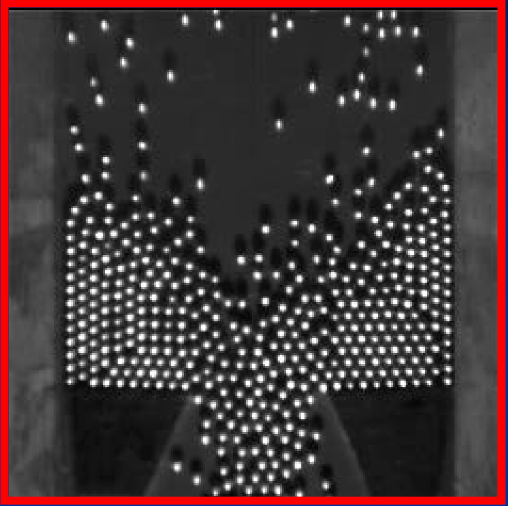

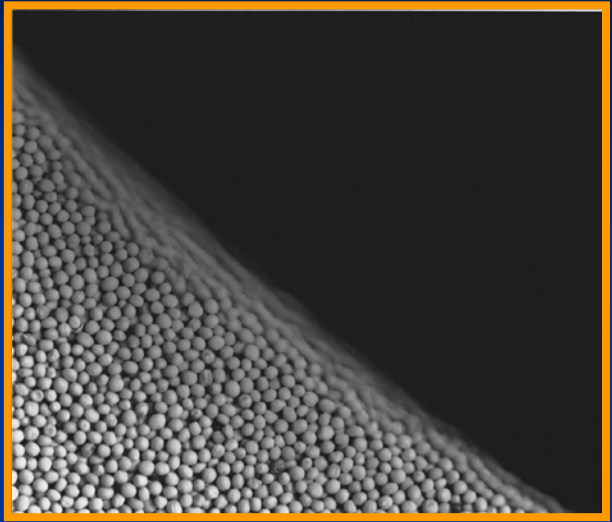

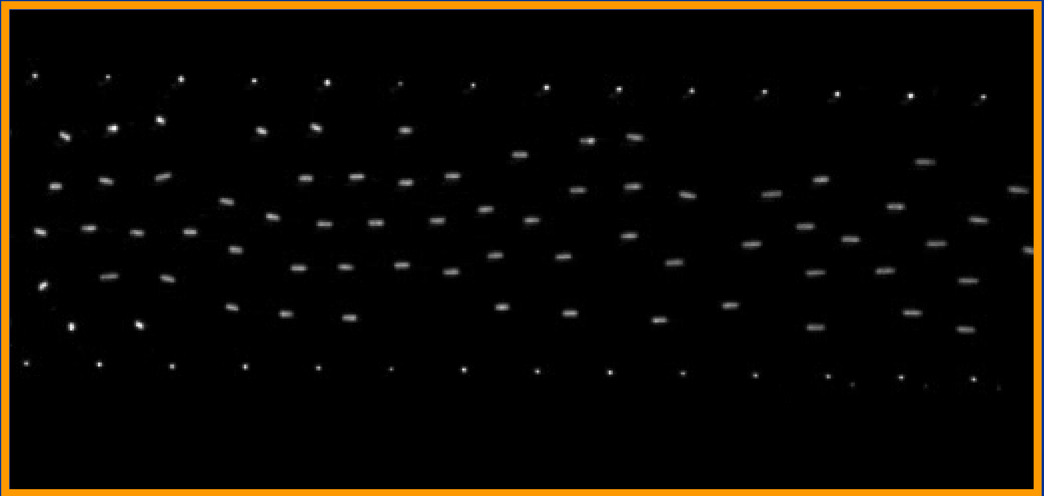

颗粒流体　　喷注、溅射现象

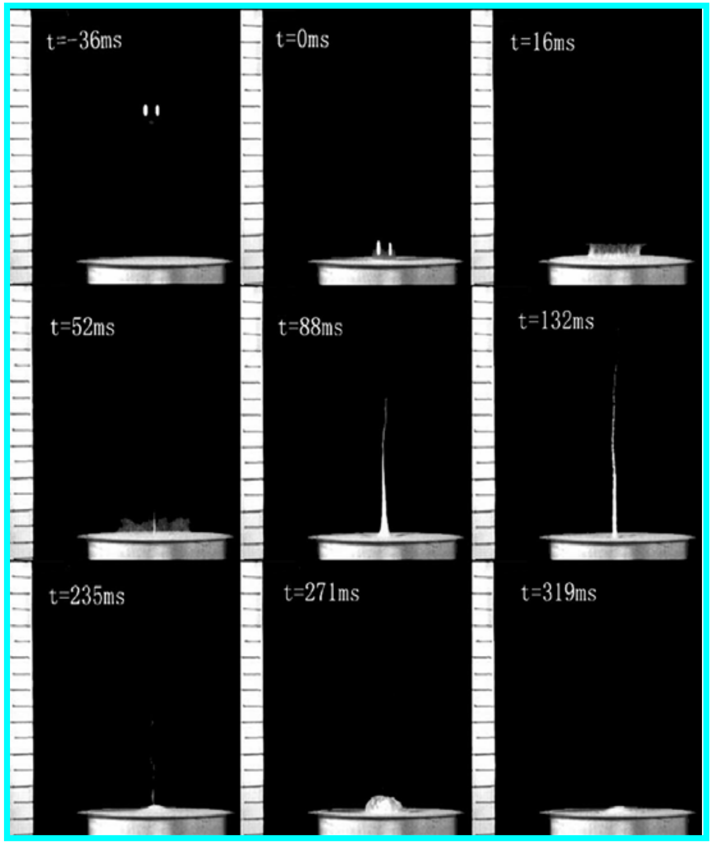

在空气中

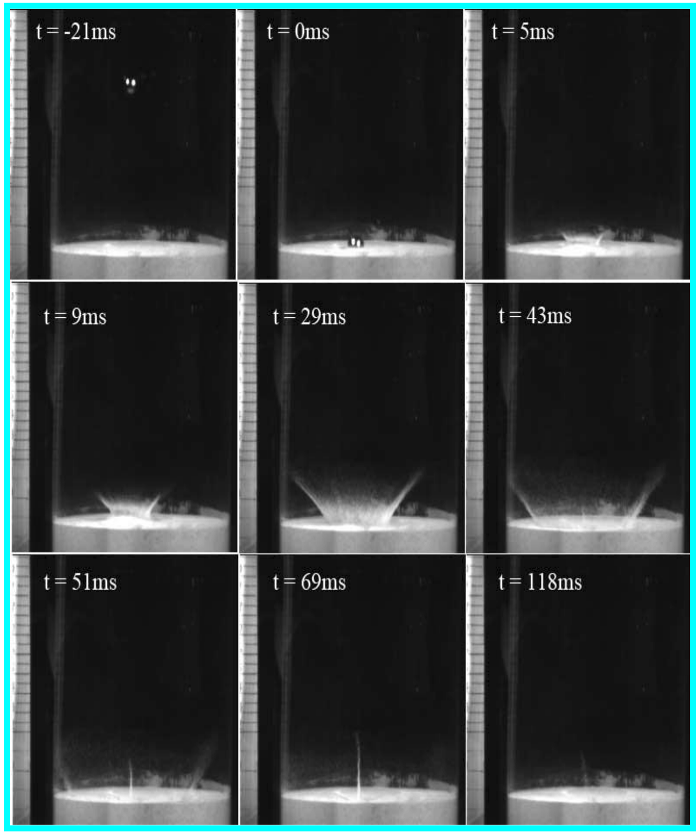

在真空中
（气压小于10^{-3}大气压）

颗粒固体

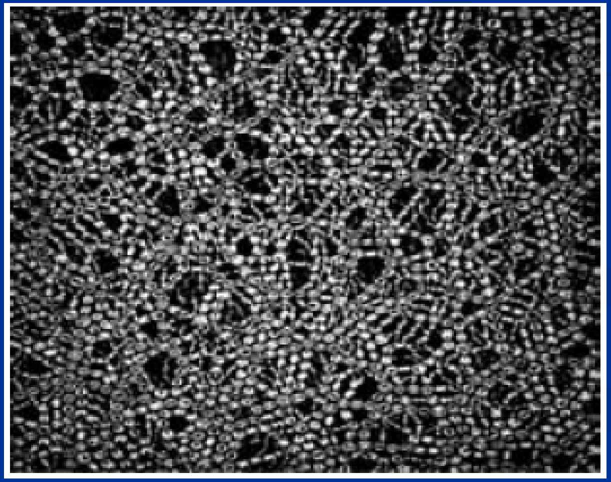

颗粒固体 力链拓扑结构

实验所得压力斑图 —弹性力学→ 颗粒受力情况 → 力链结构

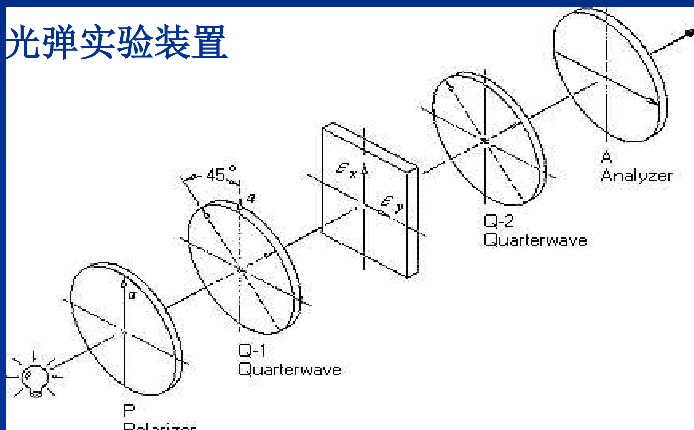

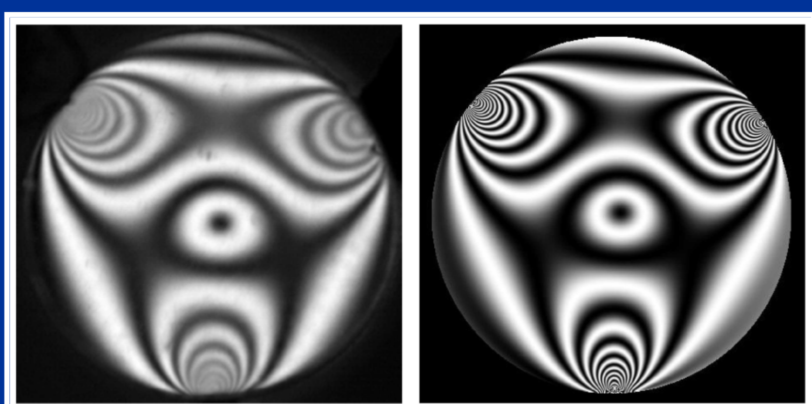

$$I=\sin^2\left(\frac{\delta}{2}\right)=\sin^2\left(\frac{\pi Ch}{\lambda}(\sigma_1-\sigma_2)\right)$$

二维剪切光弹实验

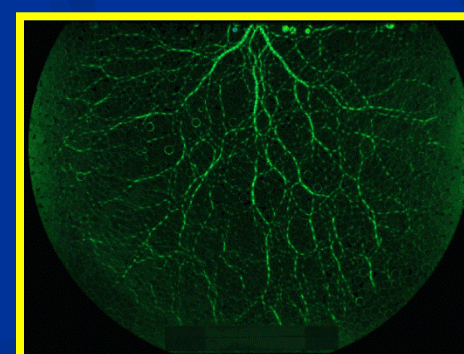

Liu et al., *Front Arch Civil Eng*, 2010

1. 颗粒气体速度分布律研究

颗粒气体

In ideal gas

- In equilibrium statistical mechanics, the kinetic theory is used to define an absolute temperature as the average translational kinetic energy of the random motions of all the particles.
- The simplest case is non-interacting particles of the ideal gas, $\frac{3}{2}k_B T_{eq} = \langle \frac{1}{2}mv^2 \rangle,$

  In a gas at equilibrium, the distribution of the particle velocities must satisfy a statistical distribution function in Gaussian form

$$f_{eq}(v) \propto \exp\left(-\frac{1}{2}\frac{mv^2}{k_B T_{eq}}\right).$$

- **that T_{eq} is connected not only to the average value of the energy, but also to the form of the distribution function.**

颗粒气体 What is the case in granular gas if we want to establish an athermal non-equilibrium thermodynamics?

$$P(v) \sim \exp[-|v/v_0|^{\zeta}]$$

with the exponent ζ=3/2.

The experimental and theoretical conditions are quite different: in the experiments, the energy is injected at the boundaries;
the theoretical model considers a homogeneous driving by a white noise, acting in the bulk of the homogeneous system.
The agreement between experiment and theory for the exponent ζ is somewhat misleading. The inconsistencies in experimental results depend on various parameters, such as number density, inelasticity, energy injection,etc.

A Barrat, E Trizac and M H Ernst, J. Phys.: Condens. Matter 17 (2005)

颗粒气体

Experiment in microgravity

Boundary Heating

Parabolic 2006

Cell = 10d x 10d
N=47 Bronze balls
Φ = 0.54

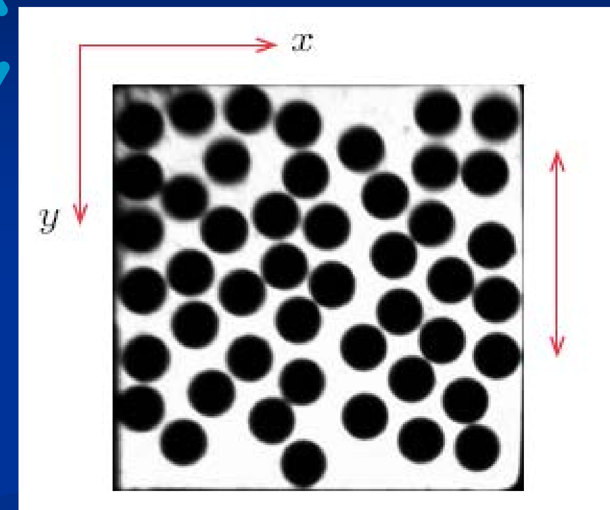

	Frequency(Hz)	A(0 – peak, mm)	$\Gamma(m/s^2)$	$V_\omega(m/s)$
1.	49	0.23	21.56	0.070
2.	97	0.11	41.28	0.067
3.	97	0.14	53.60	0.088
4.	49	0.12	11.73	0.038

颗粒气体

Vibro-fluidization

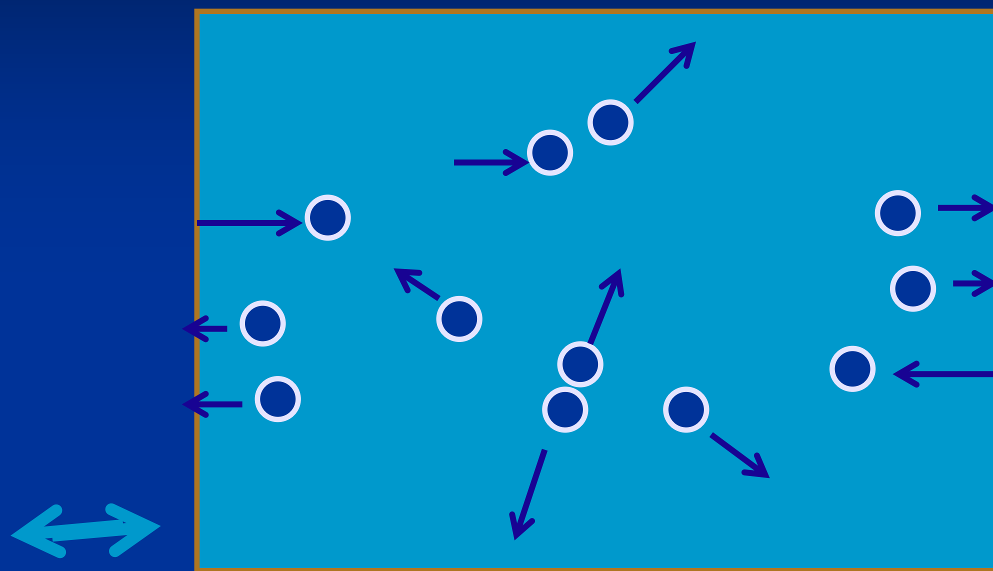

- $<V_x> = 0, <V_y> = 0,$ ⟷ y
- The boundary heating method develops gradient in density and in mean kinetic energy along the vibration direction, and $n_+(y) \neq n_-(y)$, $T_+(y) \neq T_-(y)$
- *Hydrodynamic description fails?*

颗粒气体 ffect enters into bulk: f(v) has two peaks

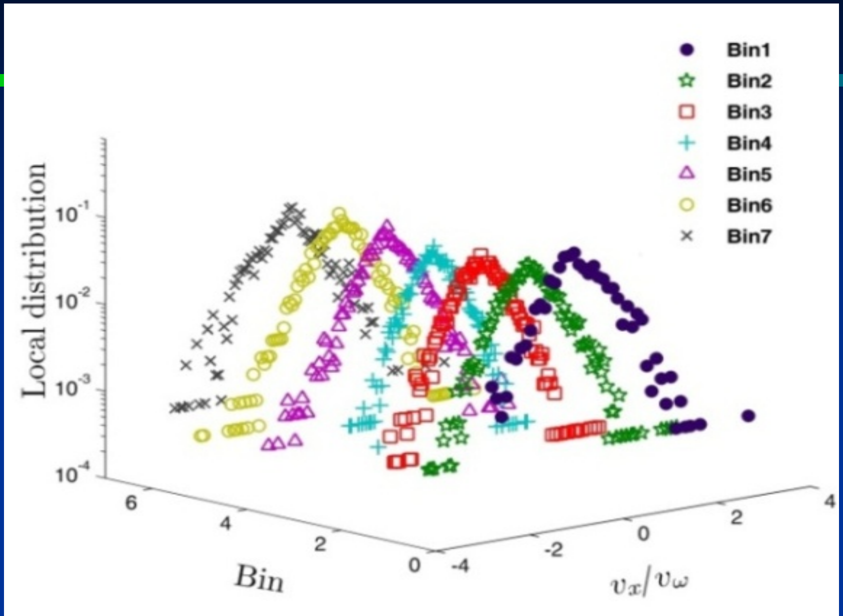

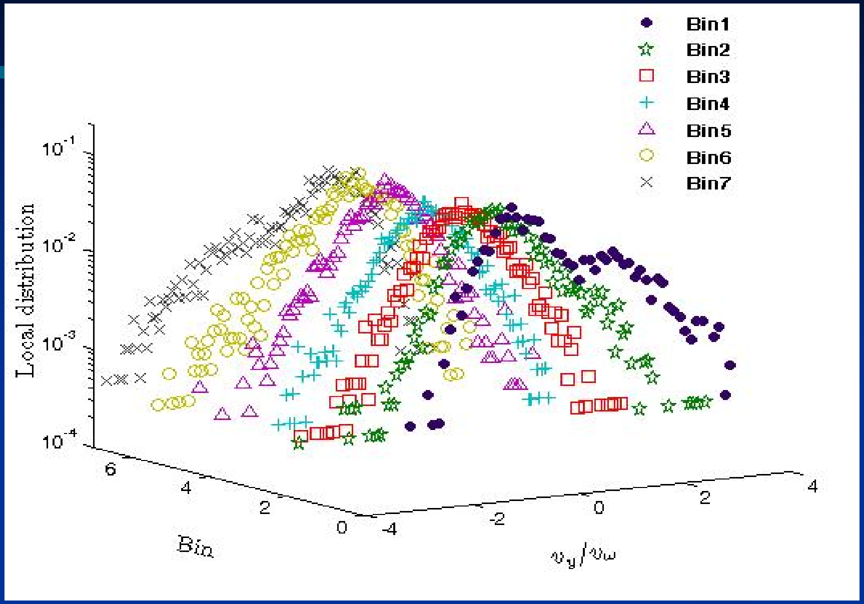

The local velocity distribution profiles of the longitudinal component are asymmetric or in two peaks near the walls, and this feature extends into the bulk, while the transverse component remains symmetric.

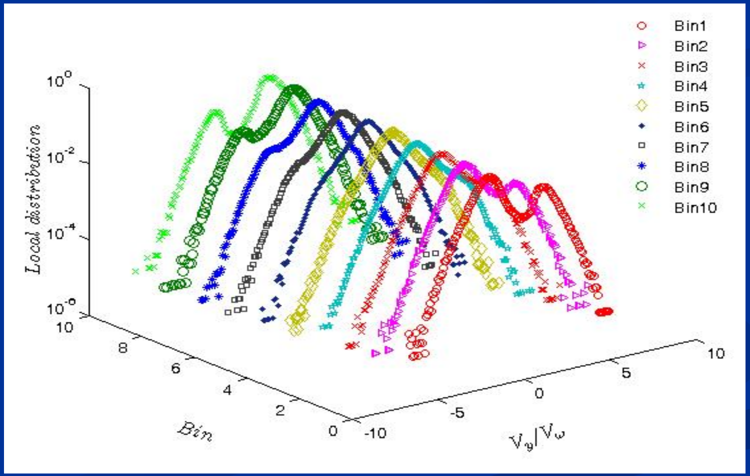

Journal of Physics: Conference Series **327** (2011) 012033

Chen Yanpei[1,2], Pierre Evesque[1], Meiying Hou[2], C. Lecoutre[3], F. Palencia[3] and Yves Garrabos[3]

Event-driven simulation by Zippelius' group (Phys. Rev. E 70,051313(2004))

Considering stress tensor in two terms: kinetic contribution and interactions between particles:

$$\sigma(r,t)=\sigma^{\mathrm{kin}}(r,t)+\sigma^{\mathrm{int}}(r,t)$$

$$\sigma_{ij}^{\mathrm{kin}}(r)=-m\int_{\mathrm{R}}dv_x\int_{\mathrm{R}}dv_y f_{\mathrm{stat}}(r,v_x,v_y)\times[v_i-U_i(r)][v_j-U_j(r)].$$

$$\sigma_{ij}^{\mathrm{int}}(r,t)=\frac{1}{\Delta t}\frac{1}{|V_r|}\sum_{t_n}\sum_{k_n} l_i^{k_n}(t_n)\Delta p_j^{k_n}(t_n).$$

$$\sigma_{ij}^{\mathrm{int}}(r)=\frac{1}{\tau}\int_{t_0}^{t_0+\tau}dt\,\sigma_{ij}^{\mathrm{int}}(r,t).$$

Event-driven simulation by Zippelius' group (Phys. Rev. E 70,051313(2004))

- They showed solid like stress tensor in such boundary heating system.
  - Anisotropic stress that $\sigma_{xx} \neq \sigma_{yy}$ and the σ_{xx} is a constant, while $\sigma_{yy}(x)$ is not, it is a function of x.
  - $T_x \neq T_y$

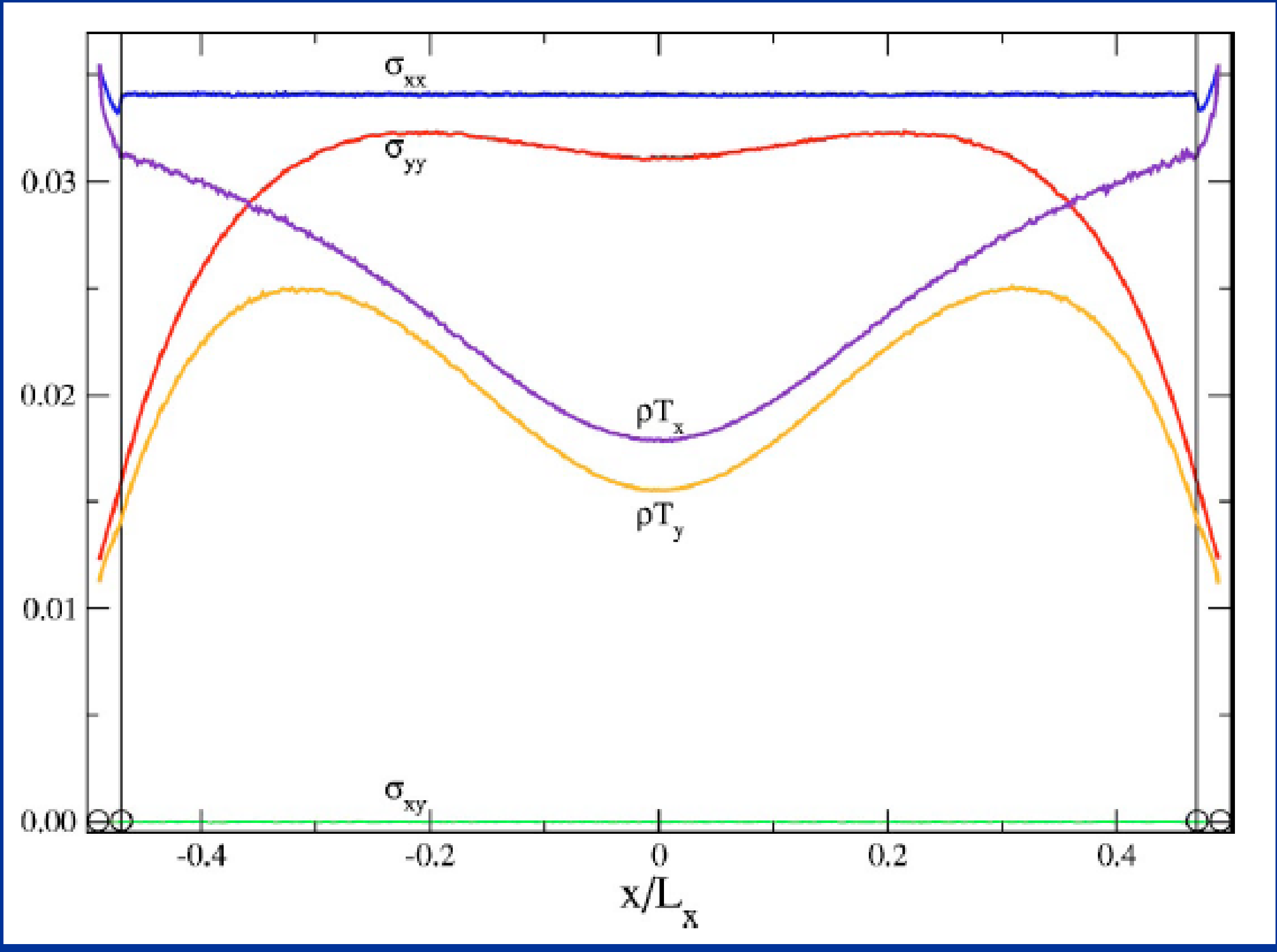

X is the vibration direction

颗粒气体

The problem:

No convective flow: $V_x = V_y = 0$

Stress, density, kinetic energy : x-dependent

Probably because of insufficient grain-grain collisions?

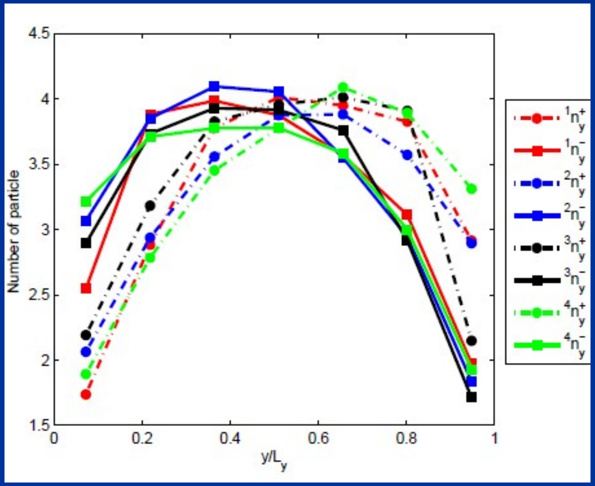

Two unusual facts:

- ❑ Wall effect enters into bulk: f(v) has two peaks
- ❑ Stress anisotropy: $\sigma_{xx} \neq \sigma_{yy}$

Haff's hydrodynamics of granular gas has to be generalized

$$\sigma_{xx} = \sigma_{yy} \quad when \quad V = 0$$

颗粒气体

Haff's hydrodynamics of granular gas

force balance $\rho d_t v_i + \nabla_k \sigma_{ik} = 0$

Flux of granular heat:

$$\iota_k = \kappa \nabla_k T_g$$

mass conservations $\partial_t \rho + \nabla_k \rho V_k = 0$

granular entropy $\partial_t s_g + \nabla_k (s_g V_k - \iota_k) = \left(R_g / T_g\right) - I$

entropy $\partial_t s + \nabla_k (s V_k - h_k) = R / T$

thermodynamic identity of stress $\sigma_{ik} = \left(\rho \frac{\partial f}{\partial \rho} - f\right)\delta_{ik} - \sigma_{ik}^D$

Viscous stress: $\sigma_{ik}^D = \eta V_{ik}$

No stress anisotropy:

$$\sigma_{xx} = \sigma_{yy} \quad when \quad V = 0$$

Production rate of entropies:

$$R = h_k \nabla_k T + \iota_k \nabla_k T_g + I T_g + \sigma_{ik}^{(D2)} V_{ik}$$

$$R_g = \sigma_{ik}^{(D1)} V_{ik}$$

颗粒气体

How to generalize the Haff's?

Expanding the set of state variables:

Poudres & Grains, 18(1):1–19, 2010

suggested:

Haff: ρ, T_g, V_i

To add

$$\rho^{(+)}, \rho^{(-)}, v^{(+)}, v^{(-)}$$

$$\rho^{(+)} + \rho^{(-)} = \rho$$

$$\rho^{(+)} v^{(+)} + \rho^{(-)} v^{(-)} = \rho v$$

Eqs. of motion?

Thermodynamics?

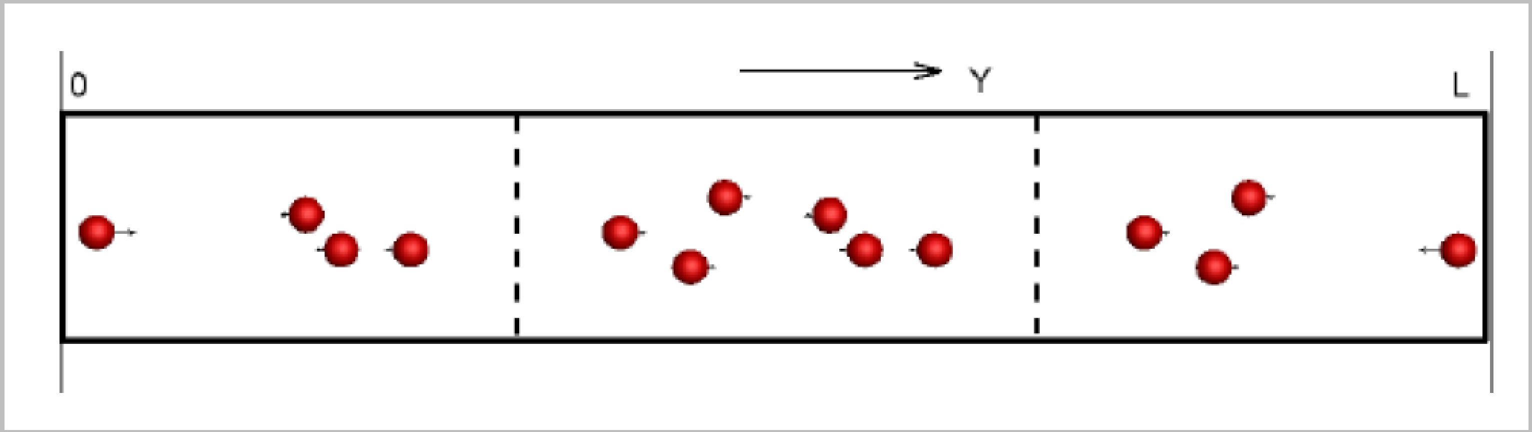

颗粒气体

How to generalize the Haff's?

Expanding the set of state variables:

Haff: ρ, s_g, v_i

$$\partial_t s_g + \nabla_k (s_g v_k - \iota_k) = \left(R_g / T_g\right) - I$$

$$R_g = \sigma_{ik}^{(D1)} v_{ik}$$

GSH: Thermodynamics

Additing two more diffusing-relaxing variables: (a vector and a tensor) → Δ_i, t_{ij}

$$\partial_t \Delta_i + \nabla_k (\Delta_i v_k - \iota_{ik}^{(\Delta)}) = -I_i^{(\Delta)}$$

$$\partial_t t_{ij} + \nabla_k (t_{ij} v_k - \iota_{ijk}^{(t)}) = -I_{ij}^{(t)}$$

$$R = h_k \nabla_k T + \iota_k \nabla_k T_g + I T_g + \sigma_{ik}^{(D2)} v_{ik} + \iota_{ik}^{(\Delta)} \nabla_k \Delta_i + \iota_{ijk}^{(t)} \nabla_k t_{ij} + I_k^{(\Delta)} \Delta_k + I_{ik}^{(t)} t_{ik}$$

The additional dissipations produce the heats

A simple choice of transport coefficients gives:

$$\sigma_{ij} = P\delta_{ij} - \eta v_{ij}^* - c\rho\alpha\Delta_i\Delta_j - e\rho\beta t_{ij}$$

颗粒气体

Reasons for a vector and a tensor: Δ_i , t_{ij}

- Two peaks of velocity distribution
- Anisotropy of kinetic energy

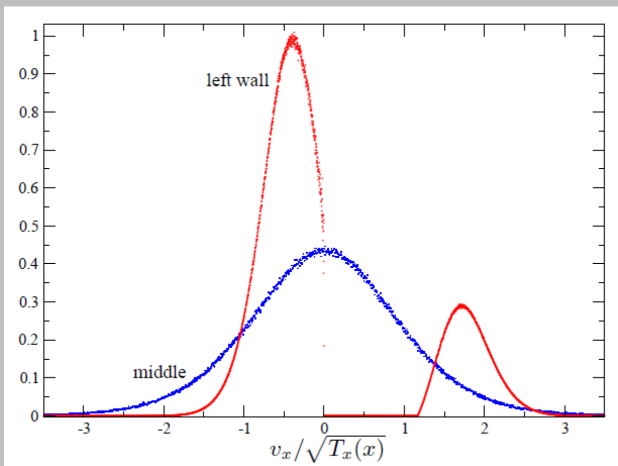

Olaf Herbst, Peter Müller, Matthias Otto, and Annette Zippelius

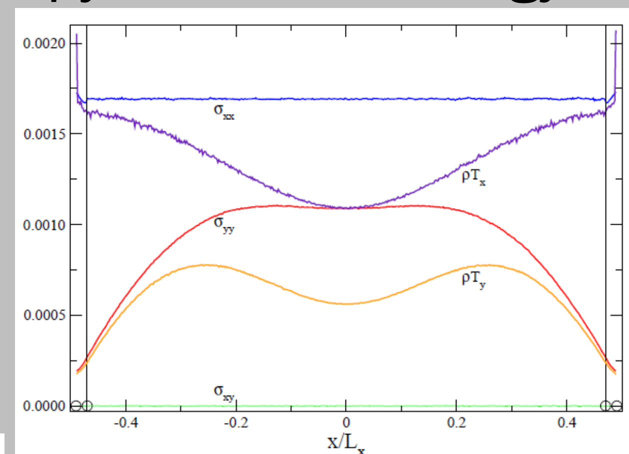

Phys. Rev. E., 70:051313, 2004.

$$for < v_i >= 0$$

$$f(v_x, v_y, v_z) \approx \alpha \exp\left[-(v_i - \xi_i)\beta_{ij}(v_j - \xi_j)\right] + \exp\left[-(v_i + \alpha\xi_i)\beta_{ij}(v_j + \alpha\xi_j)\right]$$

$$\xi_i, \beta_{ij} \Leftrightarrow \Delta_i, t_{ij}$$

颗粒气体

Free energy

$consider \qquad v = 0$

Haff: $w(\rho, T_g)$

The GSH: $w(\rho, T_g, \Delta_i, t_{ik})$

We may simply assume the Tailor expansion:

$$w = w_0 + (b\rho T_g^2 + c\rho\Delta_i^2 + e\rho t_{ij}^2)/2$$

颗粒气体

A kinetic explanation for the w

Velocity distribution:

$$f(v_x) = \frac{1}{N}\left(\alpha \exp\frac{(v_x-\xi)^2}{-T_x} + \exp\frac{(v_x+\alpha\xi)^2}{-T_x}\right)$$

$$f(v_y) = f(v_x \to v_y, T_x \to T_y, \xi = 0)$$

$$N \equiv \sqrt{\pi T_x}(1+\alpha)$$

$$\langle v_x \rangle, \langle v_y \rangle = 0$$

$$w = w_x + w_y$$

$$w_x = \frac{1}{2}\rho T_x + \rho\alpha\xi^2$$

$$w_y = \frac{1}{2}\rho T_y$$

$$\xi \to \Delta_x$$

$$T_x = b\left(T_g + t_{xx}\right)^2/4$$

$$T_y = b\left(T_g - t_{xx}\right)^2/4$$

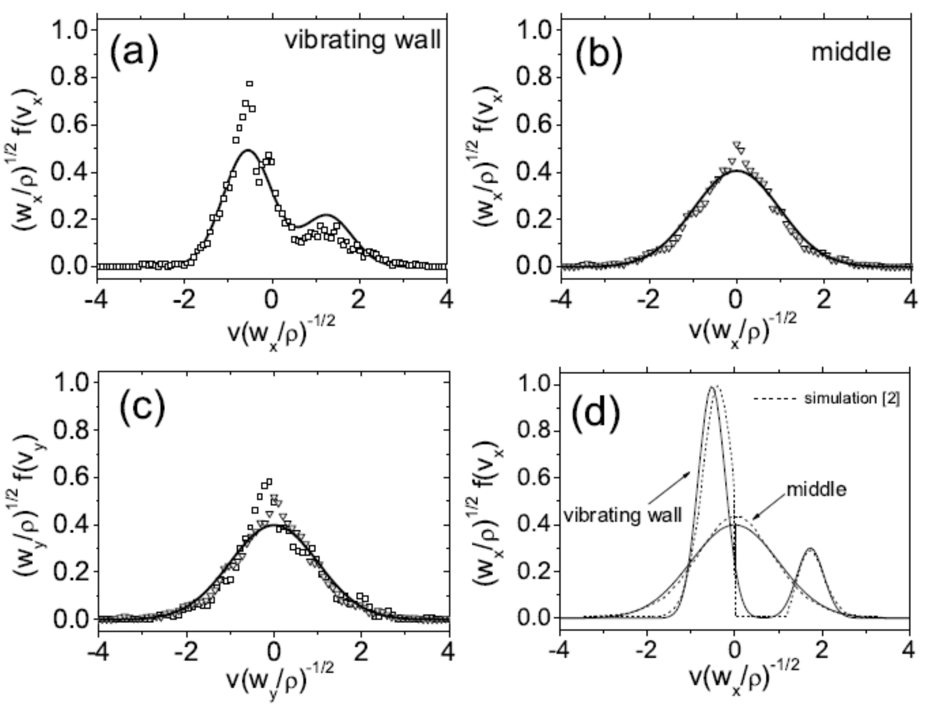

$$w = w_0 + (b\rho T_g^2 + c\rho\Delta_i^2 + e\rho t_{ij}^2)/2$$

颗粒气体

Applying the GSH to:

$$\Delta_x, t_{xx} \neq 0$$

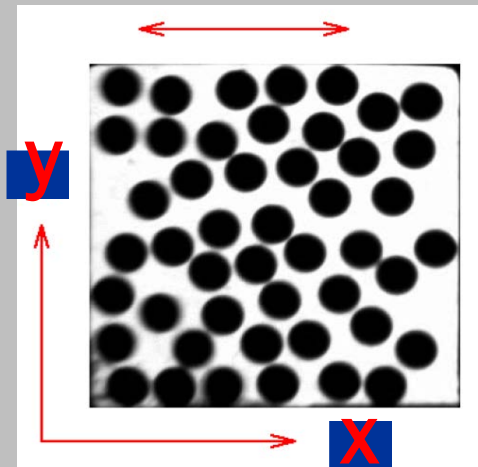

The observed behaviors could be explained.

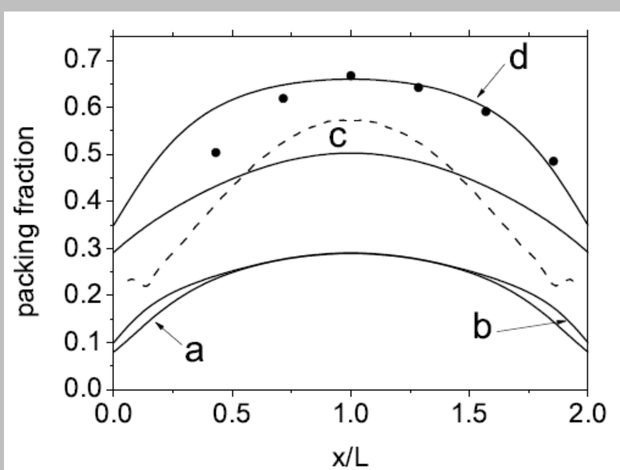

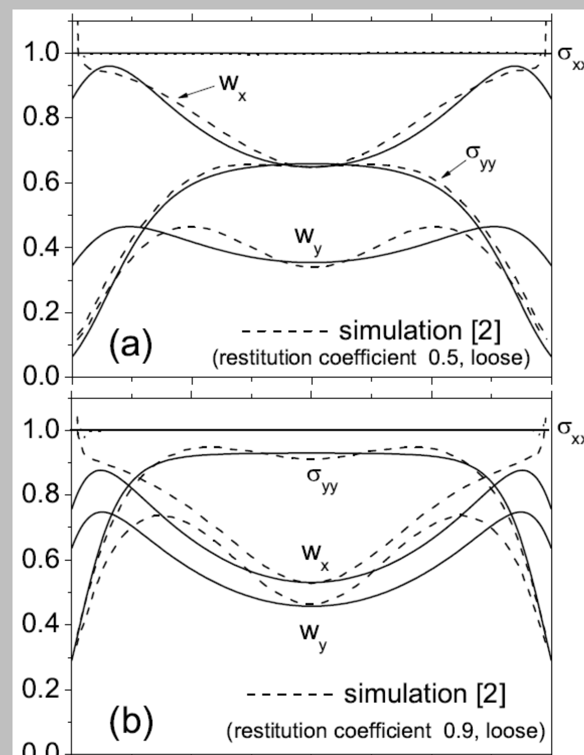

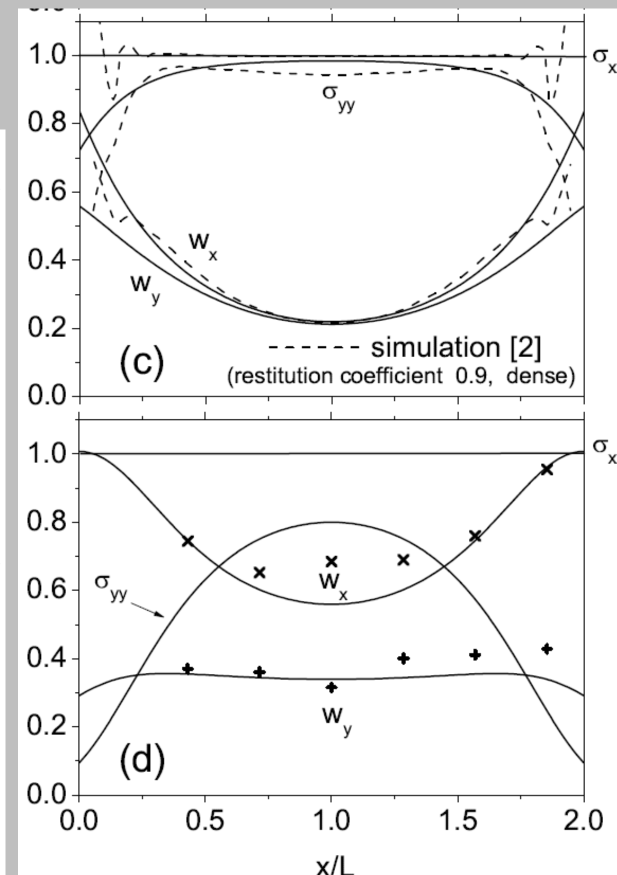

小 结

- 颗粒气体速度分布律受体系激发方式影响。振动驱动的气体体系受边壁效应引起颗粒气体具有类似固体的应力张量，使得颗粒空间密度不均匀，造成非高斯、非对称局域颗粒气体速度分布函数。

2. 颗粒气体团簇效应引起的非线性动力学与分叉行为研究

双仓振动驱动颗粒体系

体系装置

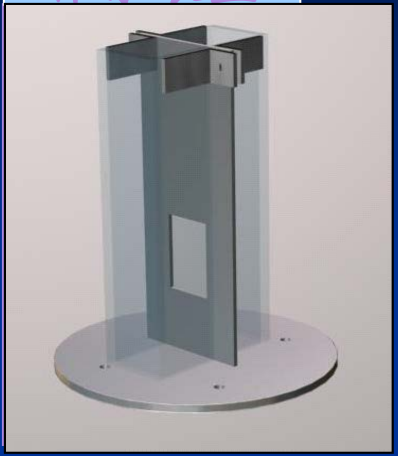

体系特点

颗粒数密度较小：

考虑成颗粒气体，颗粒间相互作用大多为两体碰撞，可用颗粒气体动力学进行建模。

横向尺寸相对较小：

避免横向密度分布不均匀带来的复杂性，体系可由三维简化为垂直方向一维系统。

能量输入方式：

颗粒与振动底板碰撞获得能量，碰撞是瞬时的，碰撞前后颗粒速度改变可根据动量守恒方便得出，边界条件相对比较简单。

两仓间通过挡板中间小缝连接：

耦合较弱，两仓可考虑成相互独立的两个部分，各自演化可考虑为准静态过程。

颗粒气体

- Considering only two body collision interaction, the clustering behavior can be studied by counting the number of particles in each compartment and/or time duration of particles in periodic oscillation.

- A rich nonlinear dynamic behavior can be obtained in such a simple classical system, which helps understanding nonlinear phenomena observed in other far from equilibrium systems.

颗粒气体 For mono-disperse granules in two-compartment cells

parameters： number of cells、 particle numbers、 driving velocity

- Segregation distributions (SEG)

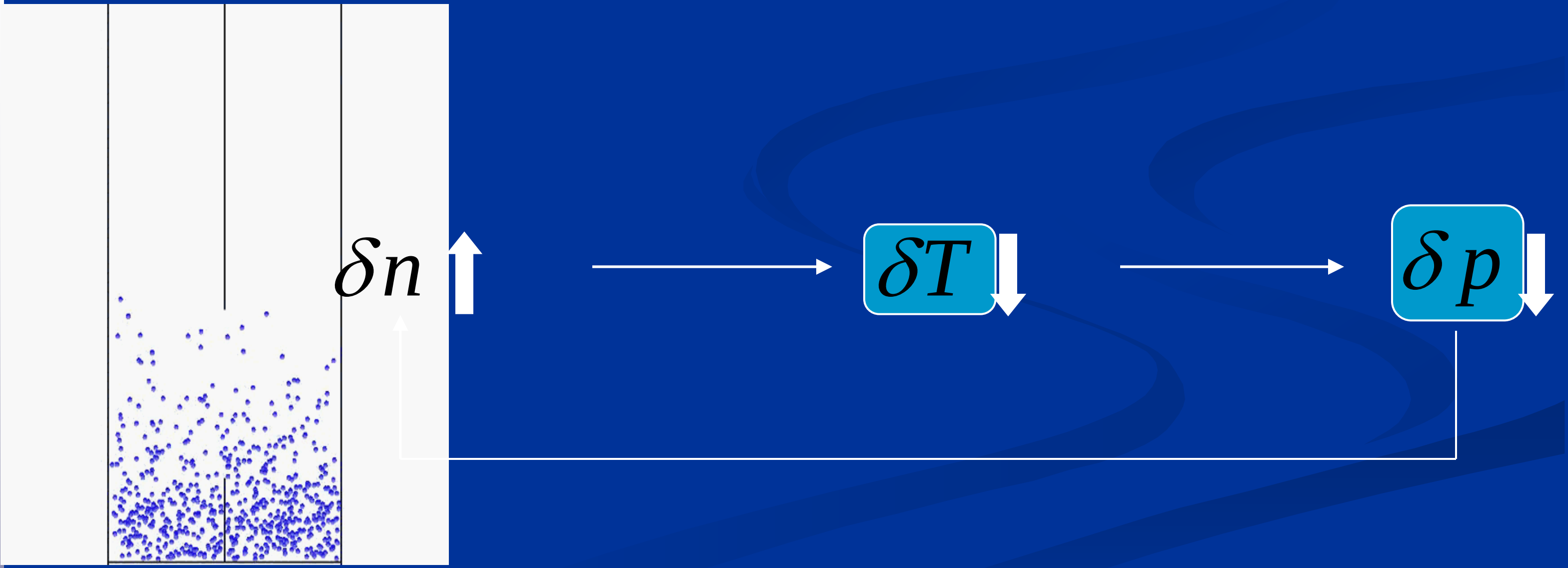

Oscillatory distribution in compartmentalized bi-disperse granular gases

Granular Clock

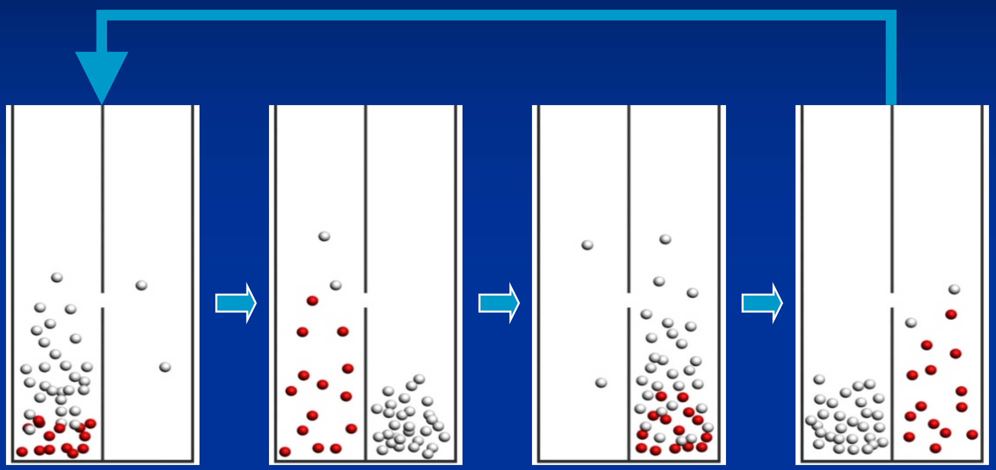

- Segregation distributions (SEG)
- Particles populate among the two compartments back and forwards periodically (OSC)

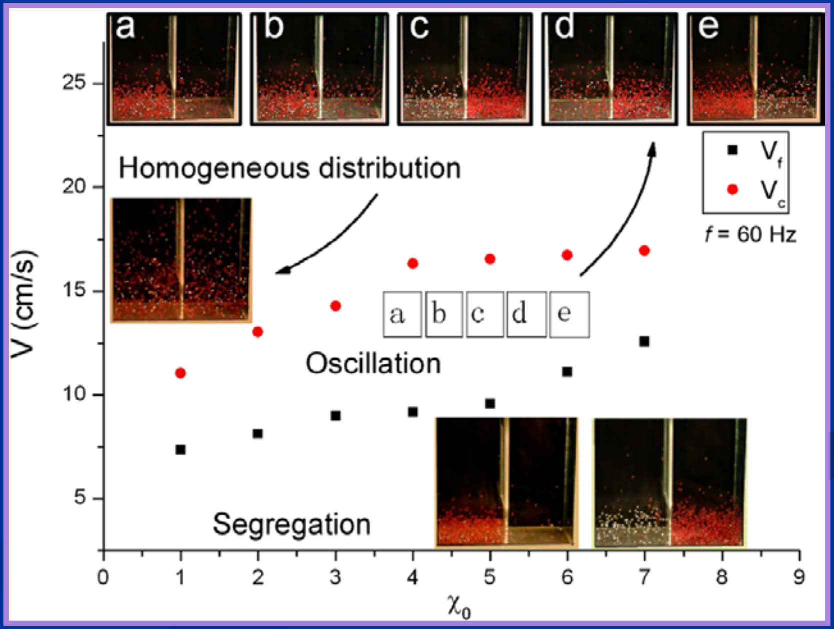

d-OSC and s-HOM states in simulation

d-OSC

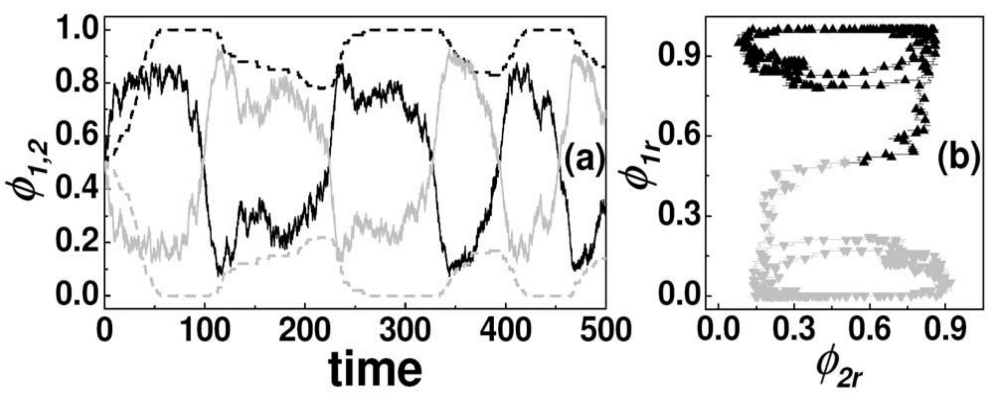

s-HOM

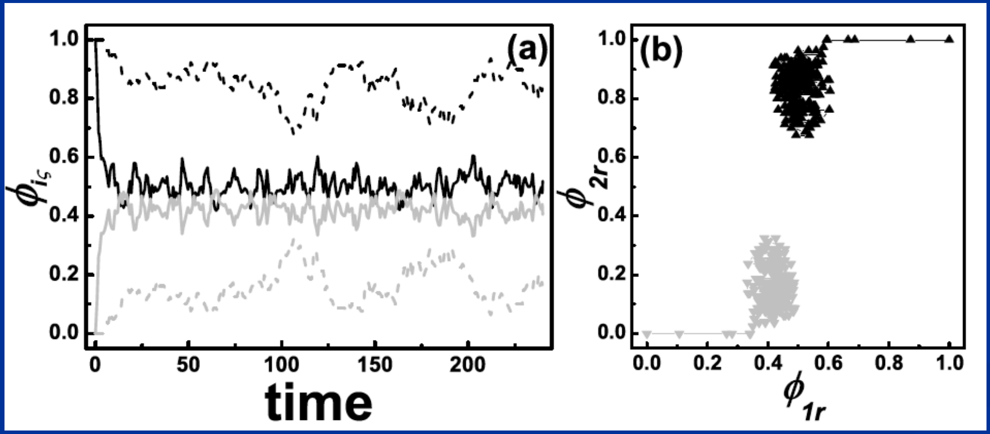

When increasing the number of heavy particles, d-OSC and s_HOM states are observed.

s-HOM:

Light particles homogenous populated in the two compartments, while the heavy particles only partly participate

d-OSC:

Light particles Oscilate between two compartments, while heavy particles only partly participate

颗粒气体

OSC

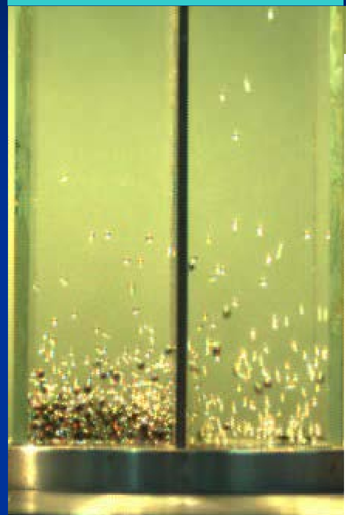

simulation

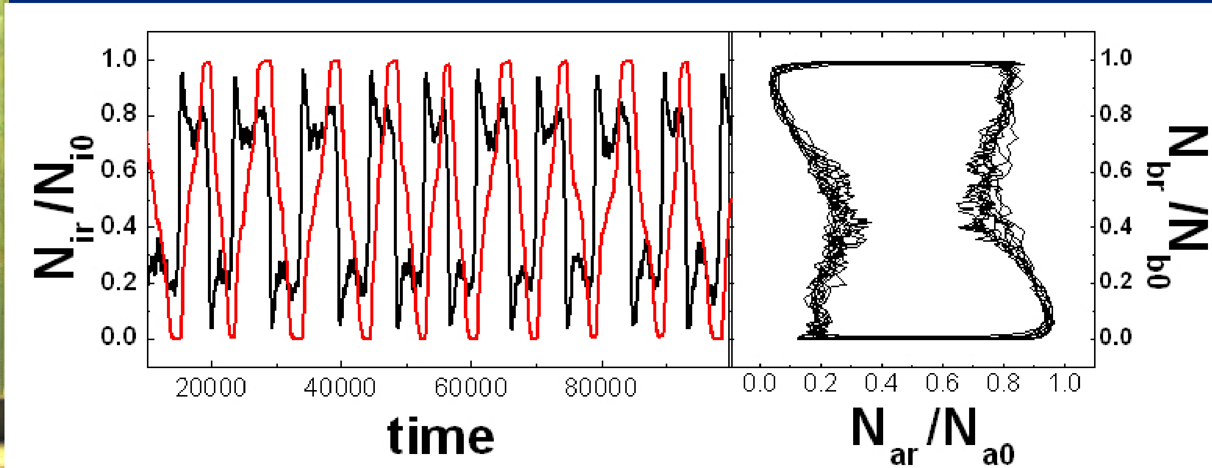

Time sequence

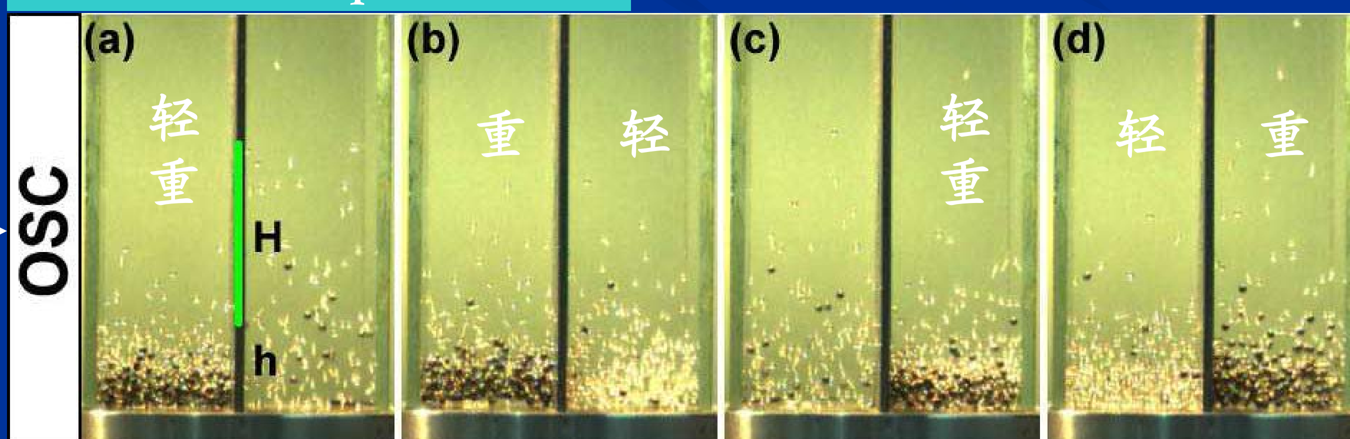

颗粒气体

d-OSC

simulation

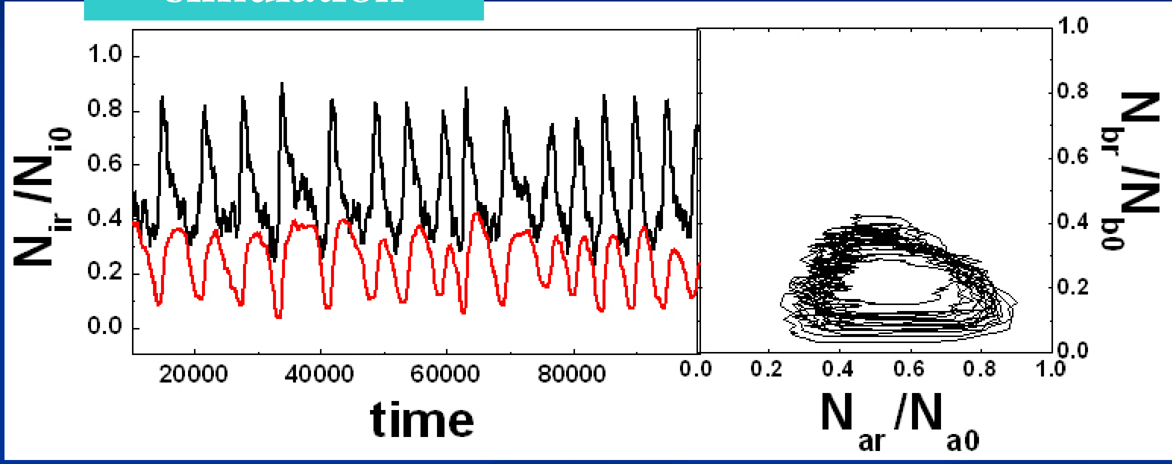

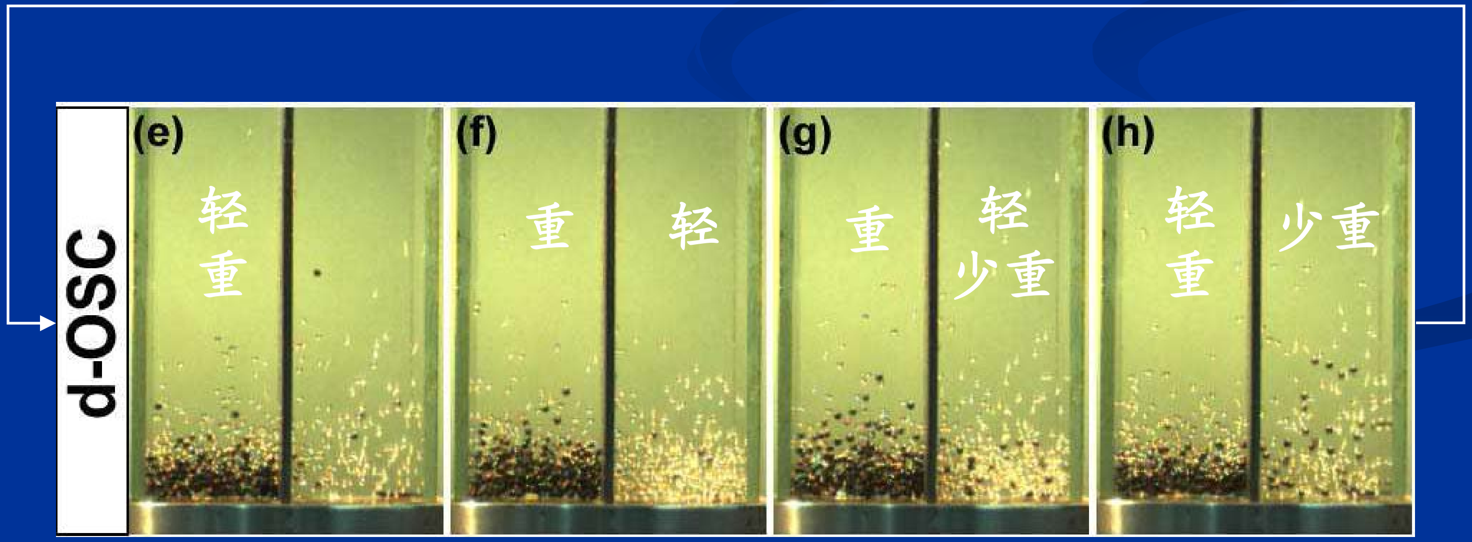

Phase diagram

V_b driving velocity

ϕ_h ratio of N_{heavy}/N_t

$N_{total} = 1000$

HOM

OSC

SEG

s-HOM

d-OSC

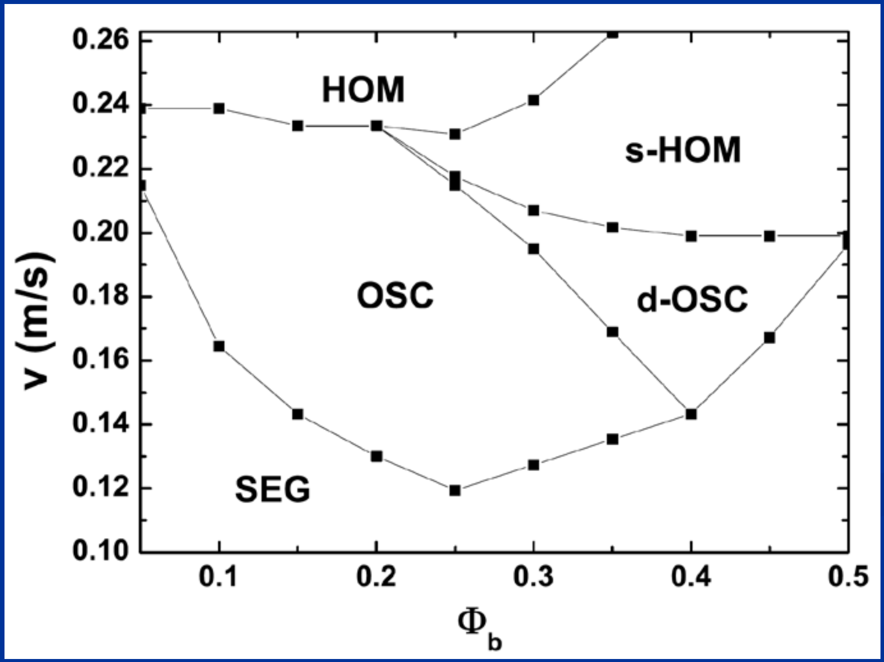

Flux model

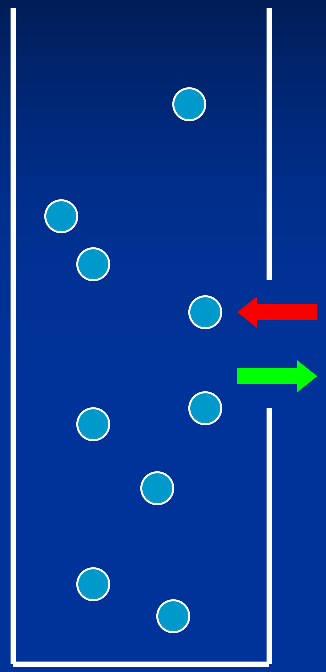

For two cell system

$$\frac{\partial N_\sigma}{\partial t} = -F(N_\sigma) + F(N_0 - N_\sigma)$$

Assume the flux is only a function of number of particles in the cell

Balance eq.

$$\partial_t n + u \cdot \nabla n + n \nabla \cdot u = 0$$

$$\partial_t u + u \cdot \nabla u + (mn)^{-1} \nabla \cdot P = 0$$

$$\partial_t T + u \cdot \nabla T + \frac{2}{3nk_B}(P : \nabla u + \nabla \cdot q + T\zeta) = 0$$

⇒ ⇒ $F(N)$

Flux function for monodiperse granular system

$$F(N) \propto n(h)\sqrt{k_B T}$$

Assume T is a constant

$$p = nk_B T$$

$$\frac{\partial p}{\partial z} = -mgn$$

$$n(z) = \frac{mgN}{\Omega k_B T} e^{-\frac{mgz}{k_B T}}$$

Assume velocity is maxwell distributed

$$Q_{dissipation} = J_{in}$$

$$Q_{dissipation} \propto N^2 \sqrt{T}$$

$$J_{in} \propto N V_b$$

$$k_B T \propto \frac{V_b^2}{N^2}$$

$$F_i(N_l, N_h) = \frac{WHg}{\sqrt{2\pi\Omega}} N_i \sqrt{\frac{m_i}{k_B T}} e^{-\frac{m_i g h}{k_B T}}$$

Flux model

monodisperse- two cells

$$\frac{\partial N_\sigma}{\partial t} = -F(N_\sigma) + F(N_0 - N_\sigma)$$

monodisperse – three cells

$$\frac{\partial N_1}{\partial t} = -2F(N_1) + F(N_2) + F(N_0 - N_1 - N_2)$$

$$\frac{\partial N_2}{\partial t} = -2F(N_2) + F(N_1) + F(N_0 - N_1 - N_2)$$

bidisperse-two cells

$$\frac{\partial N_{a\sigma}}{\partial t} = -F_a(N_{a\sigma}, N_{b\sigma}) + F_a(N_{a0} - N_{a\sigma}, N_{b0} - N_{b\sigma})$$

$$\frac{\partial N_{b\sigma}}{\partial t} = -F_b(N_{a\sigma}, N_{b\sigma}) + F_b(N_{a0} - N_{a\sigma}, N_{b0} - N_{b\sigma})$$

bidisperse –three cells

$$i = a, b$$

$$\frac{\partial N_{i1}}{\partial t} = -2F_i(N_{a1}, N_{b1}) + F_i(N_{a2}, N_{b2}) + F_i(N_{a0} - N_{a1} - N_{a2}, N_{b0} - N_{b1} - N_{b2})$$

$$\frac{\partial N_{i2}}{\partial t} = -2F_i(N_{a2}, N_{b2}) + F_i(N_{a1}, N_{b1}) + F_i(N_{a0} - N_{a1} - N_{a2}, N_{b0} - N_{b1} - N_{b2})$$

Flux model for Mono-disperse granular system

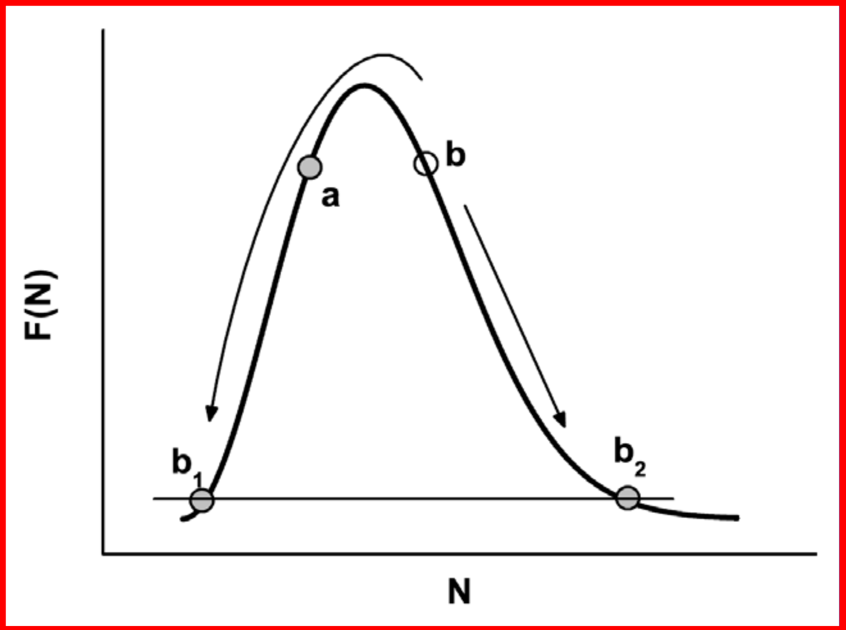

homogeneous：

$$\left.\frac{\partial N}{\partial t}\right|_{N=N_0/2} = -F(N_0/2) + F(N_0 - N_0/2) = 0$$

Small perturbation around this point

$$\frac{\partial \delta N}{\partial t} = -F(N_0/2 + \delta N) + F(N_0/2 - \delta N)$$

Around a homogenous solution

$$\frac{\partial \delta N}{\partial t} = -2\left.\frac{\partial F(N)}{\partial N}\right|_{N=N_0/2} \delta N$$

$$\left.\frac{\partial F(N)}{\partial N}\right|_{N=N_0/2} > 0, \frac{\partial \delta N}{\partial t} < 0$$

At point a， homogeneous，

$$\left.\frac{\partial F(N)}{\partial N}\right|_{N=N_0/2} < 0, \frac{\partial \delta N}{\partial t} > 0$$

At point b， segregate

Flux Function for Mono-disperse System

$$F_i \propto n_i(h)\sqrt{k_B T_i}$$

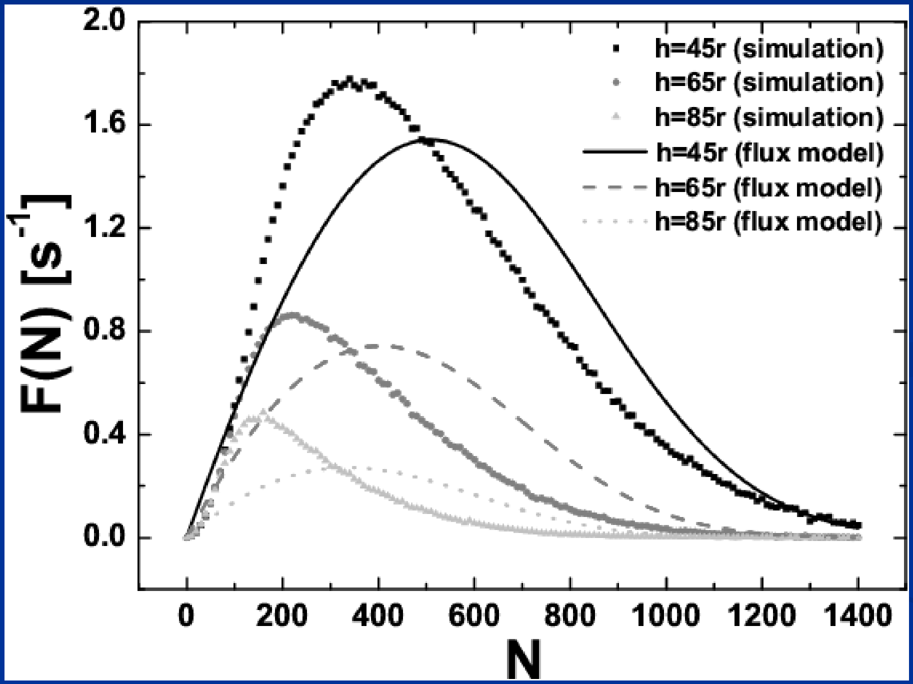

Single-peak

MD Simulation results (dots) and theoretical results (lines)

flux model for bidisperse granular system

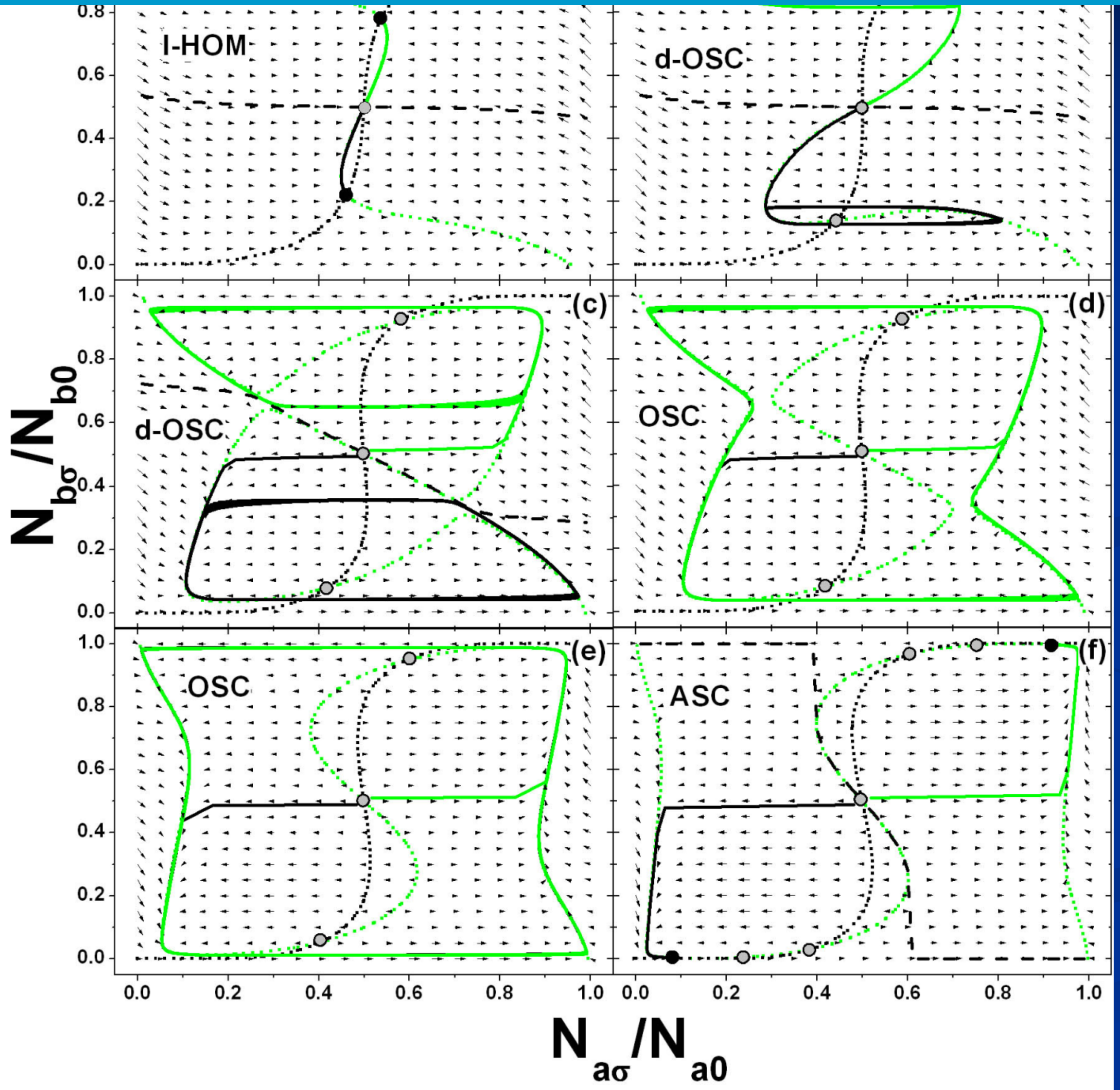

实验中所观测到的五种态均能被两种颗粒流通量模型预测。

当改变驱动速度时，由流通量模型可解出不同种颗粒数目演化行为，对应于不同的态。

图中，黑色圆点为稳定不动点，对应于不随时间变化的布局状态，如l-HOM(a)和ASC态(f)。灰色圆点代表不稳定不动点。

黑色和绿色实线代表左右仓颗粒数目演化轨道。如(b)-(d)图对应稳定的周期解（极限环）。(b)-(c)图对应d-OSC态，(d)-(e)对应OSC态。

Bi-disperse two-cell system

$$\frac{\partial N_{a\sigma}}{\partial t} = -F_a(N_{a\sigma}, N_{b\sigma}) + F_a(N_{a0} - N_{a\sigma}, N_{b0} - N_{b\sigma})$$

$$\frac{\partial N_{b\sigma}}{\partial t} = -F_b(N_{a\sigma}, N_{b\sigma}) + F_b(N_{a0} - N_{a\sigma}, N_{b0} - N_{b\sigma})$$

$$\Phi_b = N_{b0} / N_0$$

$$N_0 = 1000$$

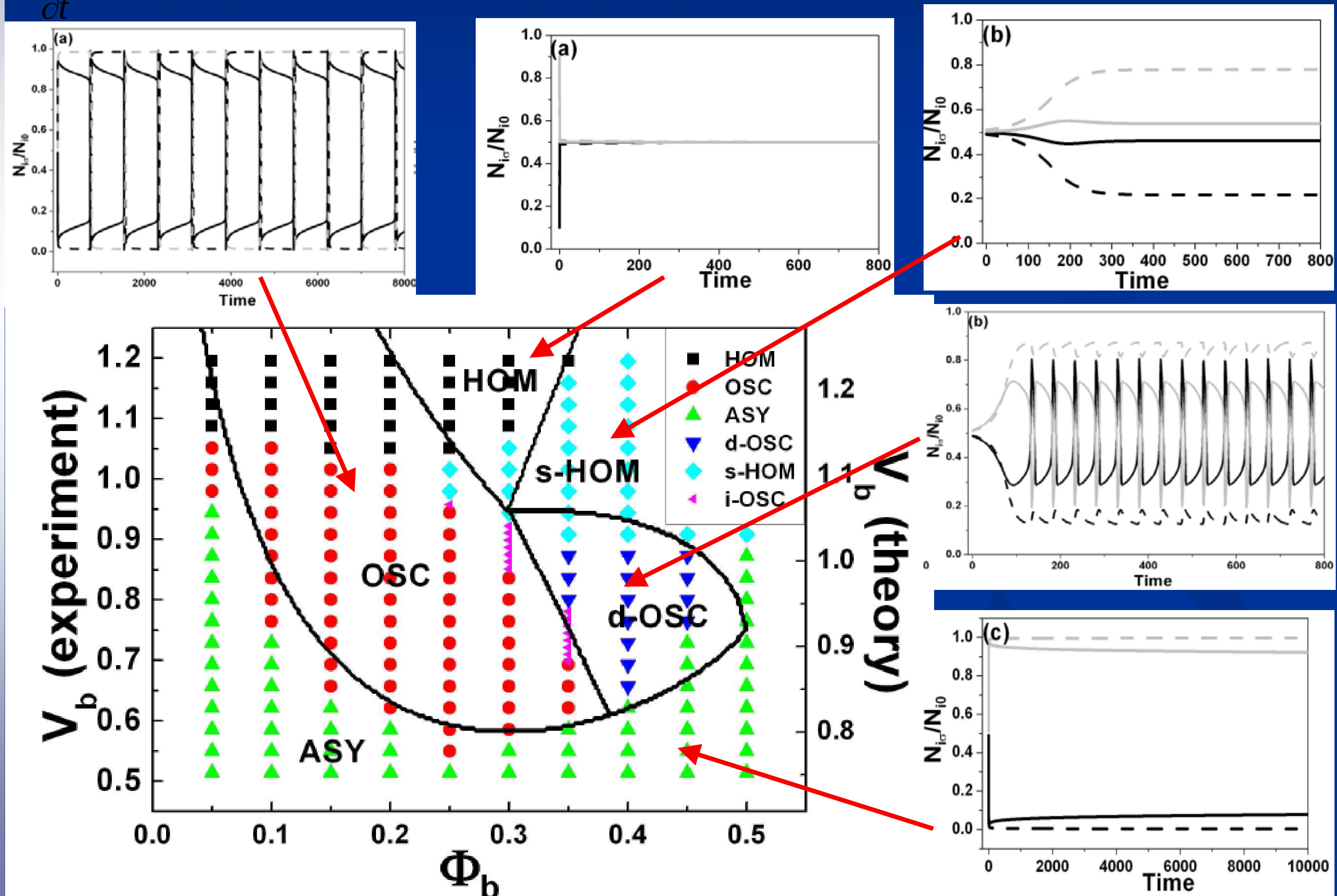

颗粒气体

Bifurcation

demonstrated by bidisperse system in two cells

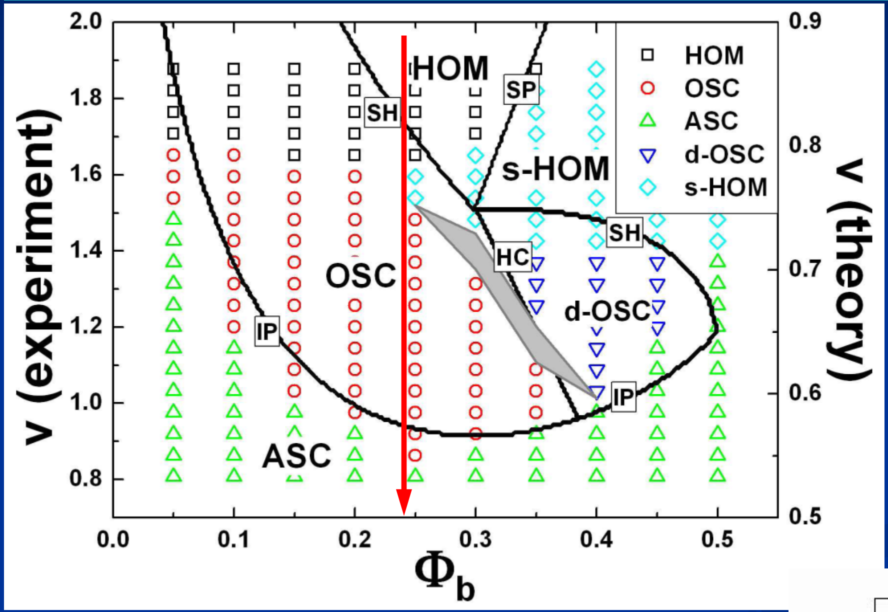

- 5-clustering states
- 7 transitions
- 6 bifurcations

Hopf bifurcation

infinite periodic bifurcation

saddle-node bifur

HOM → OSC → SEG

One fixed point	One Limit cycle	Two fixed points

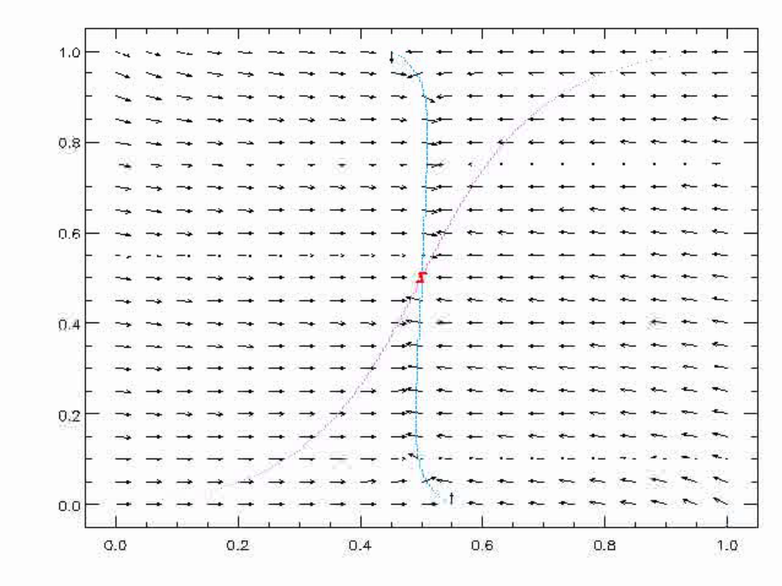

颗粒气体

bifurcation

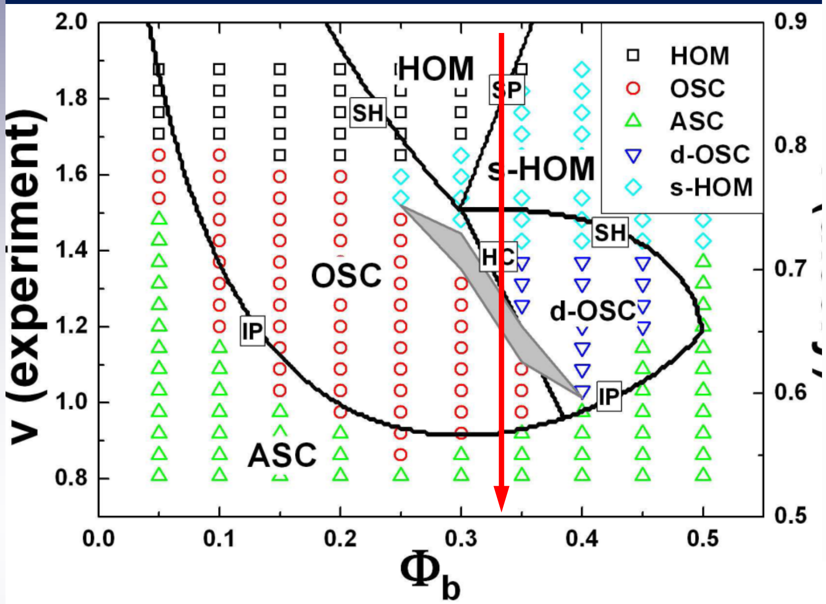

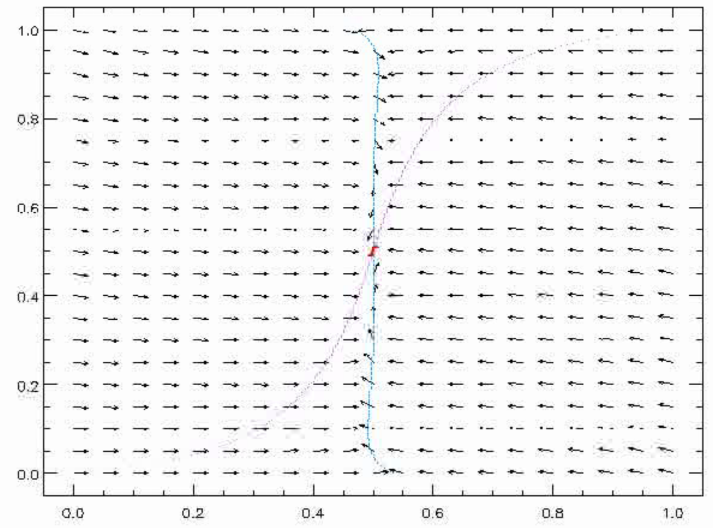

fork bifurcation → Hopf bifurcation → homoclinic bifurcation → saddlenode bifurcation

HOM → s-HOM → d-OSC → OSC → SEG

HOM	s-HOM	d-OSC	OSC	SEG
one fixed point	two fixed points	two stable cycles	one stable cycle	two fixed points

小 结

- The clustering behaviors in shaken fluidized mono-disperse and bi-disperse granular material in connected compartments were studied experimentally, by simulation and theoretically.

Granular system ⟶ a good model system for studying nonlinear bifurcation phenonema.

颗粒物质研究

颗粒的流动特性

颗 粒 流 体

振动分离

振动分离
巴西果效应

Segregation: Large grains rise to the top (Brazil nut effect).

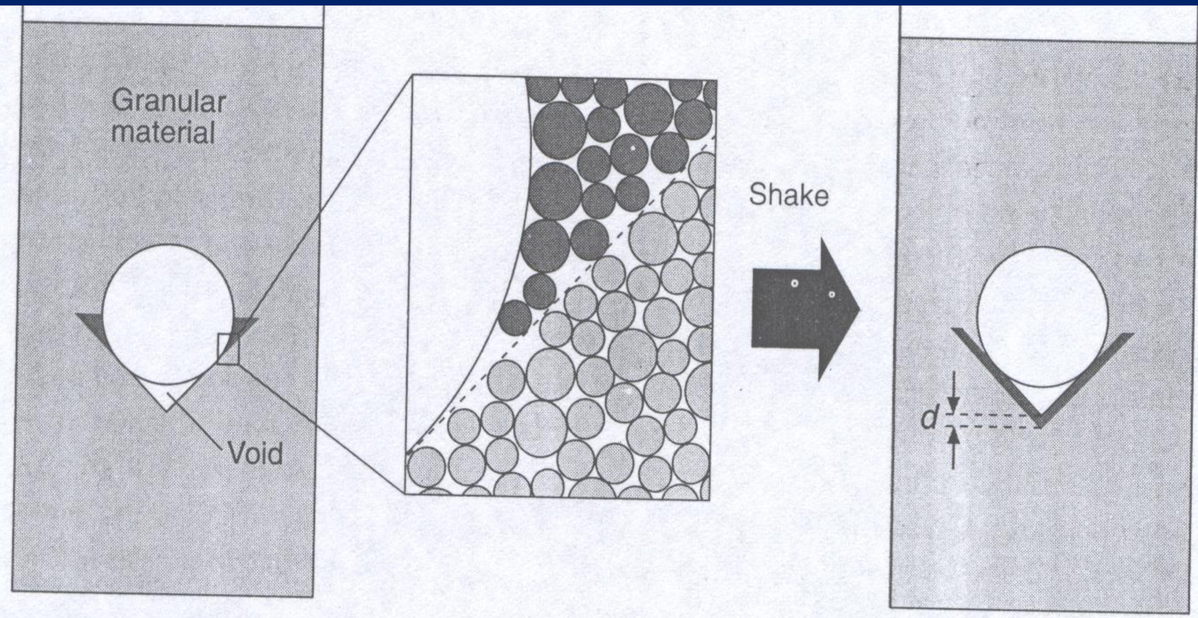

Fig. 8.1 Grains in a bed of granular material separate out according to size when it is shaken vertically, with the larger grains rising to the top. This may be due to a ratchet-like motion in which small grains fall into the space beneath larger grains as they rise during each shake. Each large grain tends to accumulate an empty space (void) below it. When the box is shaken vertically, the large white ball rises from the walls of the void, and the smaller grains in a ring (with a wedge-shaped cross-section) above it can slide down the walls of the void—here I have indicated these grains in dark grey to distinguish them from the other small (*light grey*) grains around them. When the ball settles again, it come to rests on the cone of dark grains, and so has risen a small distance *d*, roughly equal to the thickness of the dark layer. Note that the disparity in sizes is extreme in this picture, for clarity.

Nagel (PRL, 1993): Convection causing large grain from moving back down.

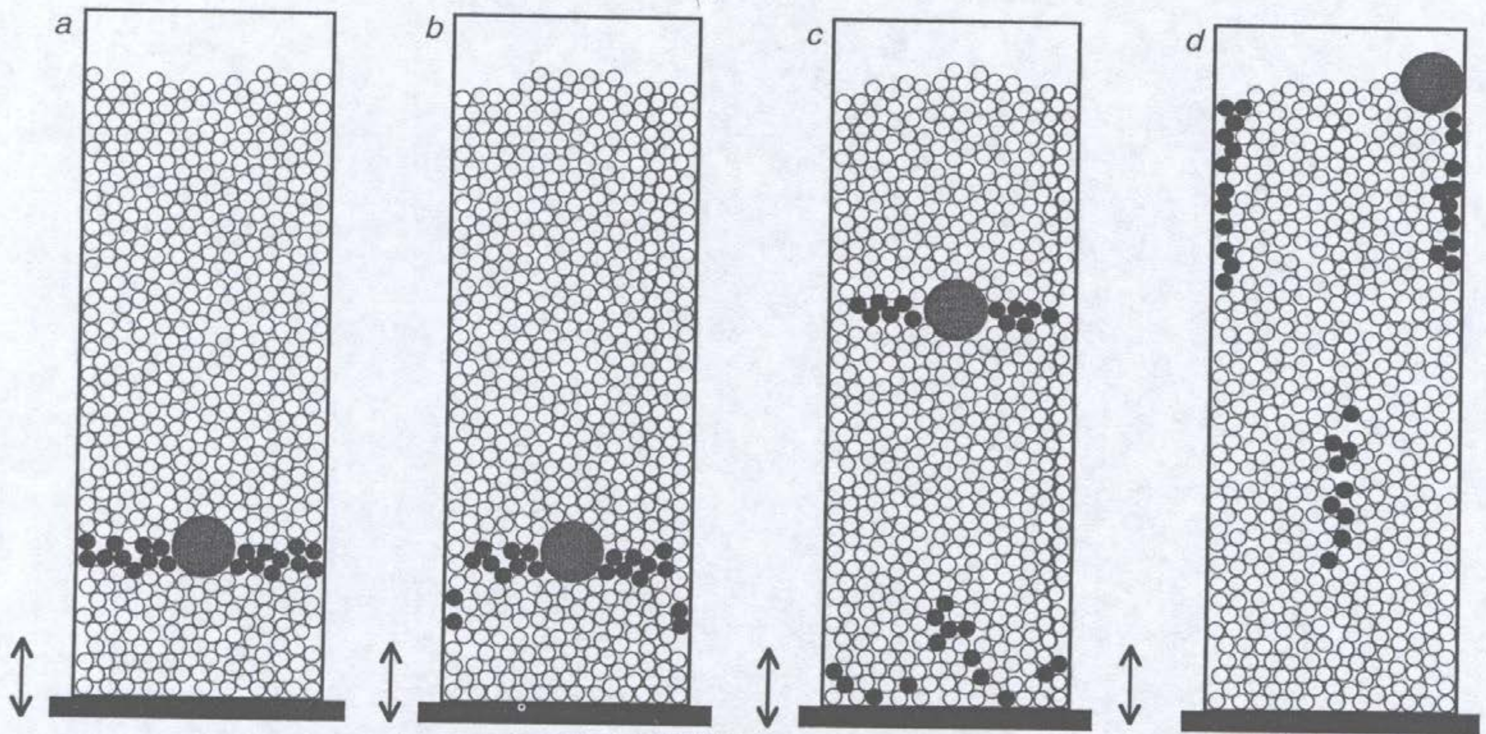

Fig. 8.2 Grains in a tall column undergo convection-like circulating motions: the grains in the centre rise upwards, and those at the edges crawl down to the bottom in a narrow band. The images shown here are reconstructions of an experiment in which some glass beads were dyed to reveal their motions. An initially flat layer near the bottom of the column (*a*) separates into down-going beads at the edges and rising beads at the centre (*b*). The latter move outwards at the top and then downwards at the walls (*d*); the former move upwards at the centre when they reach the bottom (*c*, *d*). A single large bead gets trapped at the top because it is too large to fit in the narrow down-welling band at the edges. So the convective motion causes size segregation. (Images: Sidney Nagel, University of Chicago.)

振动分离

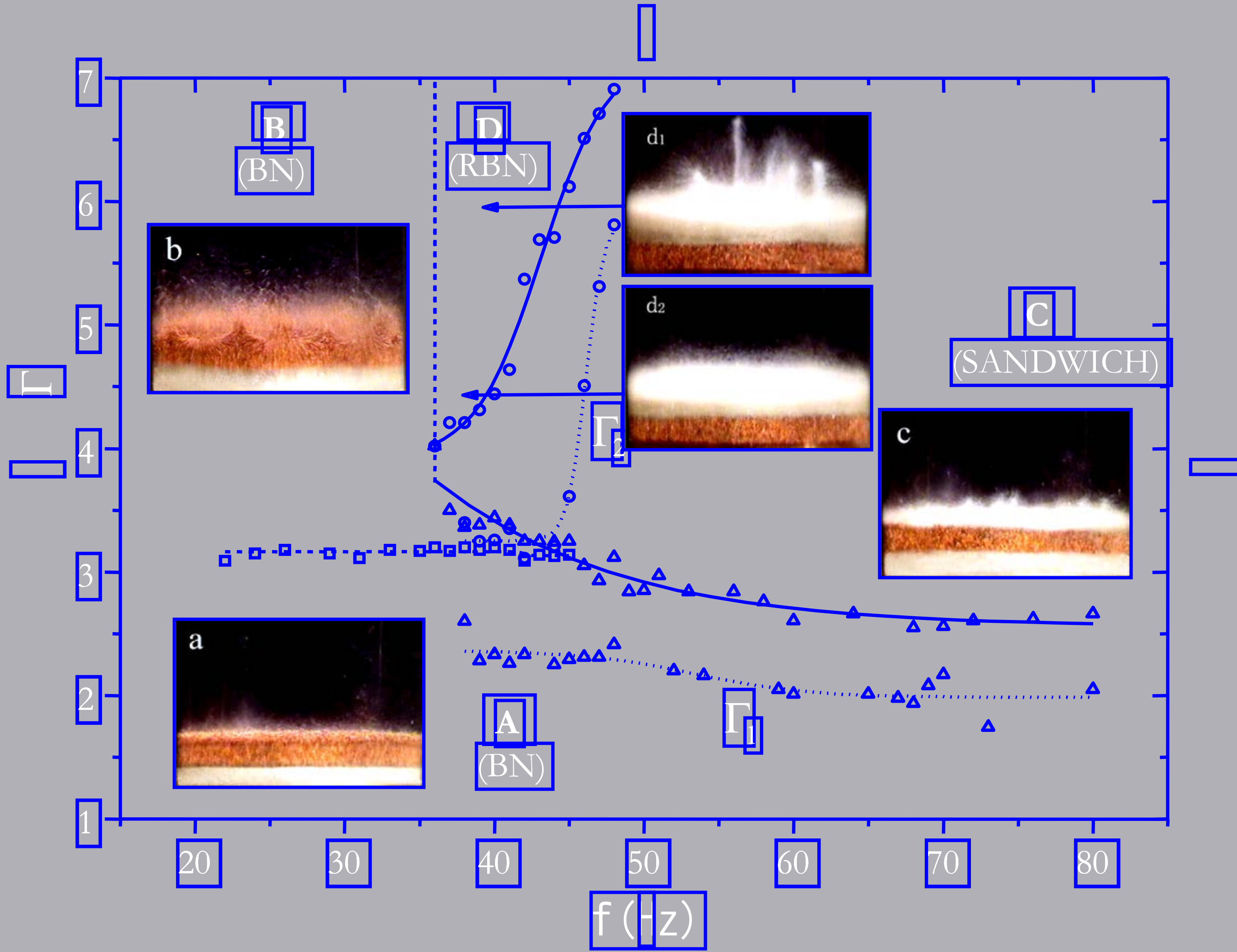
B
(BN)
D
(RBN)
C
(SANDWICH)
A
(BN)
a
b
c
d1
d2
Γ
Γ2
Γ1
1
2
3
4
5
6
7
20
30
40
50
60
70
80
f (Hz)

惯性分层：密度驱动

颗粒流体

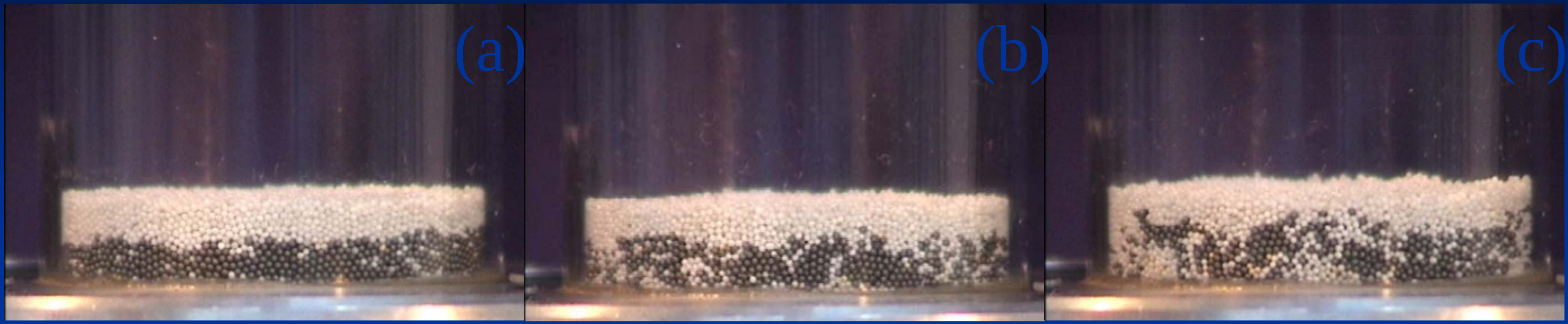

L/H　　　　L/M　　　　L/M

氧化铝 和钴硌钼合金颗粒：密度比 1.31：8.37

Φ = 0.55 mm; Γ = 6; f = 90Hz (a), 70Hz (b), 60Hz (c).

上层厚度随频率增加而增加. $f = f^{*}\sqrt{d/g}$

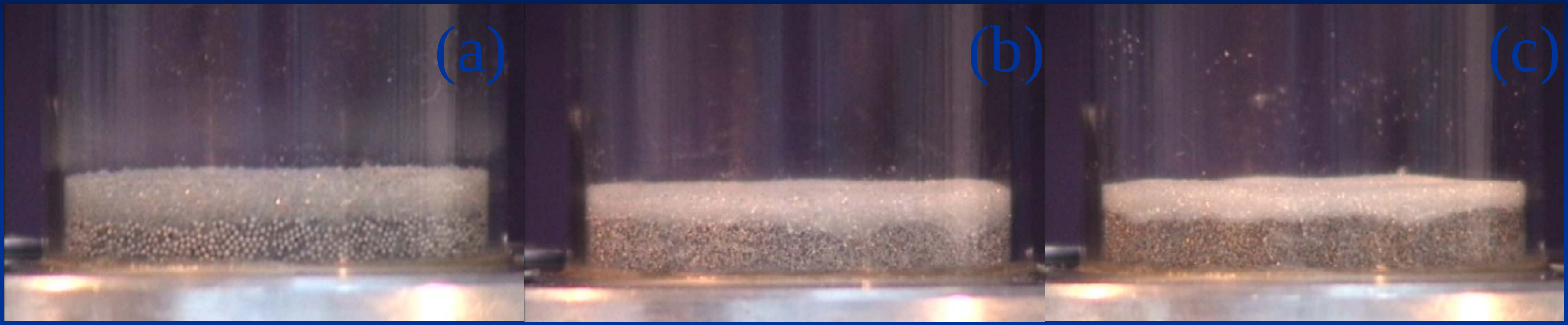

玻璃和钨合金颗粒, 密度比为 2.5 : 18

0.55mm(a),0.25mm(b),0.17mm(c)

Γ = 6, f = 90 Hz

上层厚度随颗粒尺寸增加而增加

颗粒流体
空气效应

rise/sink time of ball

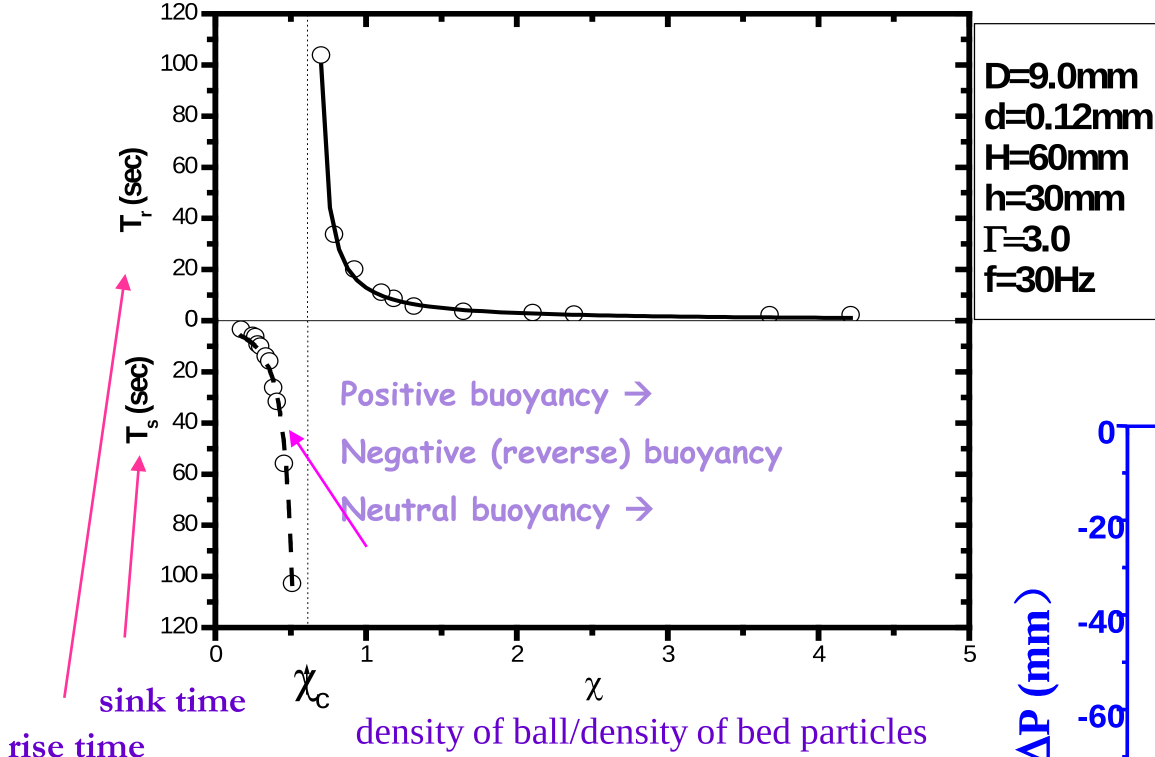

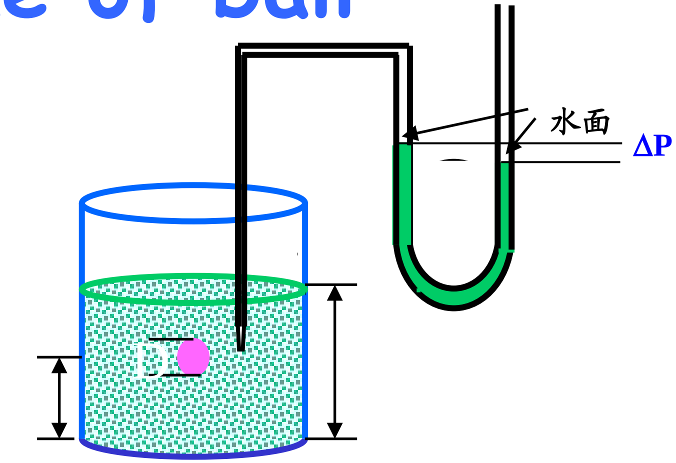

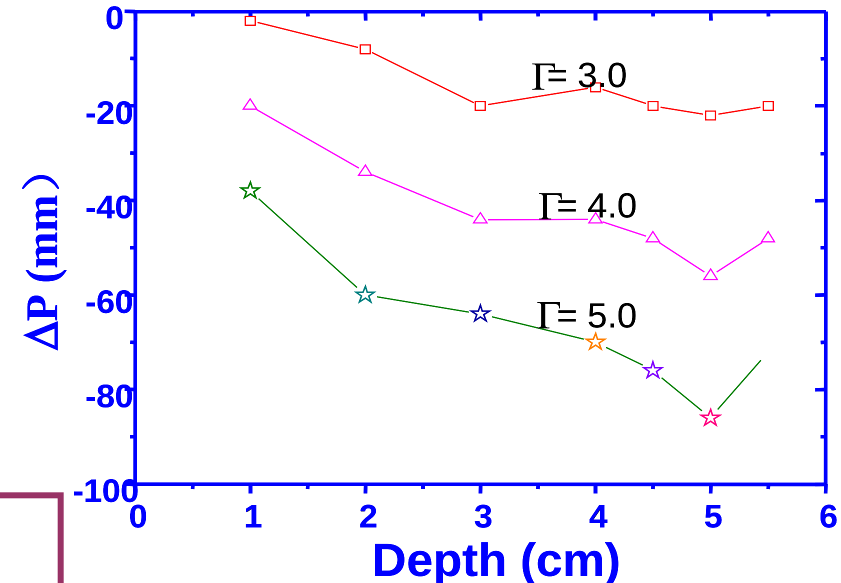

小颗粒床中(d<0.5mm)　气压为负,随Γ增大

X. Yan, Q. Shi, M. Hou, K. Lu and C. K. Chan,　PRL 91 (2003) 14302

Dilute-to-dense transition in 2D granular flow

（二维颗粒流的稀-密转变）

Dilute-to-dense transition in 2D granular flow

颗粒流体

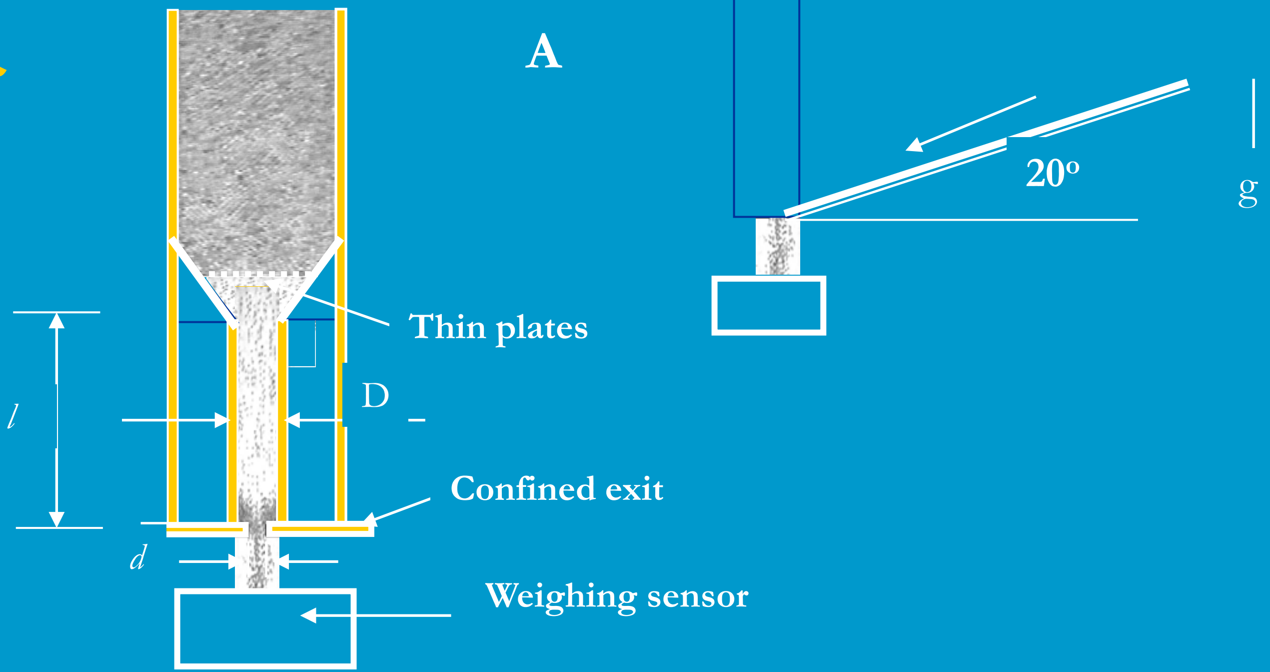

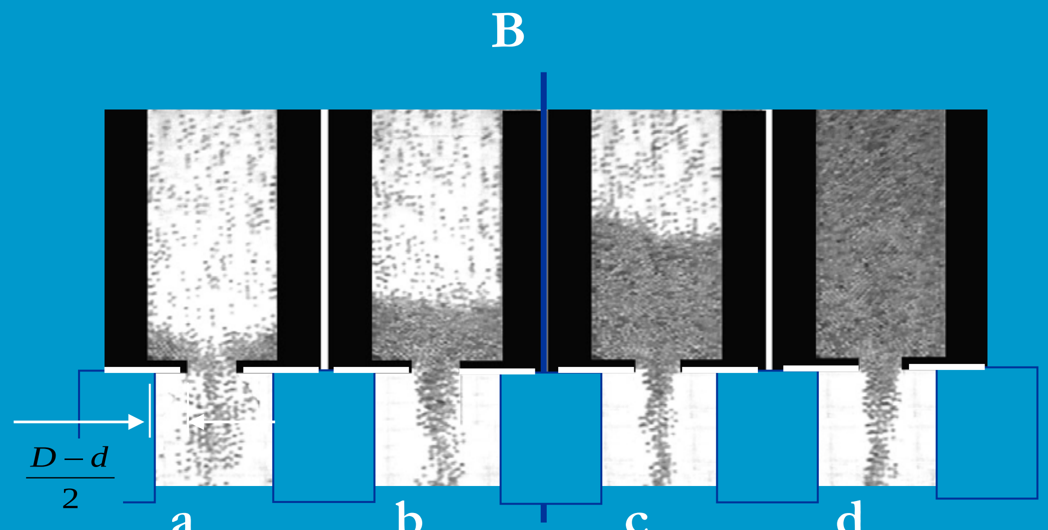

Dilute-to-dense transition in 2D granular flow

Outflow rate vs. opening size

颗粒流体

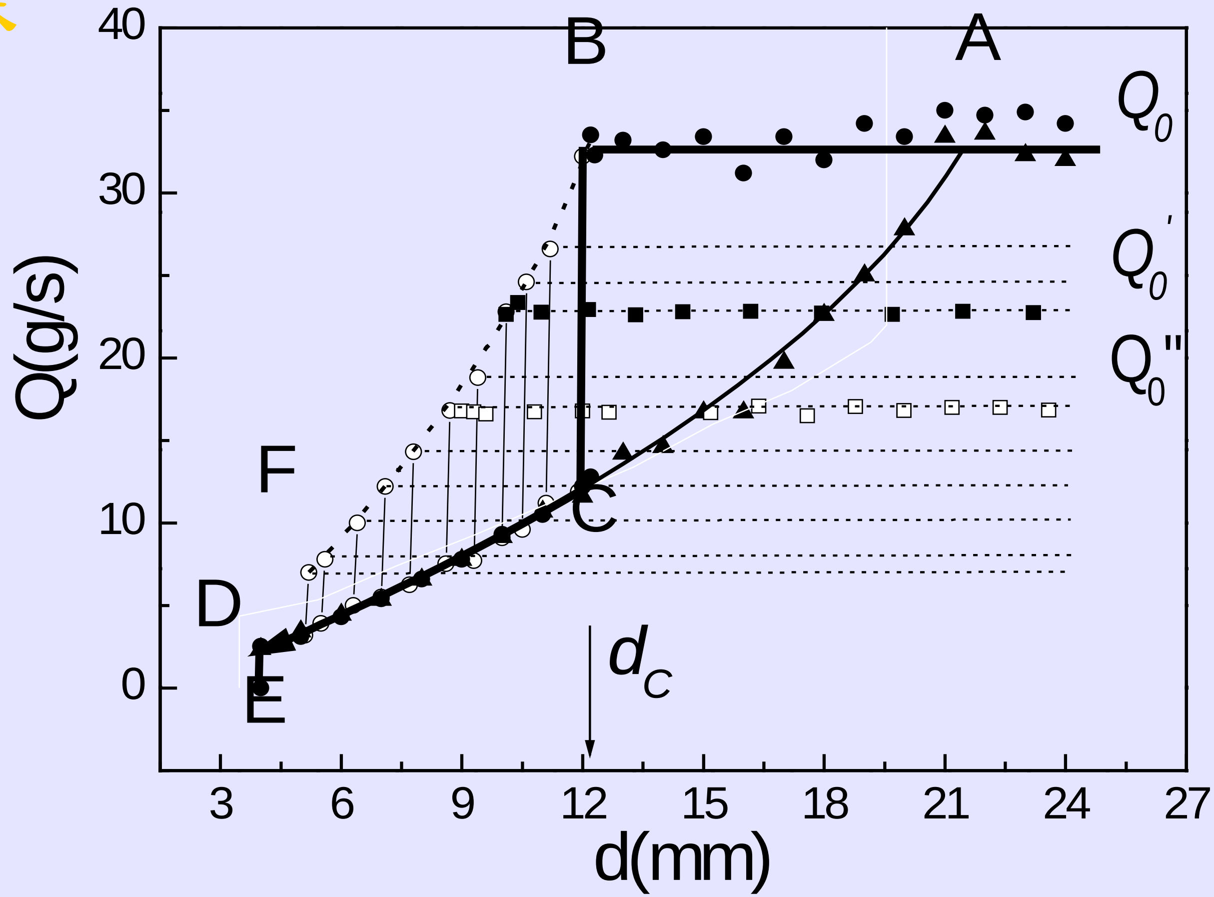

The transition occurs along Curve BF(Q_c, d_c)

Dilute-to-dense transition in 2D granular flow

颗粒流体

$$v_{in}\,\rho_{in}\,((D-d)/2) = v_{out}\,\rho_{out}\,\delta$$

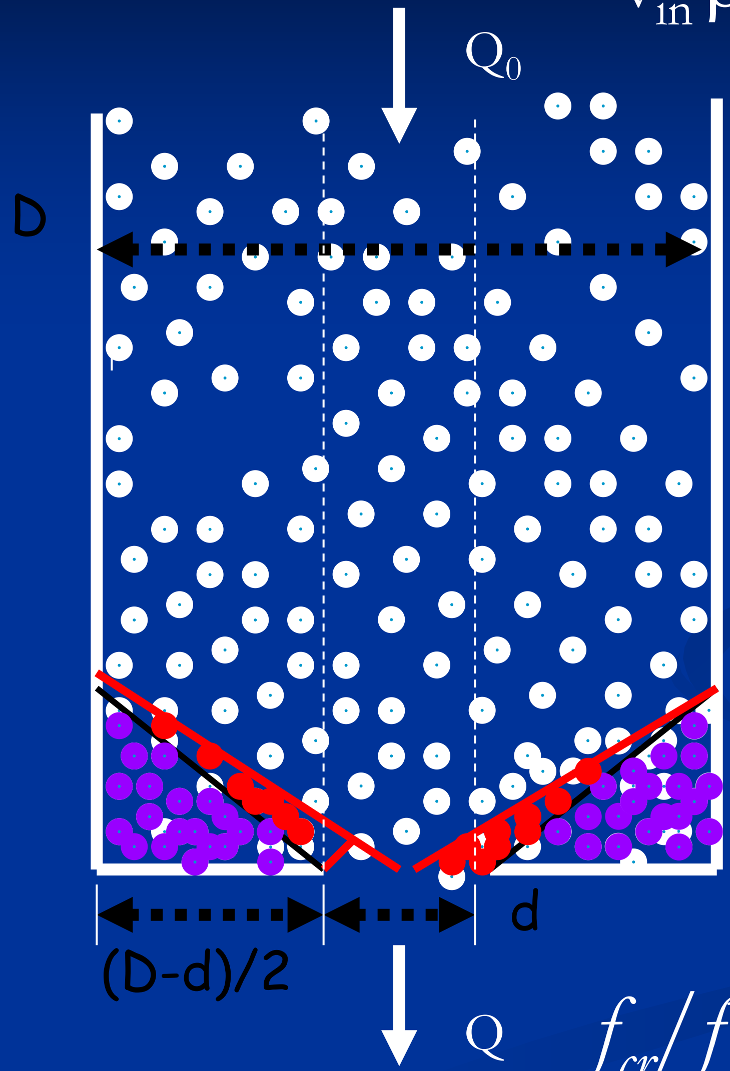

Transition occurs when

$v_{in}\,\rho_{in} = f_{cr}$, and

$$\delta = d/2$$

$$\rho_{out} = \rho_{cr}$$

$$f_{cr}/f^{*} = (d/d_0)*(d/(D - d))$$

Dilute-to-dense transition in 2D granular flow

New scaling variable

$$\lambda = (d/d_0)*(d/(D - d))$$

Dilute-to-dense transition in 2D granular flow **Rescaled flow rate vs. λ**

颗粒流体

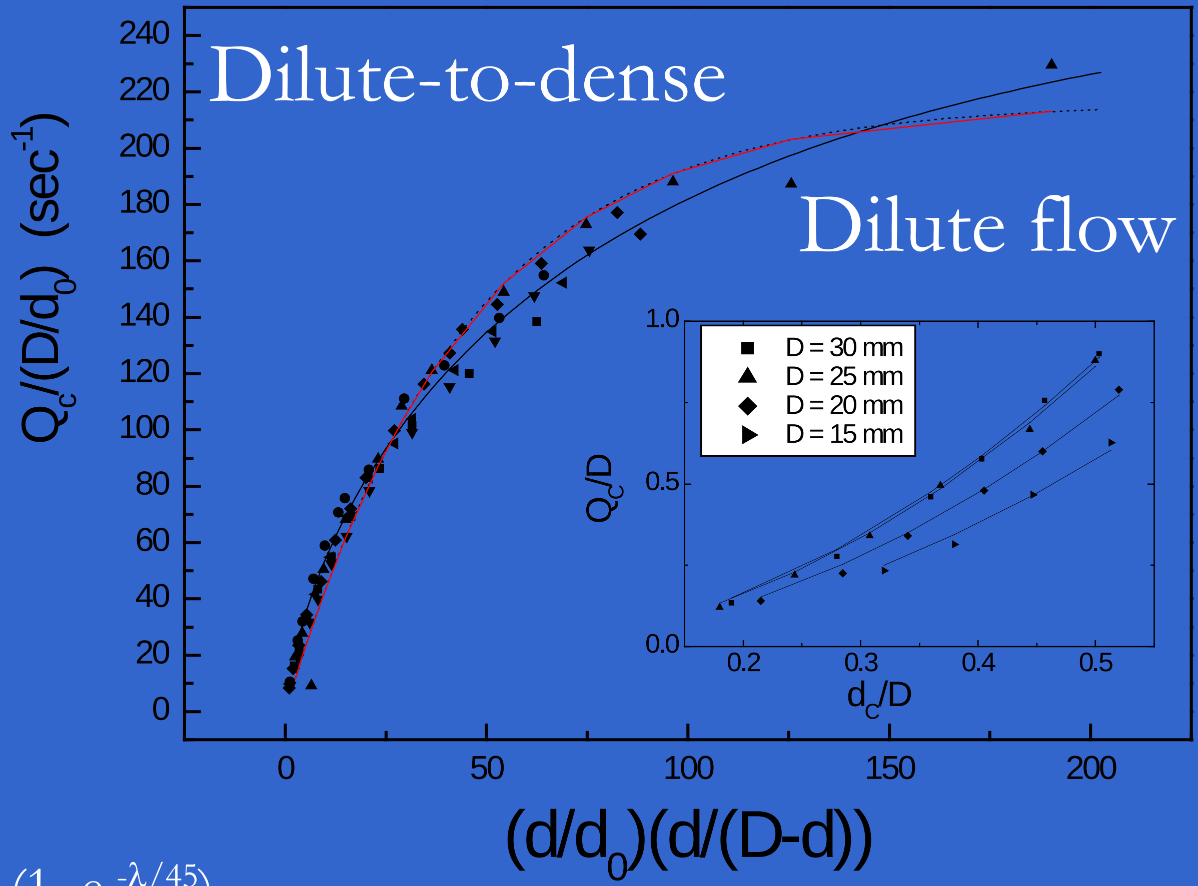

Red _ $q = 216\,(1 - e^{-\lambda/45})$

black _ $q = 270\,(1 - e^{-(\lambda/85)^{0.7}})$

颗粒喷流现象

The drag force:

$\langle F \rangle d = mgH$

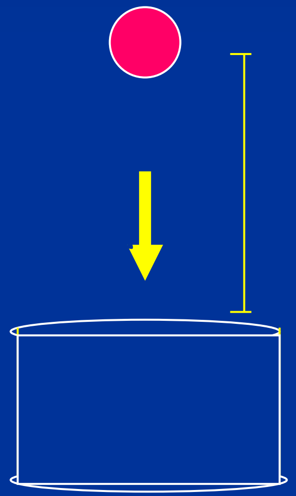

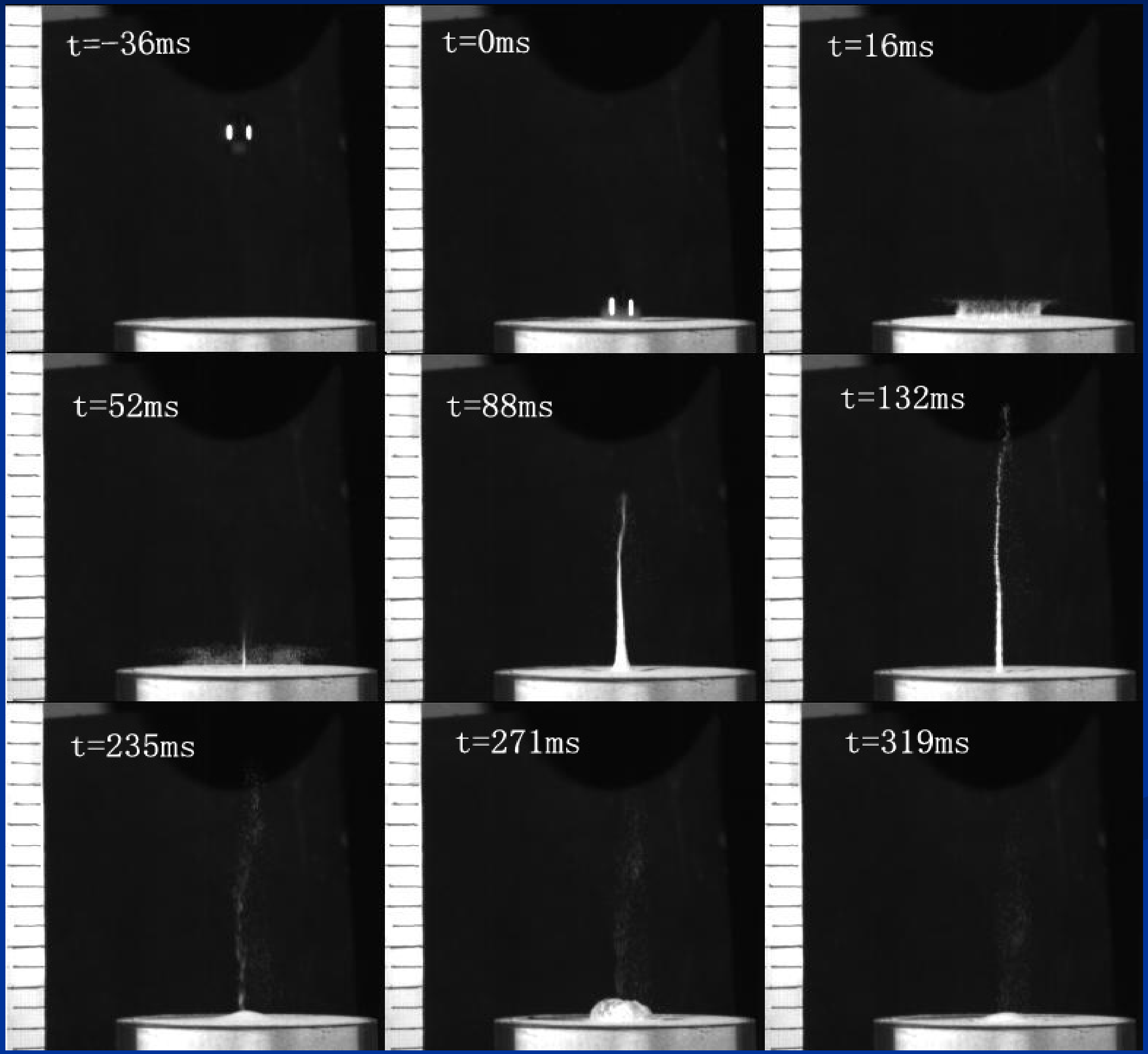

Equation of motion:

$$du/dt=-2u/\tau-z/\tau^2+g$$

The penetration distance z(t) is found to fit

$$z(t)=g\tau^2(1-e^{-t/\tau}) + (u_0-g\tau)te^{-t/\tau},$$

where g is the gravitational acceleration, and $\tau\equiv\alpha/2M$, is a characteristic time depending on α, a coefficient related to the medium "viscosity", and projectile mass M.

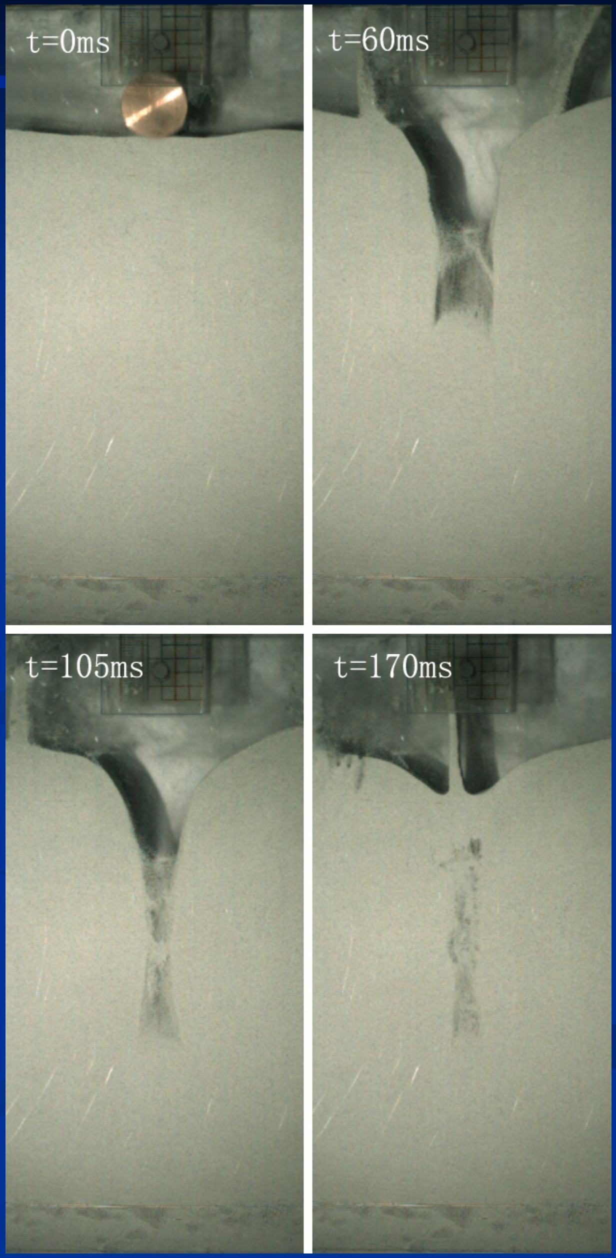

颗粒介质 ⟶ a non-Newtonian fluid

密集态颗粒流的激波结构

颗粒流的激波波前的密度与温度分布结构

激　　波（SHOCK WAVE）

SHOCK WAVE is a thin transitive area propagating with supersonic speed in which there is a sharp increase of density, pressure and speeds of substance.

$M = v/c < 1$

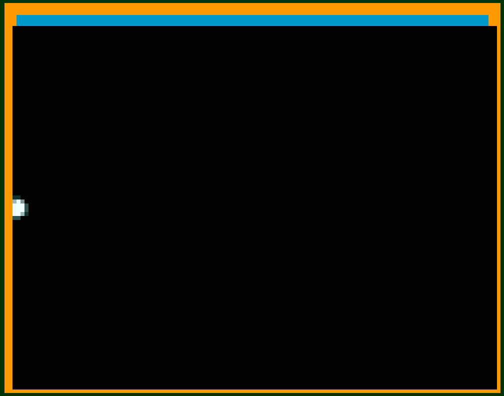

$M = v/c = 1$

$M = v/c > 1$

声 速

- 空气中：

$$c_{\text{air}} = 331.3\text{m}\cdot\text{s}^{-1}\sqrt{1+\frac{\vartheta}{273.15^\circ\text{C}}}$$

- 固体中:

$$c_1 = \sqrt{\frac{K+\frac{4}{3}G}{\rho}} = \sqrt{\frac{E(1-\nu)}{\rho(1+\nu)(1-2\nu)}}$$

$$c_s = \sqrt{\frac{G}{\rho}},$$

for a typical steel alloy,
K = 170 GPa, 压缩模量
G = 80 GPa 剪切模量 and
ϱ = 7700 kg/m3, yielding
a longitudinal velocity c_l of 6000 m/s.
The shear velocity c_s = 3200 m/s

颗粒介质中的声速

（Speed of sound in granular medium）

Kai Huang, Guoqing Miao, Peng Zhang, Yi Yun, and Rongjue Wei, Phys. Rev. E 73, 041302 (2006)

$$c = \sqrt{T\,\chi(1+\chi+\frac{\nu}{\chi}\frac{\partial\chi}{\partial\nu})}$$

$$\chi = 1 + 2(1 + e\nu[1 - (\nu/\nu_{\max})^{4\nu_{\max}/3}]^{-1})$$

$$T \equiv \langle \delta v^2 \rangle = \langle (v - \langle v \rangle)^2 \rangle$$

$$c \approx 0.20 m/s$$

激波在颗粒流经常可见

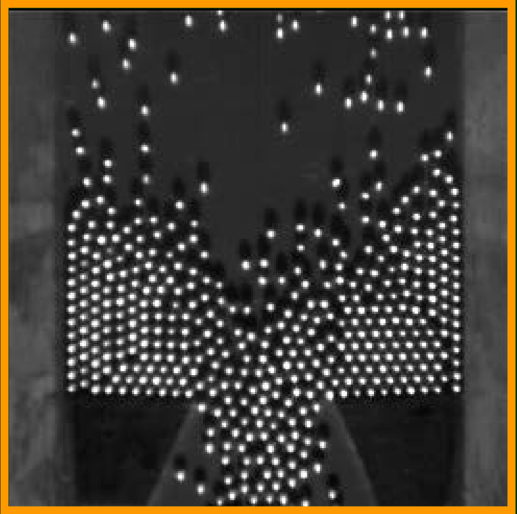

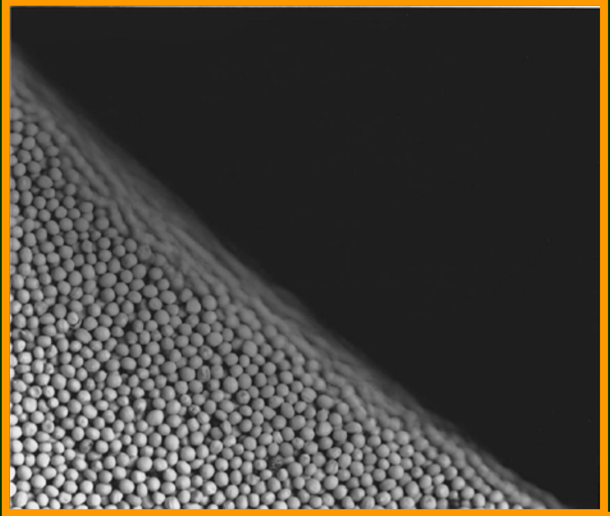

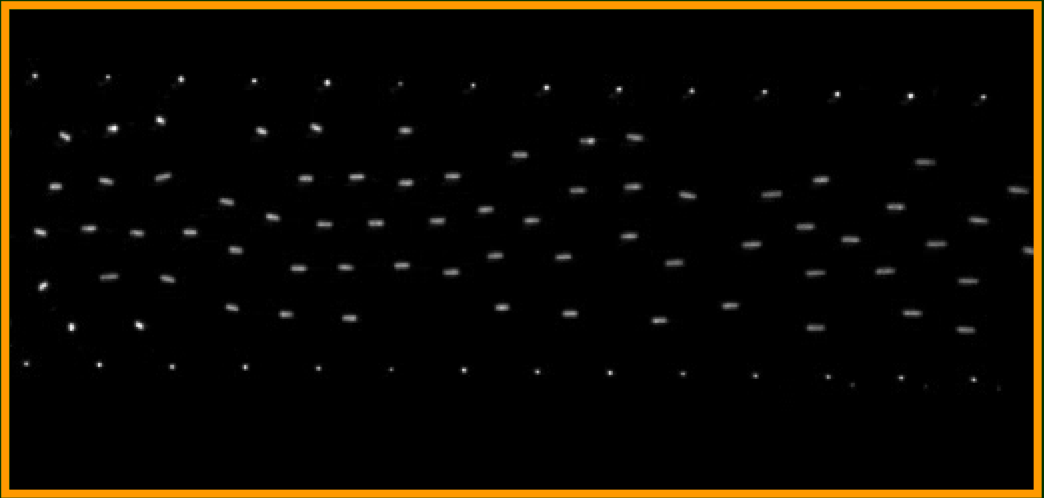

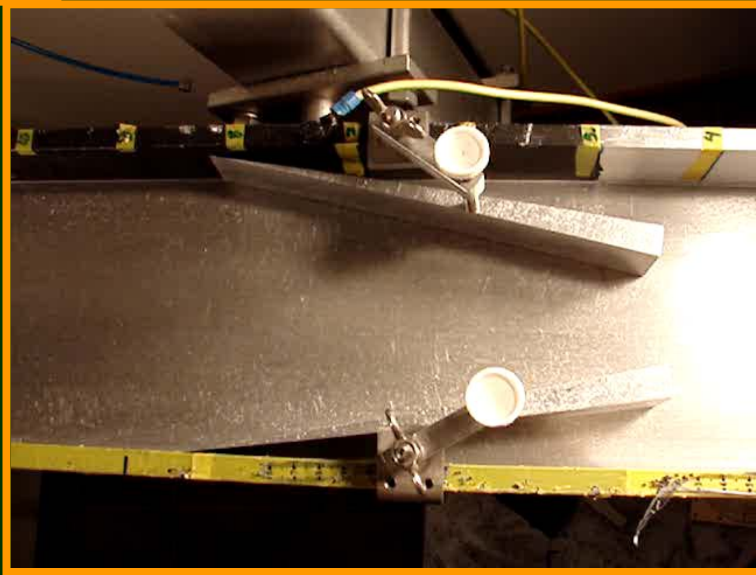

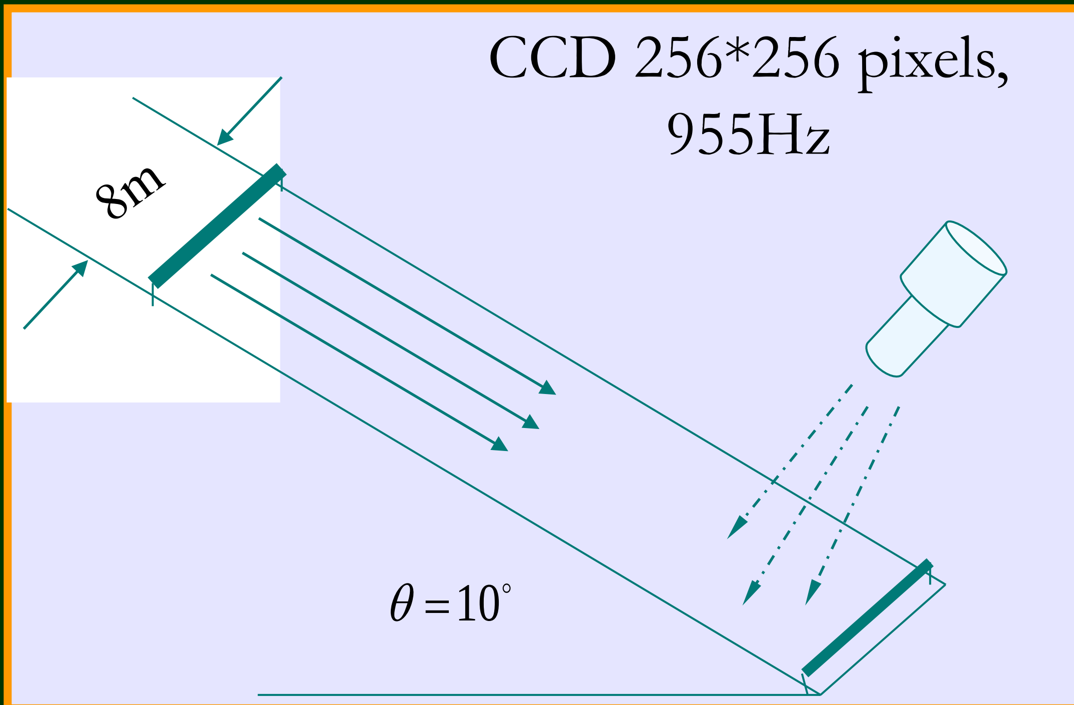
CCD 256*256 pixels,
955Hz
8m
θ =10°

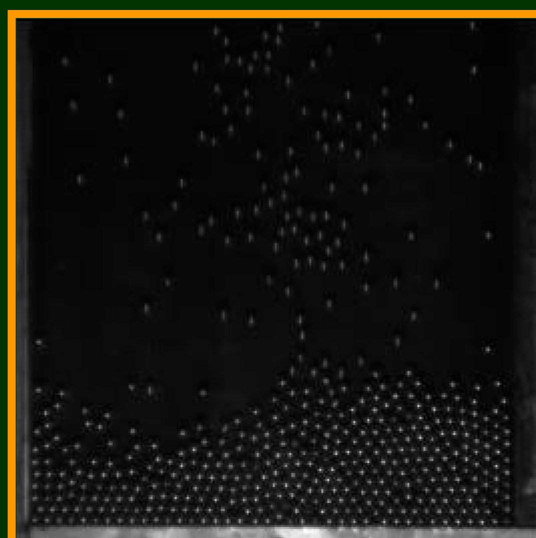

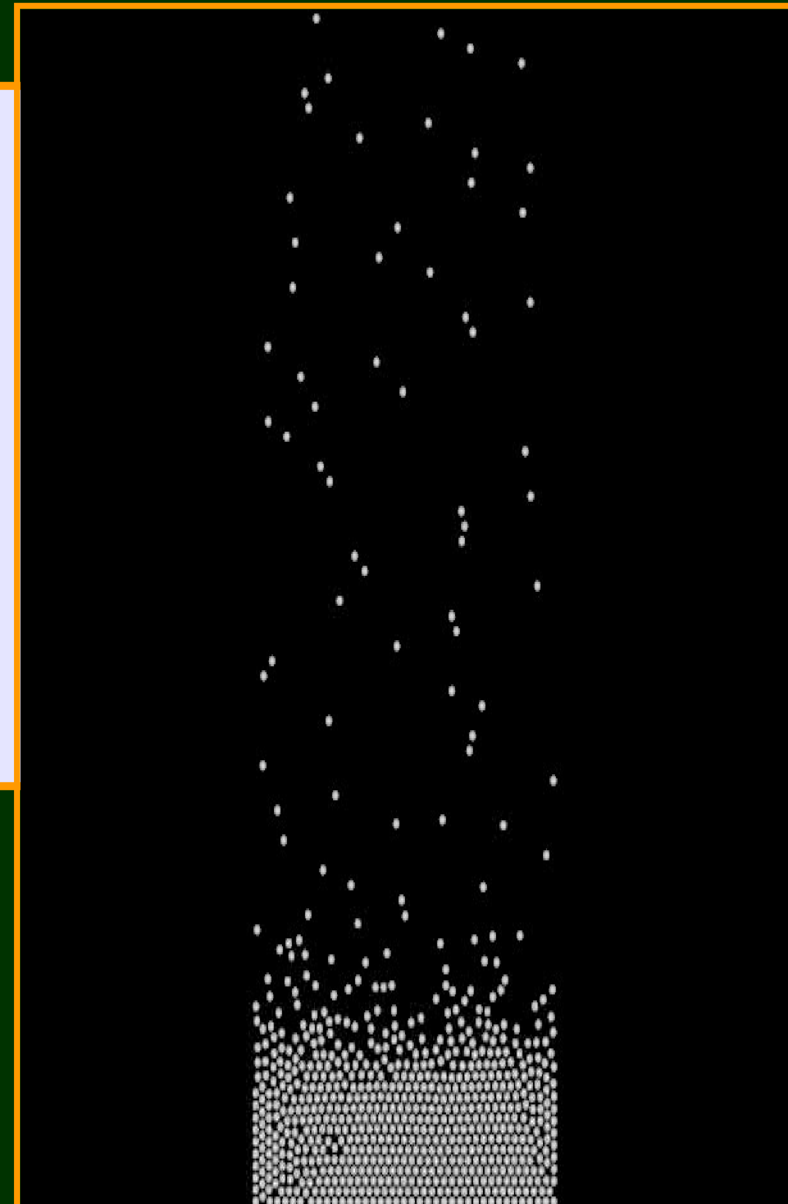

波前密度形貌

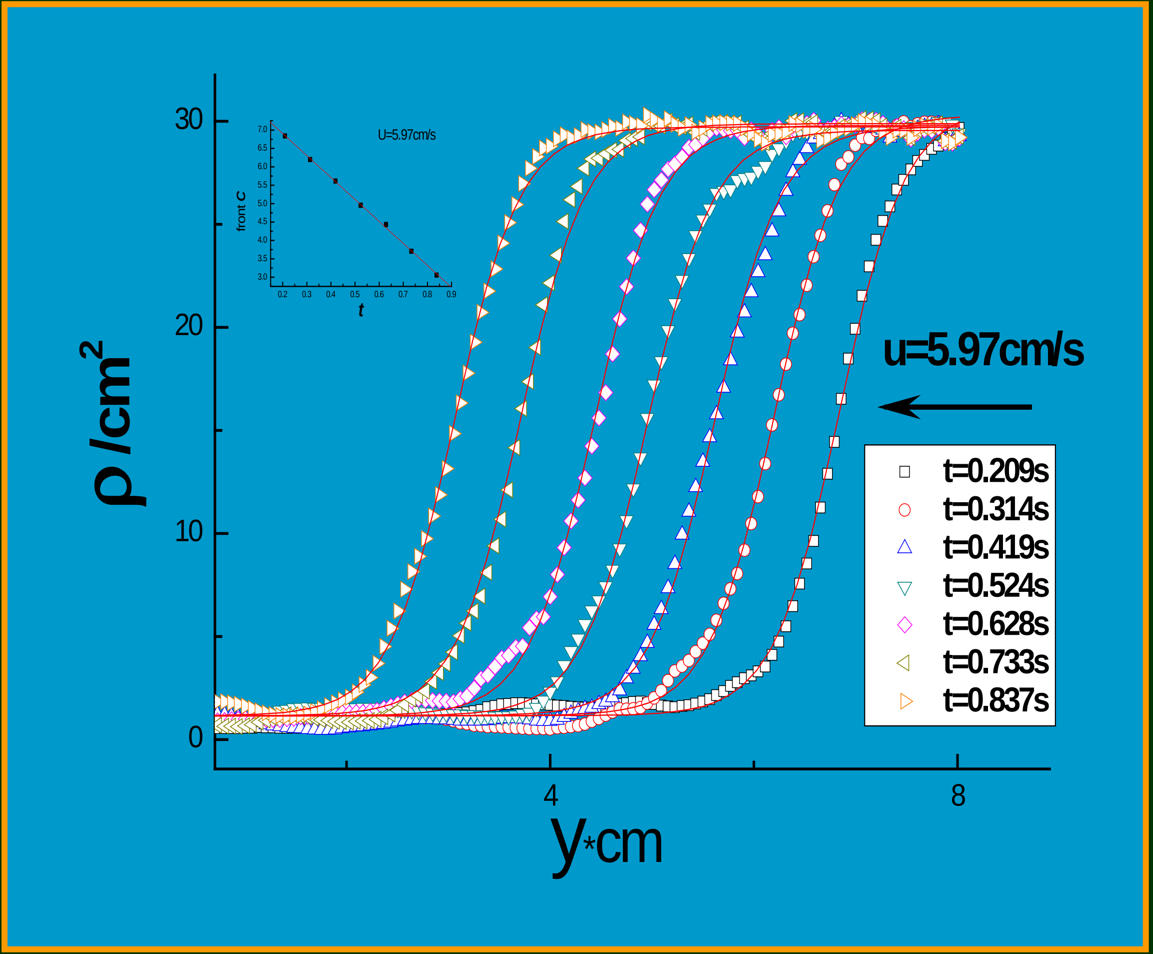

U=5.97cm/s
front c
t
u=5.97cm/s
t=0.209s
t=0.314s
t=0.419s
t=0.524s
t=0.628s
t=0.733s
t=0.837s
ρ /cm²
y*cm

波前密度形貌可用可压缩流体的密度函数拟合

Phys. Of Fluids 11, 2757, 1999

The density profile of the granular shock front can be fitted to a generic density profile used in compressible fluids:

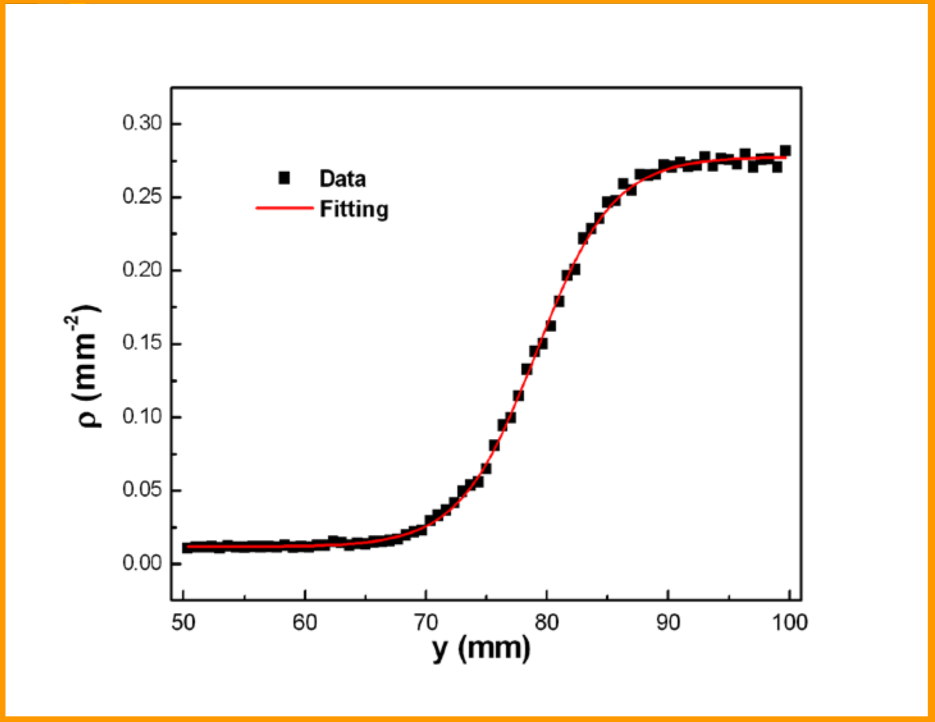

$$n(y',t)=\frac{n_0 e^{-(y'-ut)/\lambda}+n_d}{e^{-(y'-ut)/\lambda}+1}$$

$$y = y' - ut$$

$$n(y)=\frac{n_0 e^{-y/\lambda}+n_d}{e^{-y/\lambda}+1}$$

速度1.2m/s下不同初始流量的颗粒流在堆积时，作用区的密度分布

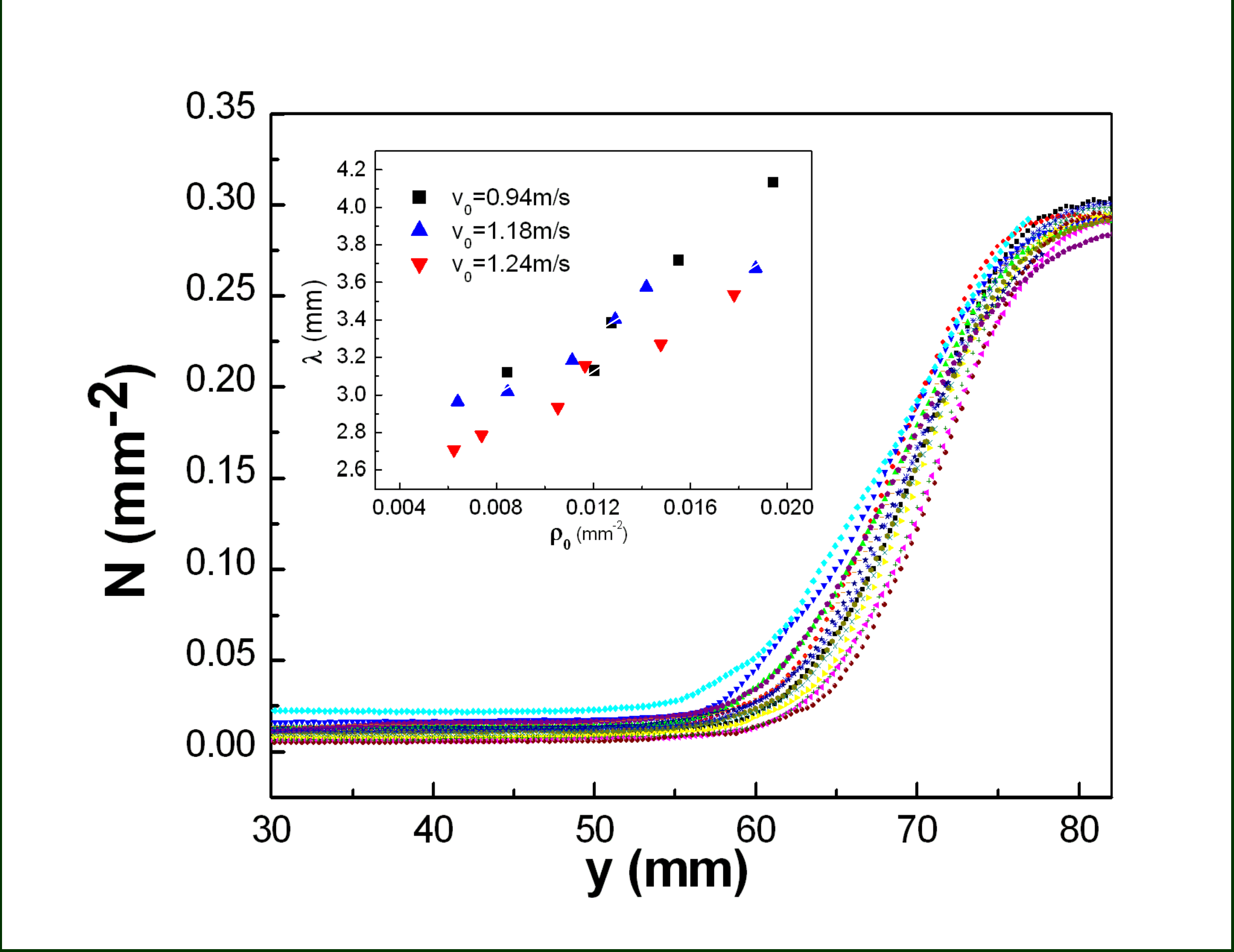

两类颗粒：流动颗粒+热运动颗粒

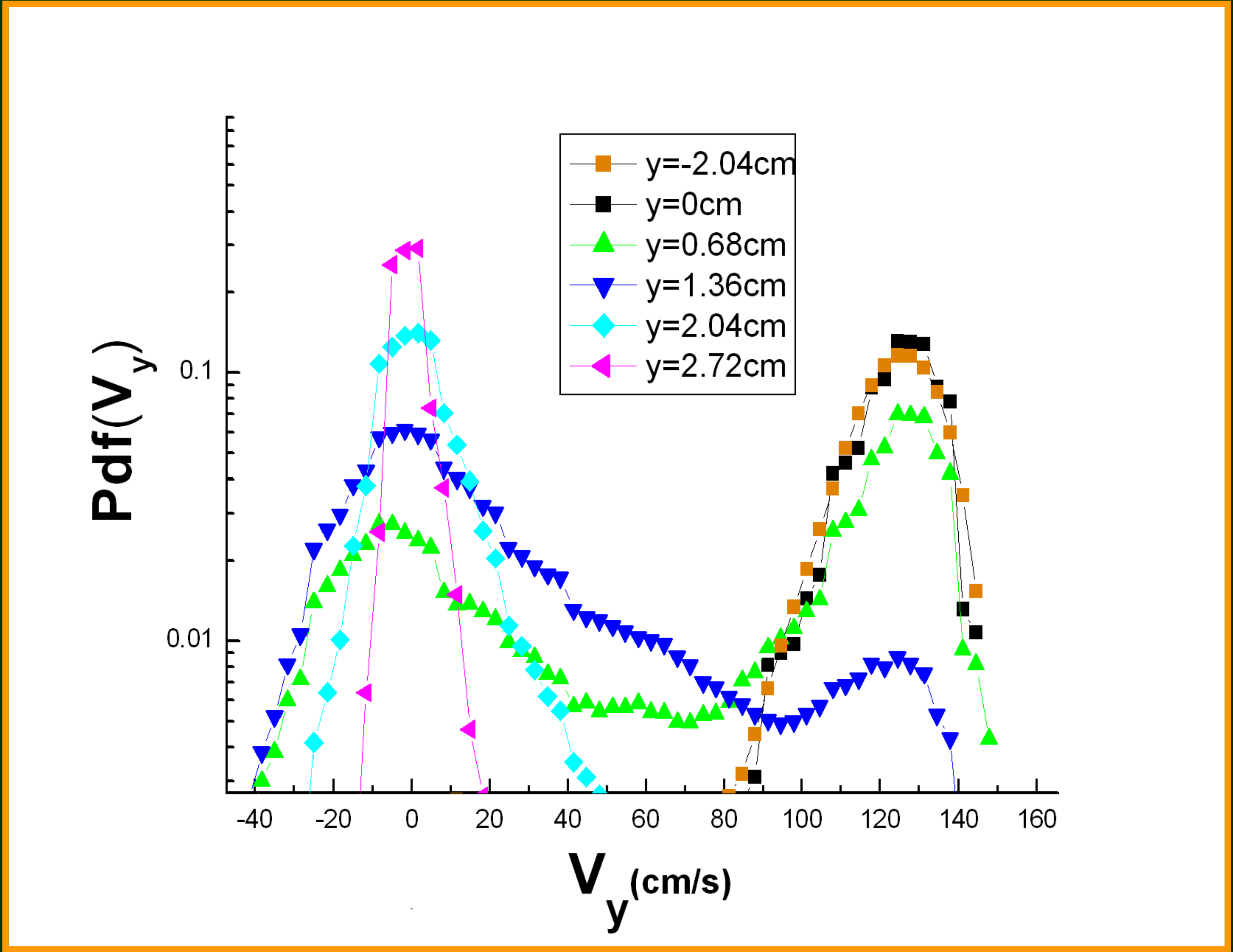

速度分布：由流动到熱涨落

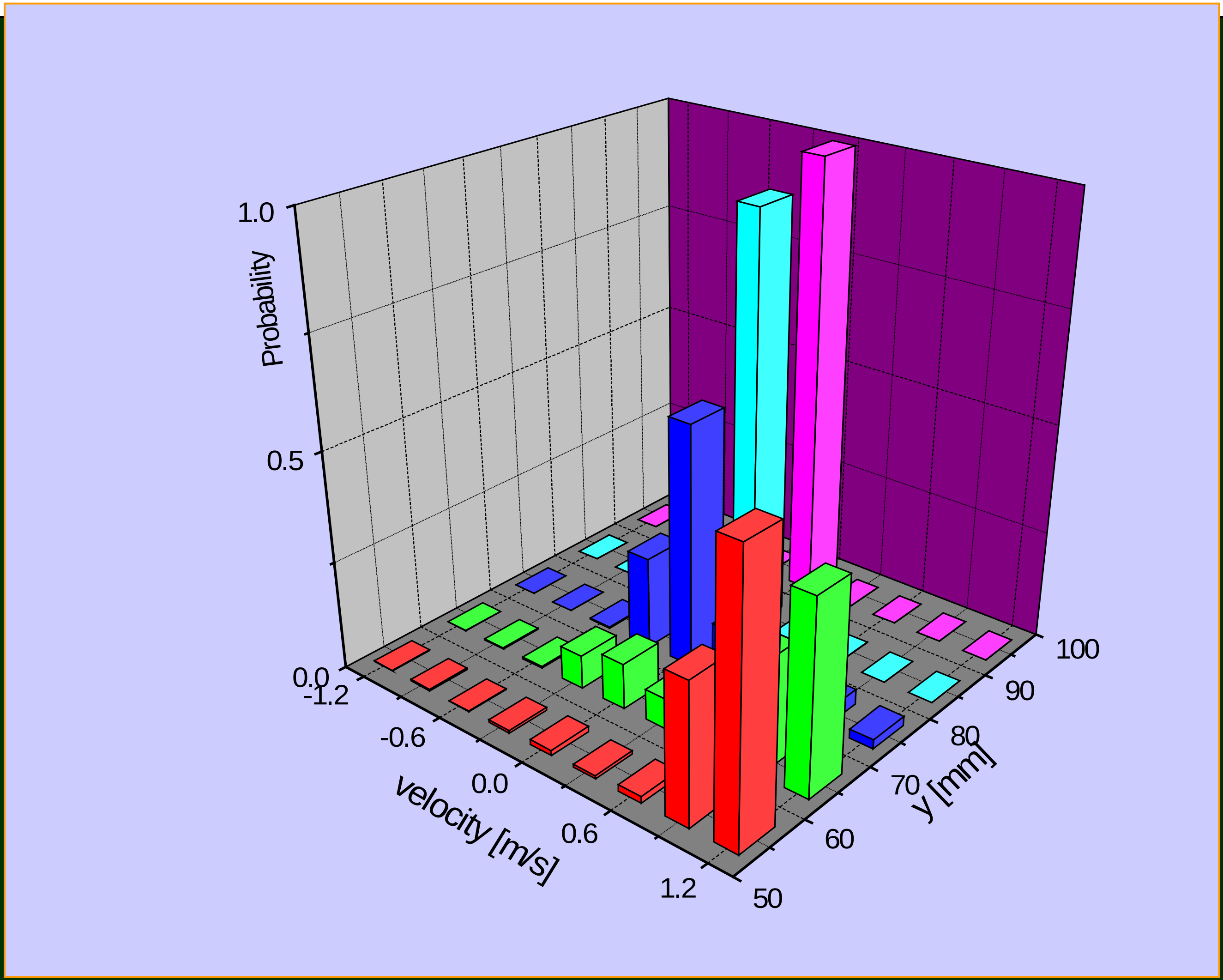

第一类颗粒的含量f

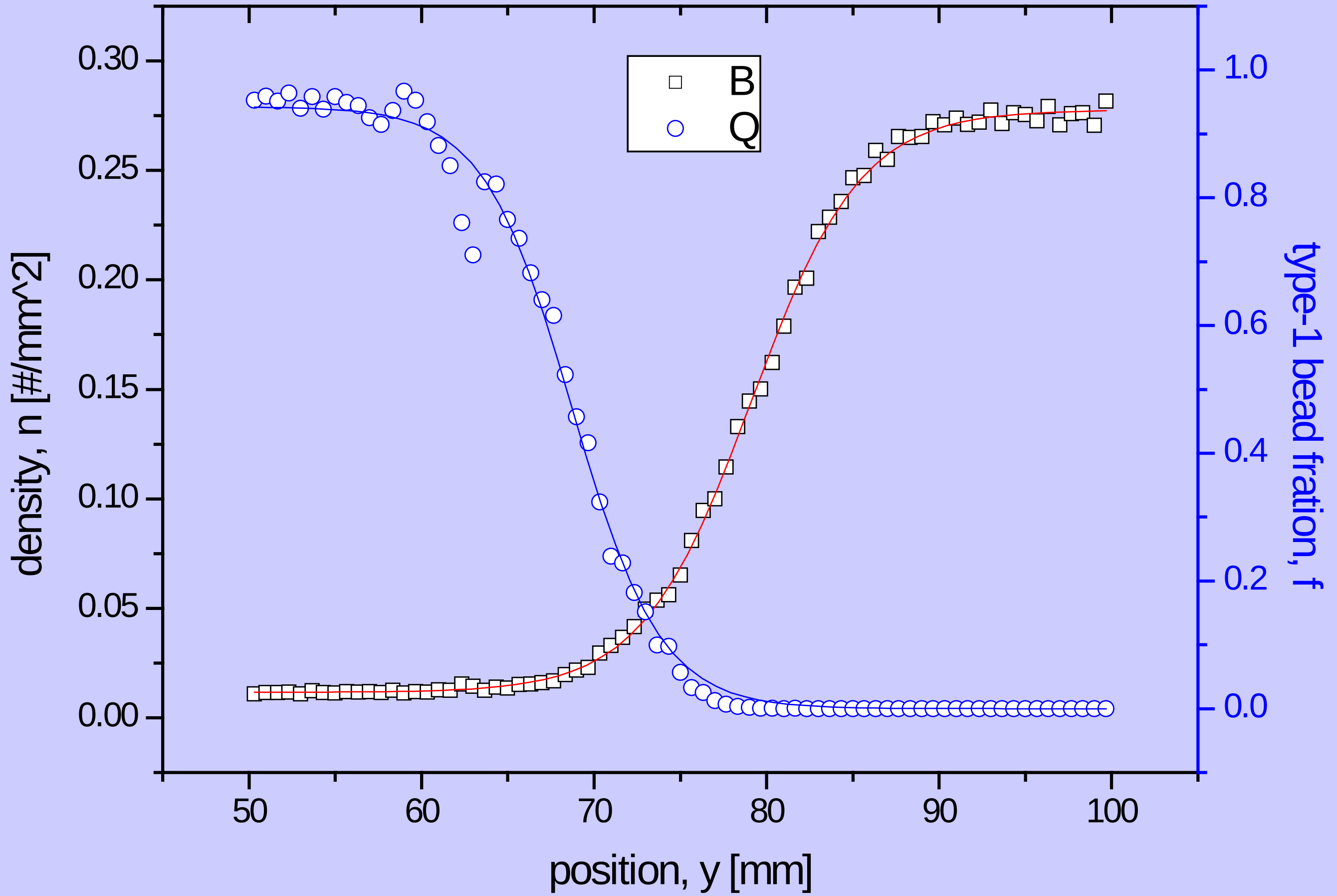

B
Q
0.30
0.25
0.20
0.15
0.10
0.05
0.00
density, n [#/mm^2]
1.0
0.8
0.6
0.4
0.2
0.0
type-1 bead fration, f
50
60
70
80
90
100
position, y [mm]

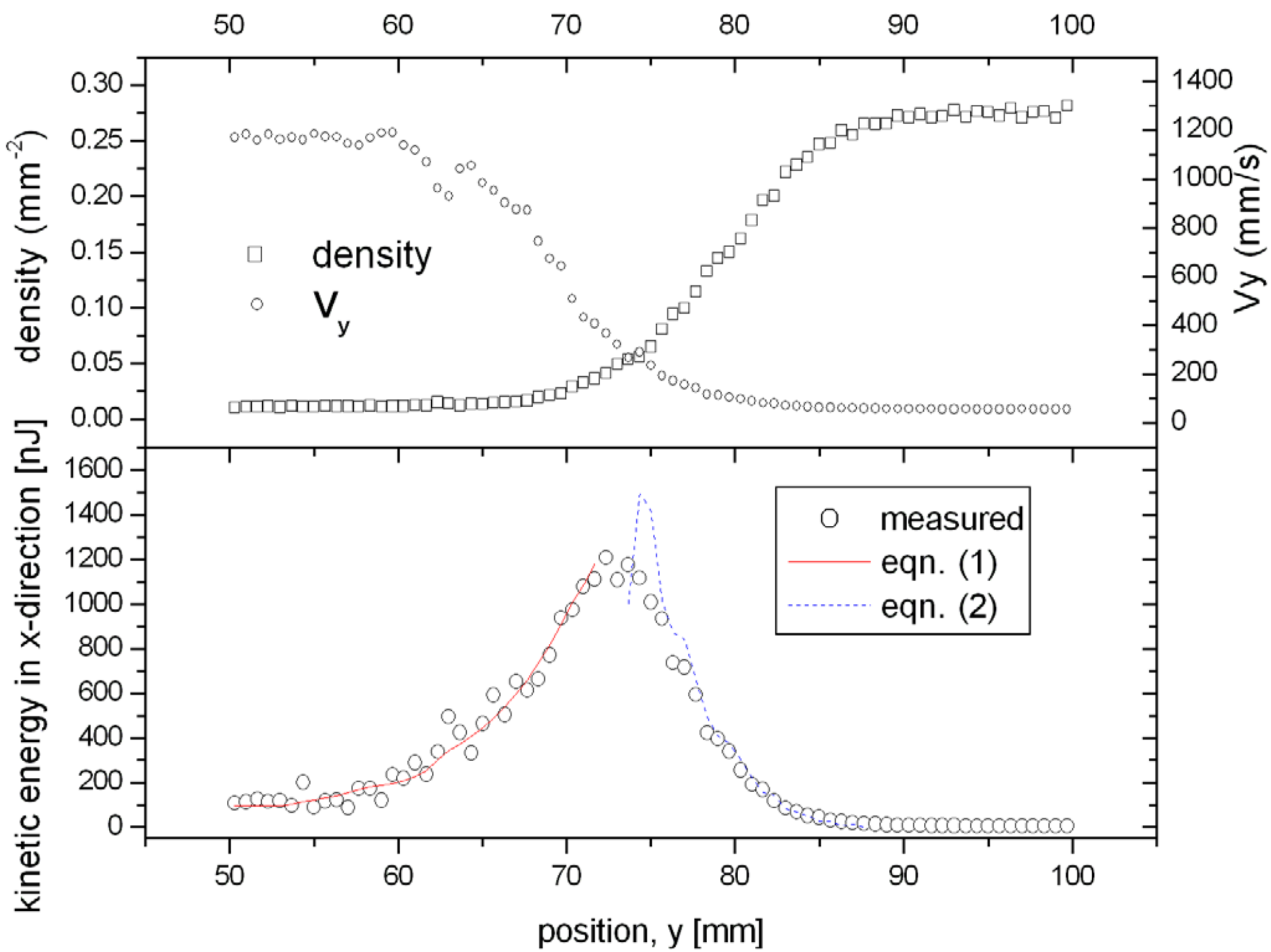

50 60 70 80 90 100
0.30 0.25 0.20 0.15 0.10 0.05 0.00
density (mm^{-2})
1400 1200 1000 800 600 400 200 0
Vy (mm/s)
density
V_y
1600 1400 1200 1000 800 600 400 200 0
kinetic energy in x-direction [nJ]
measured
eqn. (1)
eqn. (2)
50 60 70 80 90 100
position, y [mm]

热能分布

$$\frac{dE_x}{dy} = \frac{\alpha}{u} E_y n_1 n_2$$

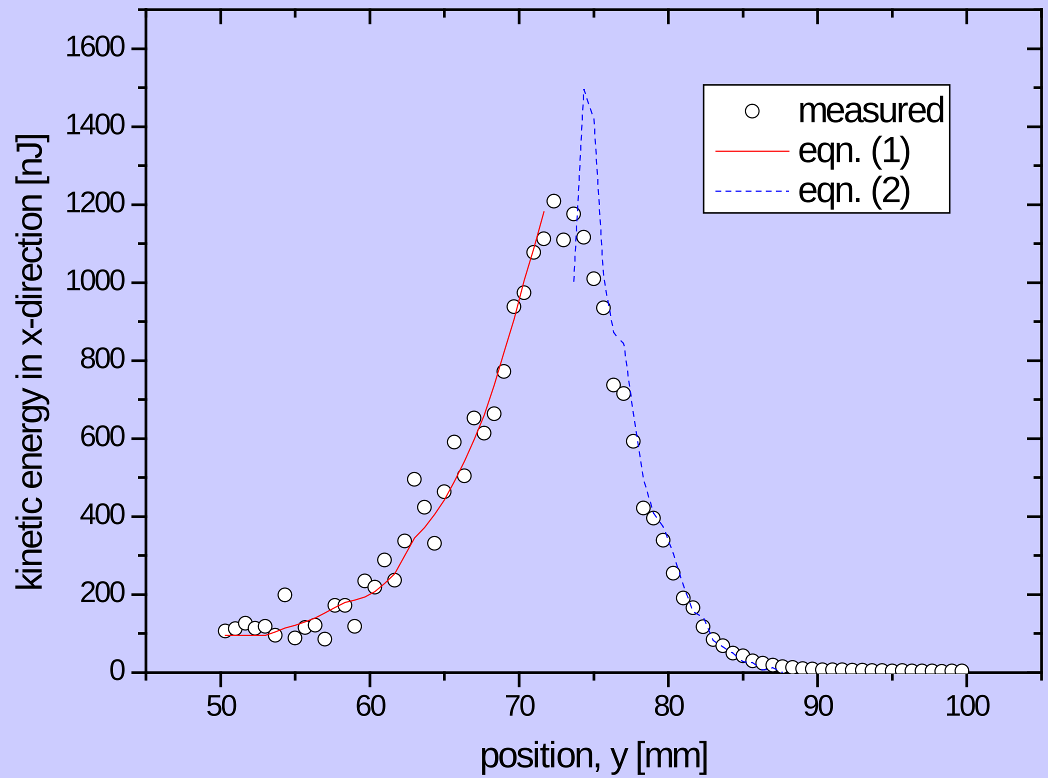

equation(1):

$$E_x = \int_{y_0}^{y} dy \frac{\alpha}{u} E_y n_1 n_2 + E_x(y_0)$$

equation(2):

$$E_x = \frac{(n_1 T_{1x} + n_2 T_2/2)}{(n_1 + n_2)}$$

$$P_2 + n_2 v_2^2 + n_1 v_1^2 = C$$

$$E_x = \frac{(n_1 E_{1x} - n_2 E_{2x})}{(n_1 + n_2)}$$

小 结

- 颗粒流的激波波前密度分布形貌与连续介质相似，但温度的形貌分布与连续介质不同。
- 波前的温度分布可以动力学模型拟合

颗粒经典非平衡系统
涨落耗散关系

布朗运动

- Albert Einstein noted in his 1905 paper on Brownian motion that the same random forces that cause the erratic motion of a particle in Brownian motion would also cause drag if the particle were pulled through the fluid. In other words, the fluctuation of the particle at rest has the same origin as the dissipative frictional force one must do work against, if one tries to perturb the system in a particular direction.
- Einstein-Smoluchowski relation: $D = \mu k_B T$
- linking D, the diffusion constant, and μ, the mobility of the particles. (μ is the ratio of the particle's terminal drift velocity to an applied force, $\mu = v_d / F$). $k_B \approx 1.38065 \times 10^{-23}$ m^2 kg s^{-2} K^{-1} is the Boltzmann constant, and T is the absolute temperature.

Stochastic processes

The Langevin equation

粒子悬浮在流体中，受到正比于速度的一个阻力和一个随 $\vec{F}(t)$

$$\frac{d\vec{r}}{dt} = \vec{v}$$

$$\frac{d\vec{v}}{dt} = -\xi\vec{v} + \vec{F}$$

摩擦系数为 ξ $\quad \xi = 6\pi\eta a/m$

上式的解为 $\vec{v}(t) = \vec{v_0}e^{-\xi t} + \int_0^t d\tau e^{-\xi(t-\tau)}\vec{F}(\tau)$

$$<\vec{v}(t)\cdot\vec{v}(t)>_{\vec{v_0}} = v_0^2 e^{-2\xi t} + 2\int_0^t d\tau e^{-\xi(2t-\tau)}\vec{v_0}\cdot<\vec{F}(\tau)>_{\vec{v_0}}$$
$$+\int_0^t d\tau' \int_0^t d\tau e^{-\xi(2t-\tau-\tau')} <\vec{F}(\tau)\cdot\vec{F}(\tau')>_{\vec{v_0}}$$

$$<\vec{F}(t)>=0$$
$$<\vec{F}(t)\cdot\vec{F}(t')>_{\vec{v_0}} = C_{\vec{v_0}}\delta(t-t')$$

$$<\vec{v}(t)\cdot\vec{v}(t)>_{\vec{v}_0}=v_0^2 e^{-2\xi t}+\frac{C_{\vec{v}_0}}{2\xi}(1-e^{-2\xi t})$$

For large t, 式左边等于 $3kT/m$

The fluctuation-dissipation theorem $<\vec{F}(t)\cdot\vec{F}(t')>=6\frac{kT}{m}\xi\delta(t-t')$

then we get

$$\vec{r}(t)=\vec{r}_0+\vec{v}_0\frac{1}{\xi}(1-e^{-\xi t})+\int_0^t d\tau\int_0^\tau d\tau' e^{-\xi(t-\tau)}\vec{F}(\tau')$$

from which we calculate the mean square displacement

$$\left\langle\left(\vec{r}(t)-\vec{r}_0\right)^2\right\rangle_{\vec{v}_0}=\frac{v_0^2}{\xi^2}(1-e^{-\xi t})^2+\frac{3kT}{m\xi^2}(2\xi t-3+4e^{-\xi t}-e^{-2\xi t})$$

for very large t this becomes

$$\left\langle\left(\vec{r}(t)-\vec{r}_0\right)^2\right\rangle=\frac{6kT}{m\xi}t$$

from which we get the Einstein relatio $D=\frac{kT}{m\xi}$

where we have used $\left\langle\left(\vec{r}(t)-\vec{r}_0\right)^2\right\rangle=6Dt$

胶体中的自推进现象

➢ 颗粒中的”自推进”现象

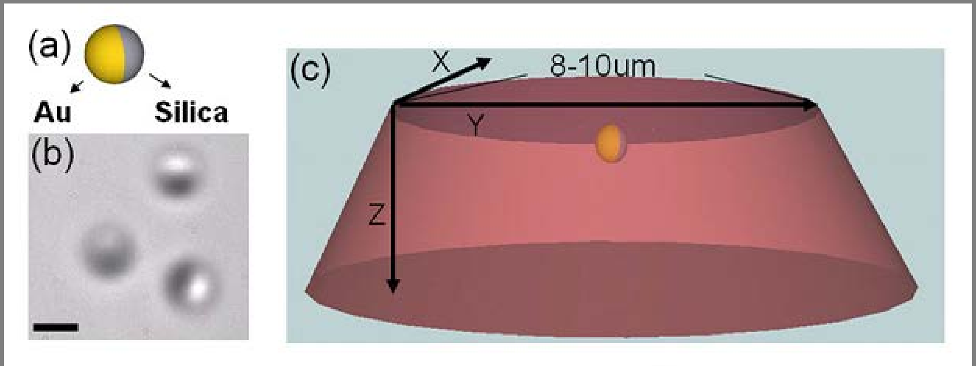

Hong-Ren Jiang *et. al.*
PRL 105, 268302(2010)

Janus Particles

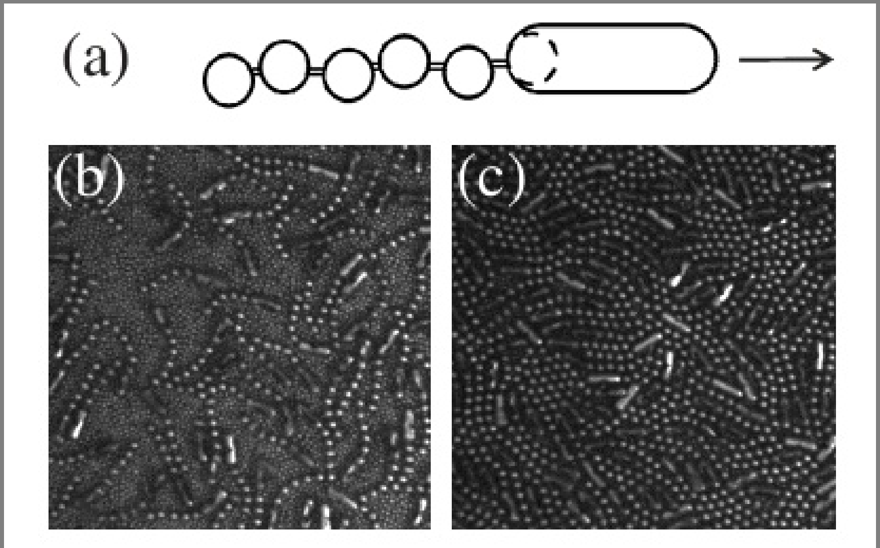

Arshad Kudrolli
PRL 104, 088001 (2010)

在没有热涨落布朗运动的宏观颗粒（大于1微米）体系中，通过对称链状颗粒在环境势垒中的定向运动，我们是否能实验构建一个类似于热涨落-耗散关系的模型体系？

Measurement of the created potential landscapes by generating a nonequilibrium steady state

实验设计

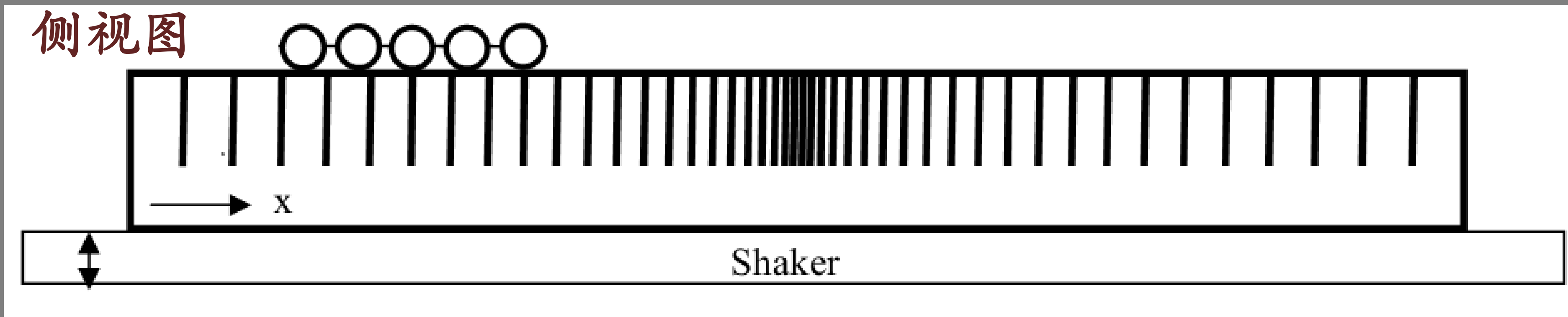

俯视图（I和II：不同初始位置） (比实际速度快5倍)

I
II

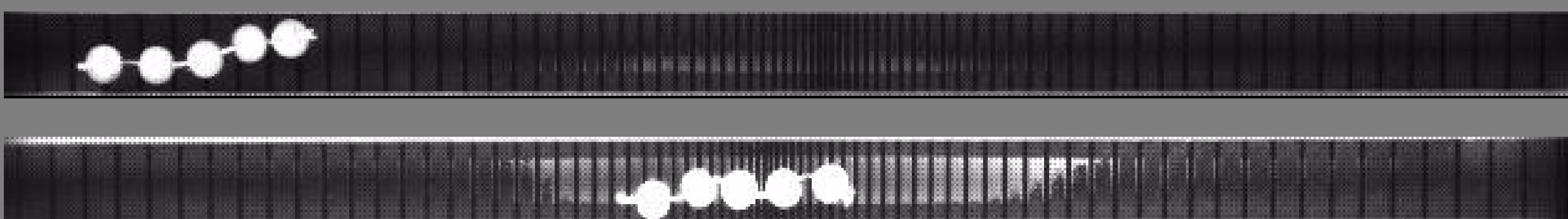

颗粒链: 5 个直径 6mm玻璃珠, 总链长约41mm, 总重约1.8克。

底板: 铁板每隔5mm到0.5mm刻槽，槽宽1mm，板长30厘米。

高速摄像： 50 或100 fps, 总帧数 30,000*30 。

振动加速度： $\Gamma = 2.4$ g (f=50Hz, a=1.5mm)。

Potential reconstruction

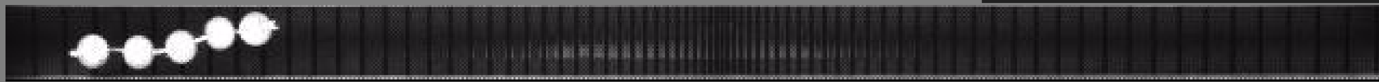

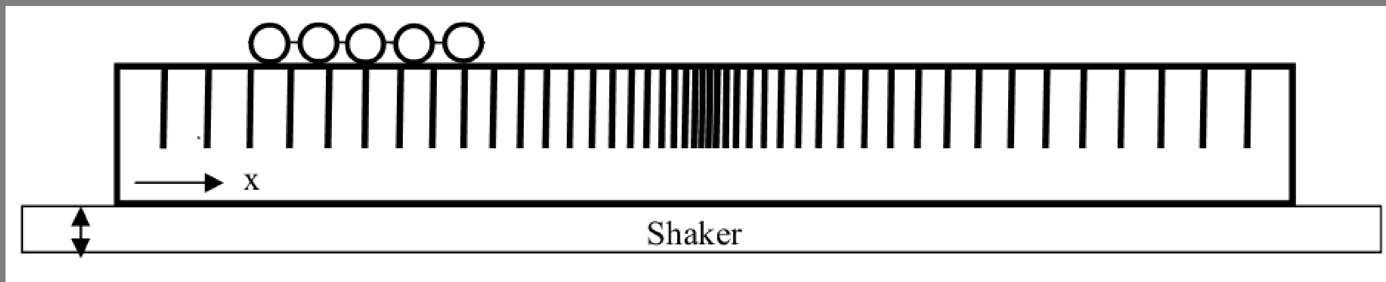

侧视

100 fps, total
10000*60 frames,
Γ =2.4 g

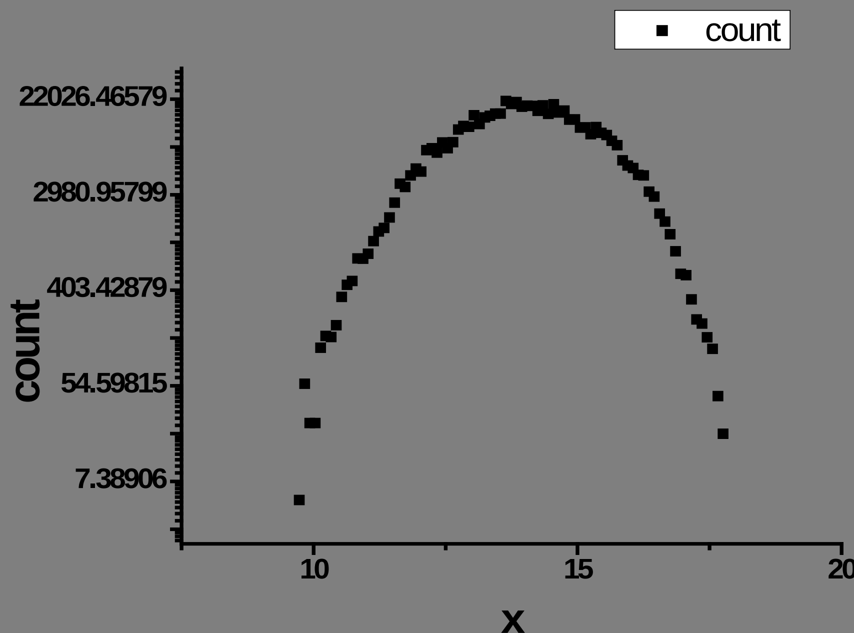

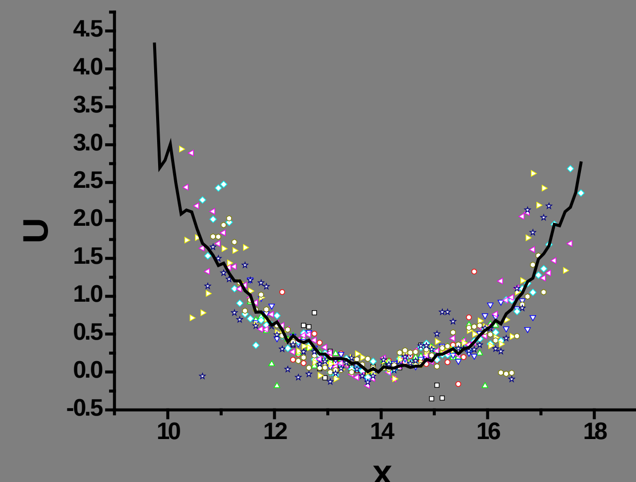

$$U(x) = -k_B T \log[P(x)]$$

$$P(x)$$

From the probability distribution , we construct an effective Boltzmann type potential, kT is arbitrarily chosen to be 1.

Potential reconstruction

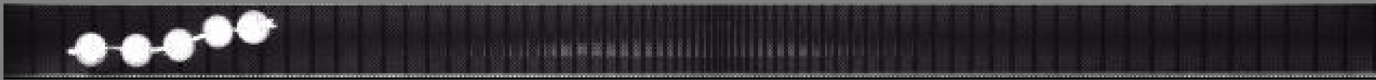

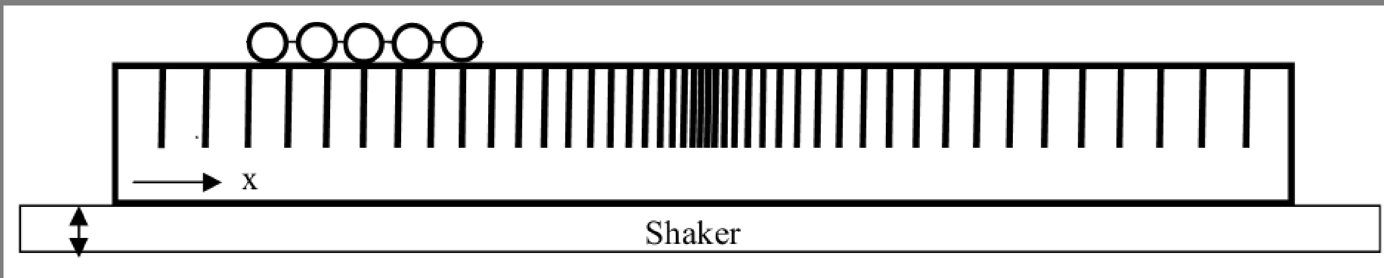

俯视

侧视

100 fps，total
10000*60 frames,
Γ =2.4 g

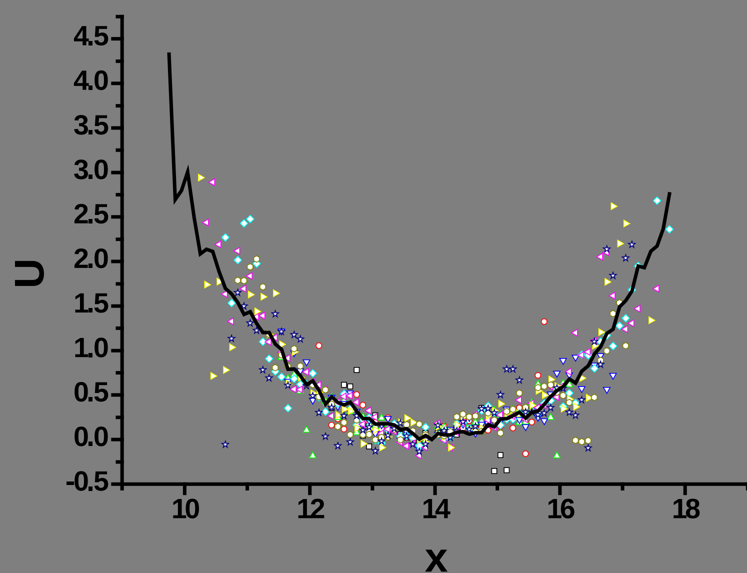

$$\dot{x} = \gamma^{-1} F(x) + \zeta(t)$$

$\zeta(t)$ Thermal

$$\langle \zeta(t)\zeta(t')\rangle = 2(k_B T/\gamma)\delta(t-t'),$$

$$\gamma = \frac{1}{3\pi\eta d}$$

$$F(x) = -V'(x) + f$$

The gradient of a potential $-V'(x)$

driving force f.

$$V(\mathbf{r}) = -k_B T \ln p_{eq}(\mathbf{r})$$

实验结果

- 位移分布 $\delta x(t) = x(t + t_f) - x(t)$

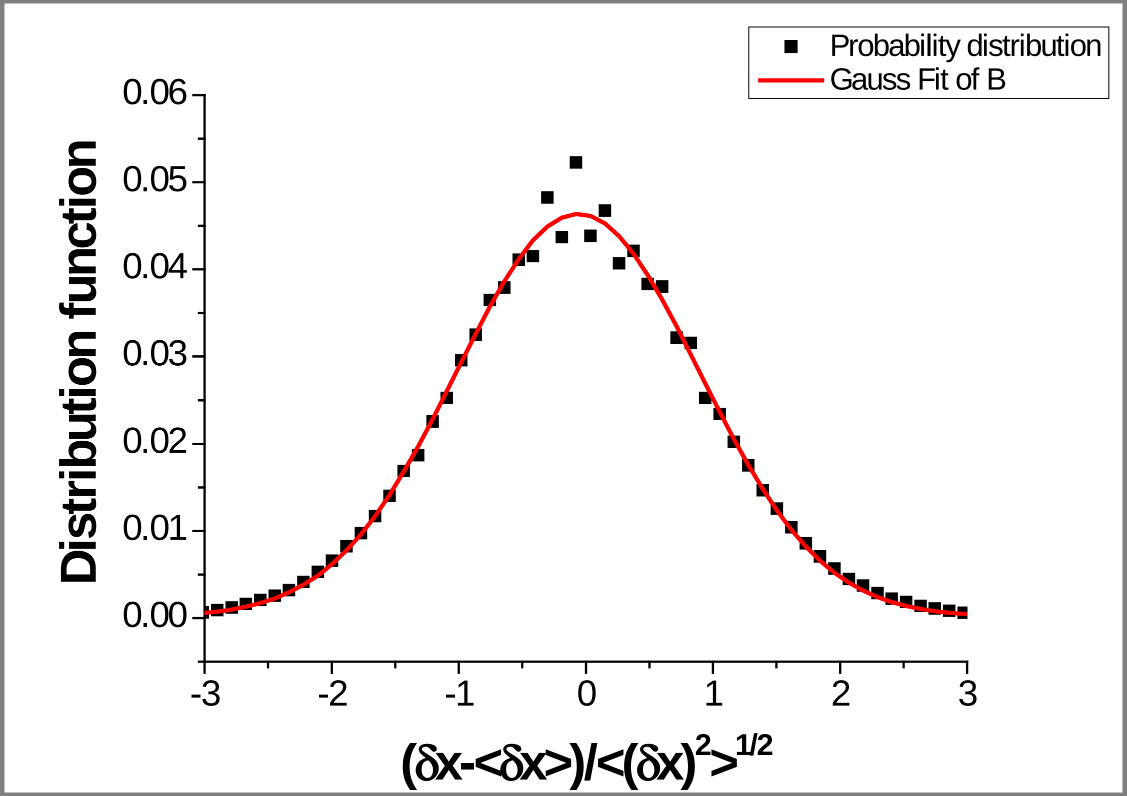

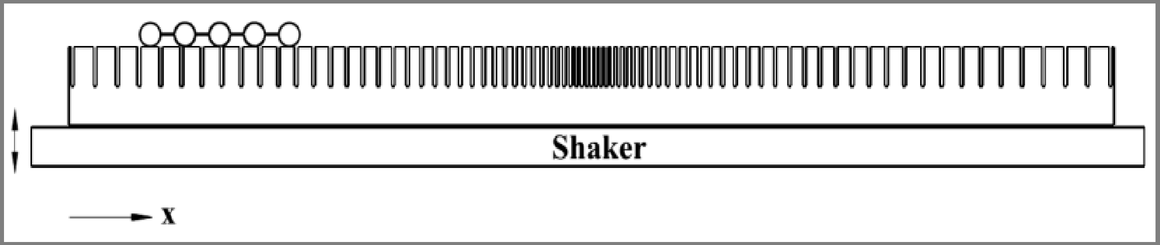

Shaker
x

- 瞬时速度分布

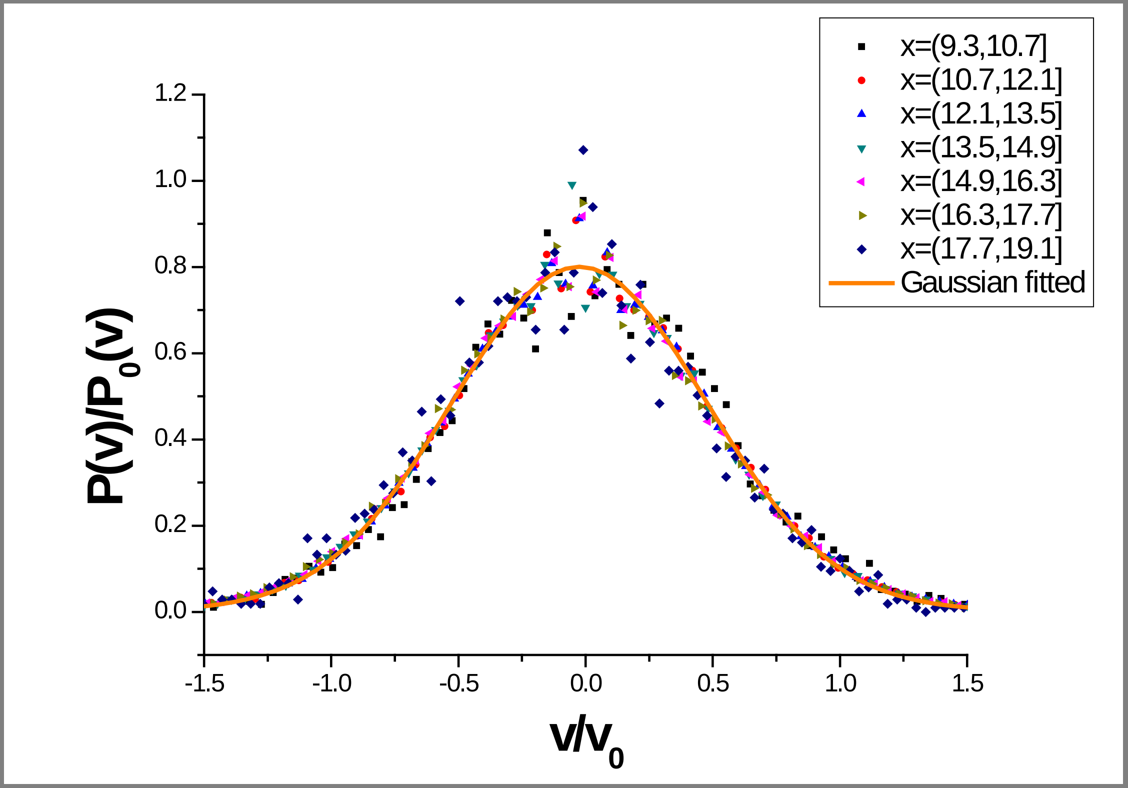

x=(9.3,10.7]
x=(10.7,12.1]
x=(12.1,13.5]
x=(13.5,14.9]
x=(14.9,16.3]
x=(16.3,17.7]
x=(17.7,19.1]
Gaussian fitted
1.2
1.0
0.8
0.6
0.4
0.2
0.0
-1.5
-1.0
-0.5
0.0
0.5
1.0
1.5
P(v)/P0(v)
v/v0

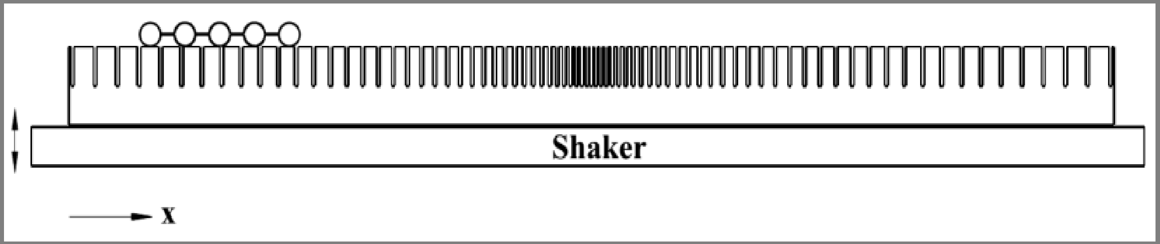
Shaker
x

- 瞬时加速度分布

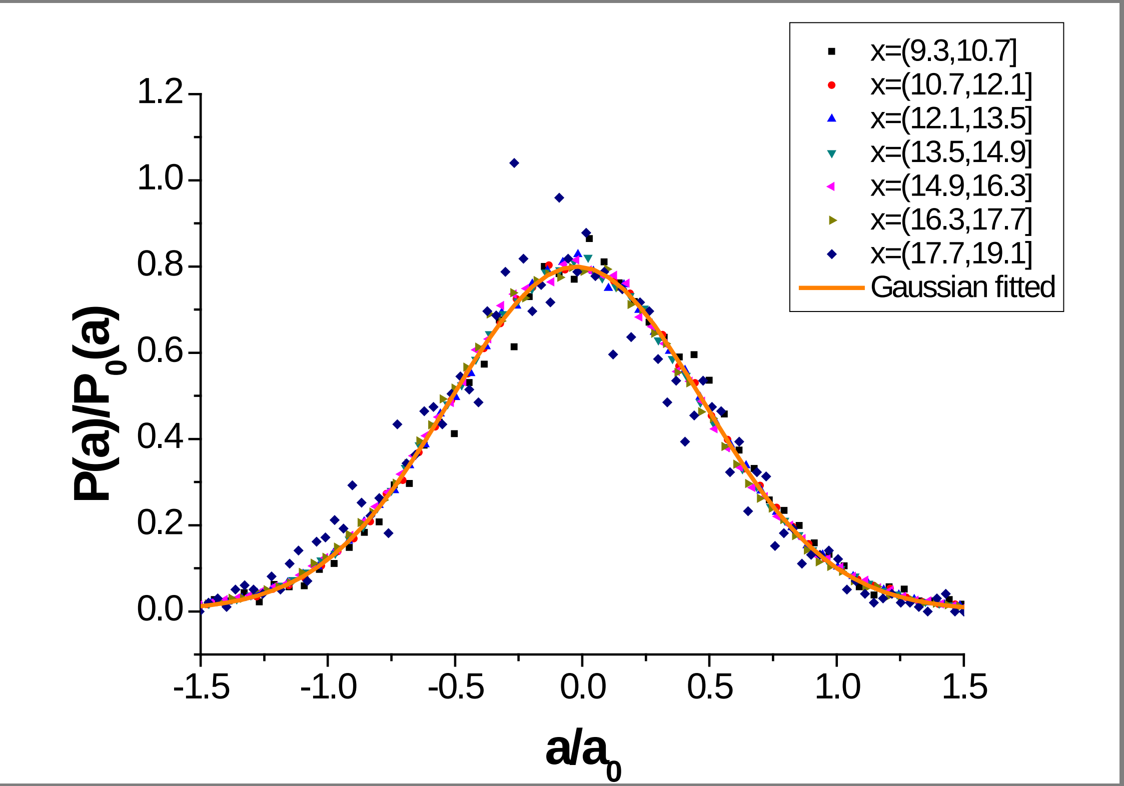
x=(9.3,10.7]
x=(10.7,12.1]
x=(12.1,13.5]
x=(13.5,14.9]
x=(14.9,16.3]
x=(16.3,17.7]
x=(17.7,19.1]
Gaussian fitted
1.2
1.0
0.8
0.6
0.4
0.2
0.0
P(a)/P0(a)
-1.5
-1.0
-0.5
0.0
0.5
1.0
1.5
a/a0

Experimental test of Bier-Astumian Fluctuation theorem in a granular system

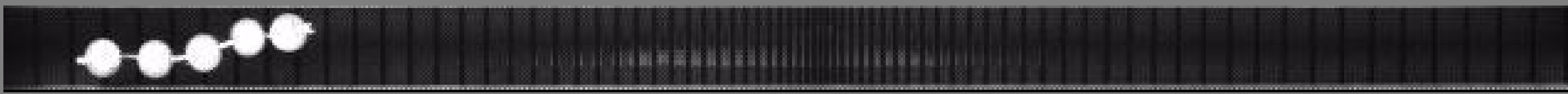

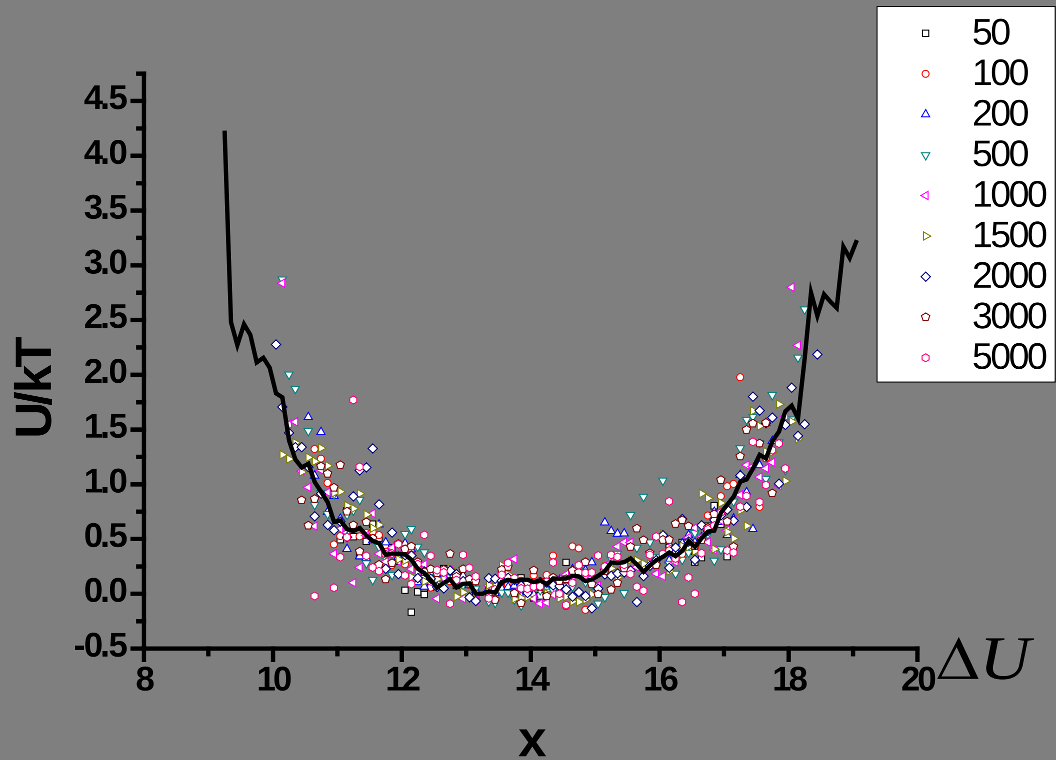

涨落耗散关系

Bier and Astrumian discovered that the transition probability of particle trajectories between two positions in space with defined potential U satisfies

$$\Delta U = -k_B T \log\left[\frac{P(x_0 \rightarrow x;\Delta t)}{P(x \rightarrow x_0;\Delta t)}\right]$$

$$\frac{P(x_a \rightarrow x_b;\Delta t)}{P(x_b \rightarrow x_a;\Delta t)} = \exp\left(-\frac{\Delta U}{k_B T}\right)$$

$$\Delta U = -k_B T \log[P(x)] - U_0$$

平均位移和均方位移（MSD）

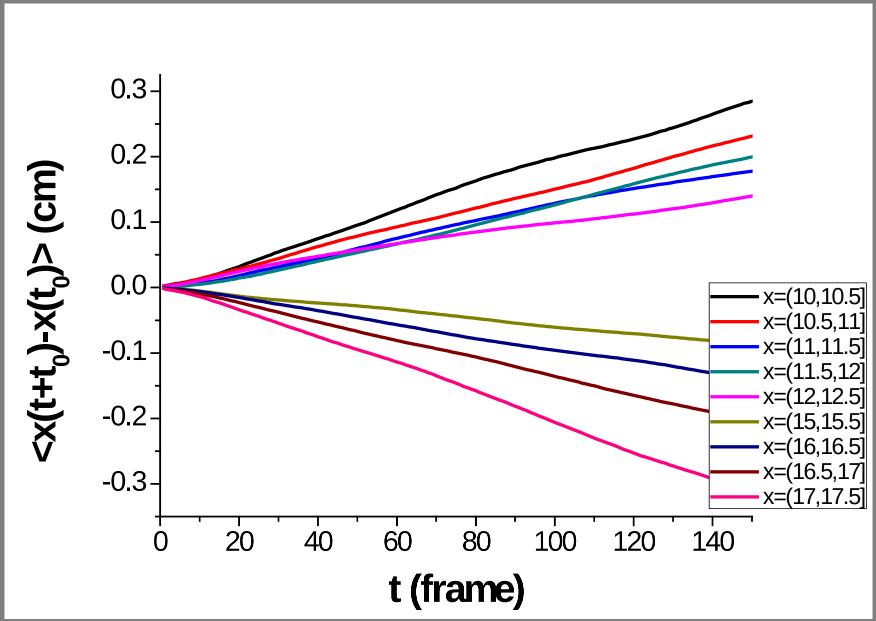

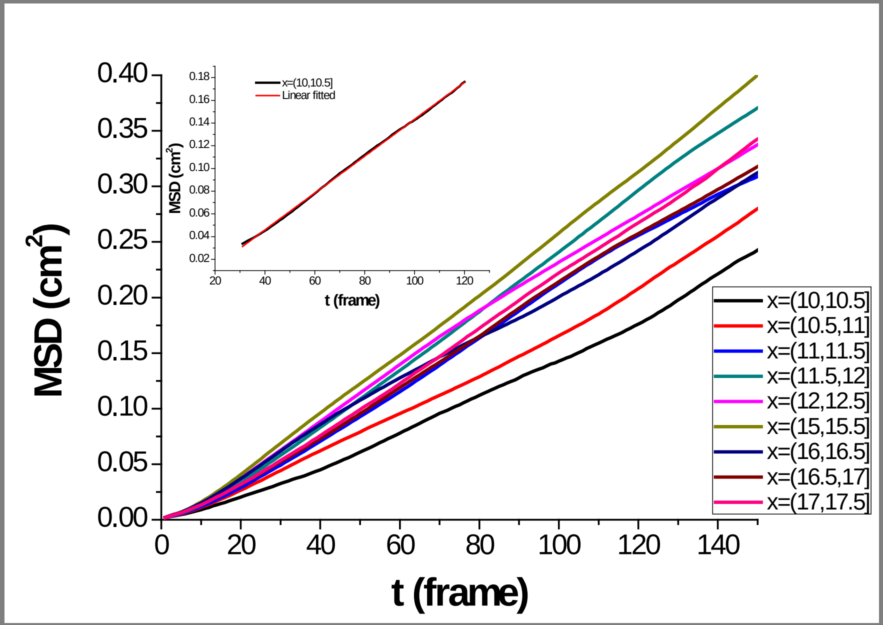

$$< x(t+t_0) - x(t_0) >= v_d t$$

$$< [x(t+t_0) - x(t_0)]^2 >= 2Dt$$

Drift velocity, force, diffusion

as a function of position

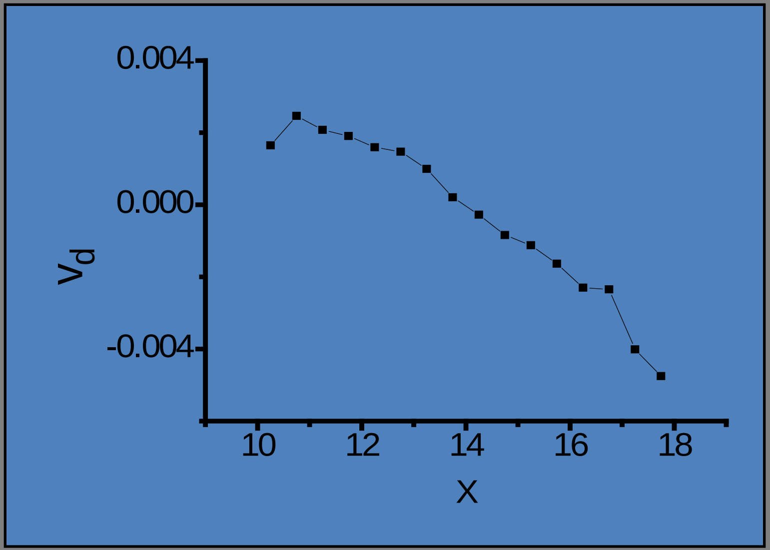

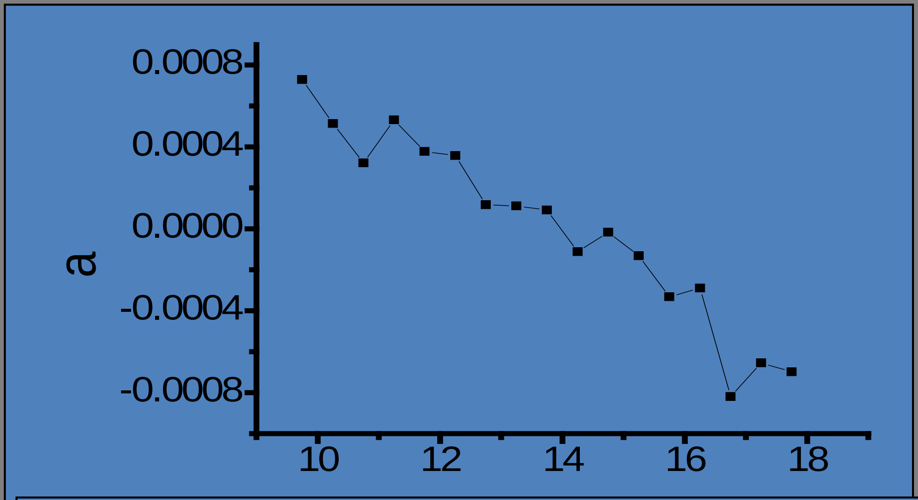

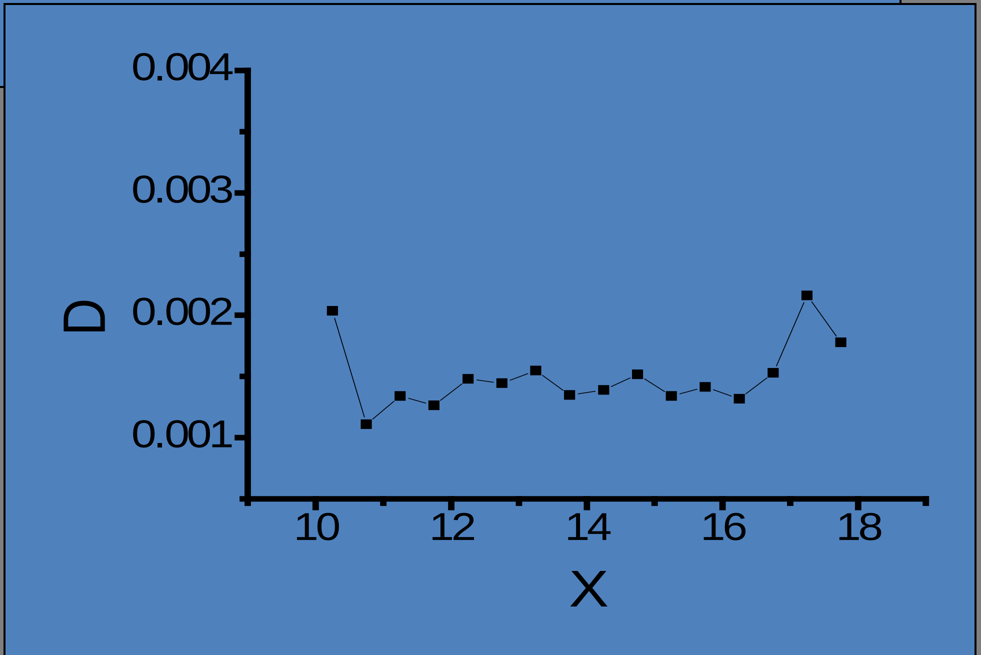

➢ 有效温度（Effective temperature）

$$< x(t+t_0) - x(t_0) > = v_d t \qquad <[x(t+t_0) - x(t_0)]^2> = 2Dt \qquad F(x) = v_d(x)\gamma(x)$$

$$<[x(t+t_0) - x(t)]^2> = 2T_{eff} < x(t+t_0) - x(t) > / F$$

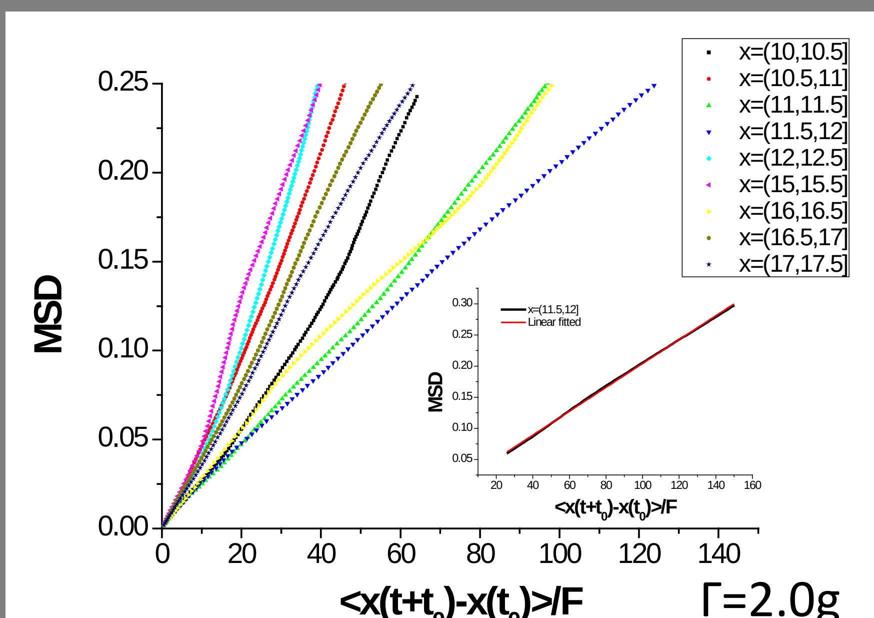

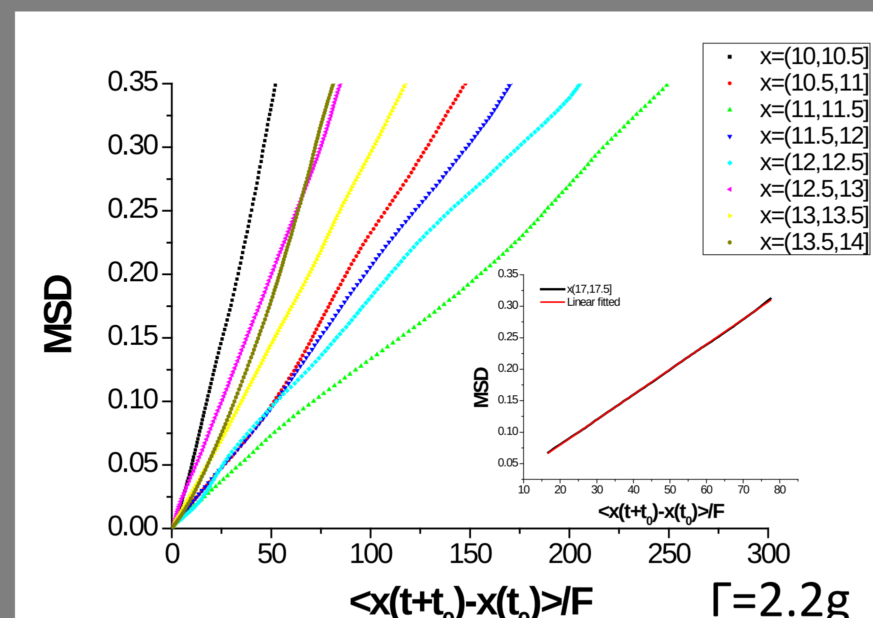

实验结果

➢ 有效温度与颗粒温度 $T_g = \langle |v - \langle v \rangle|^2 \rangle \approx \langle v^2 \rangle$

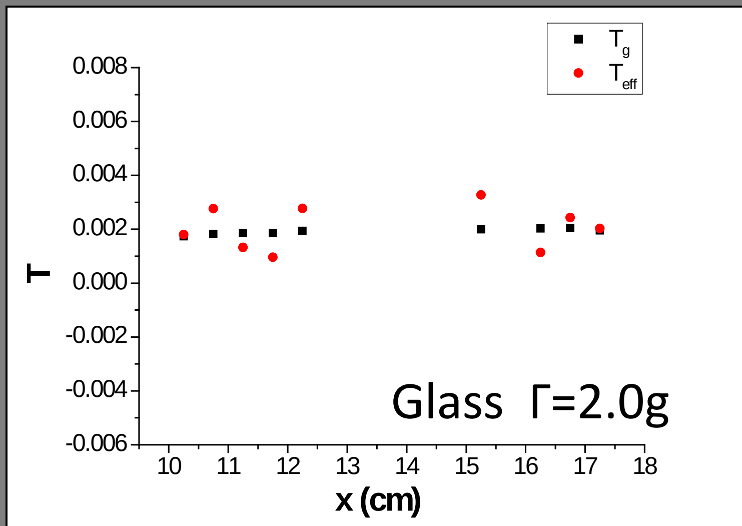

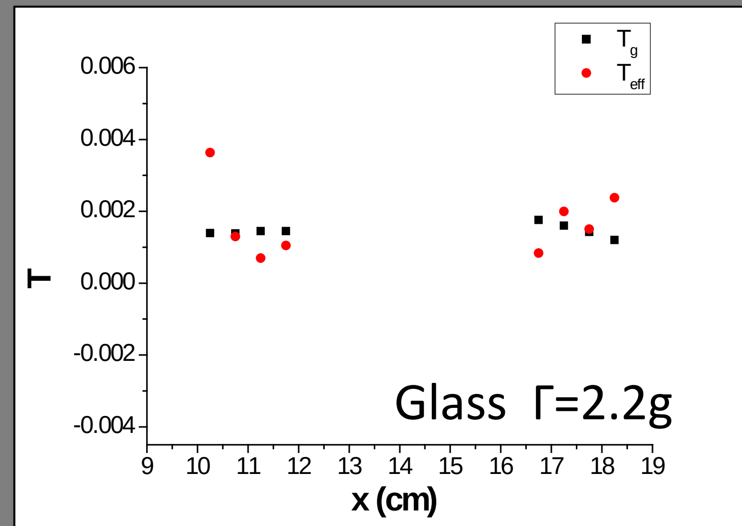

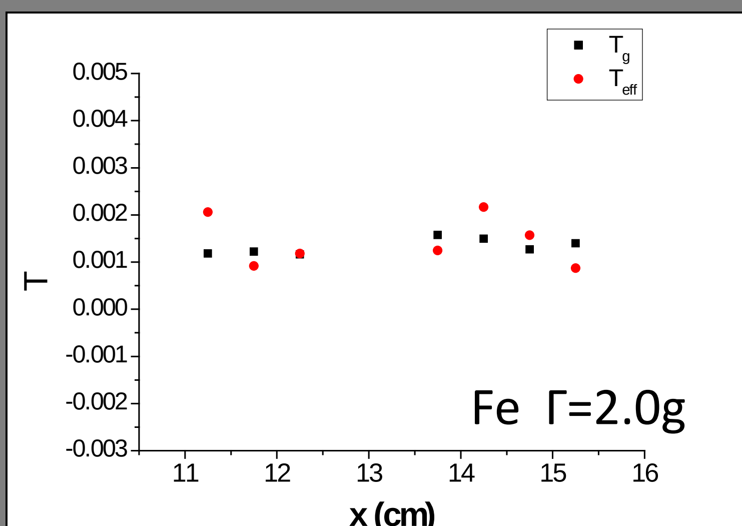

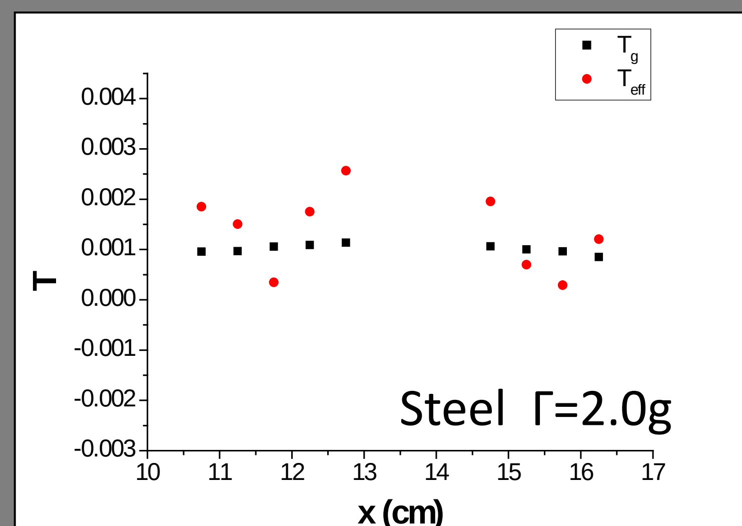

T_{eff} 随着 T_g 变化

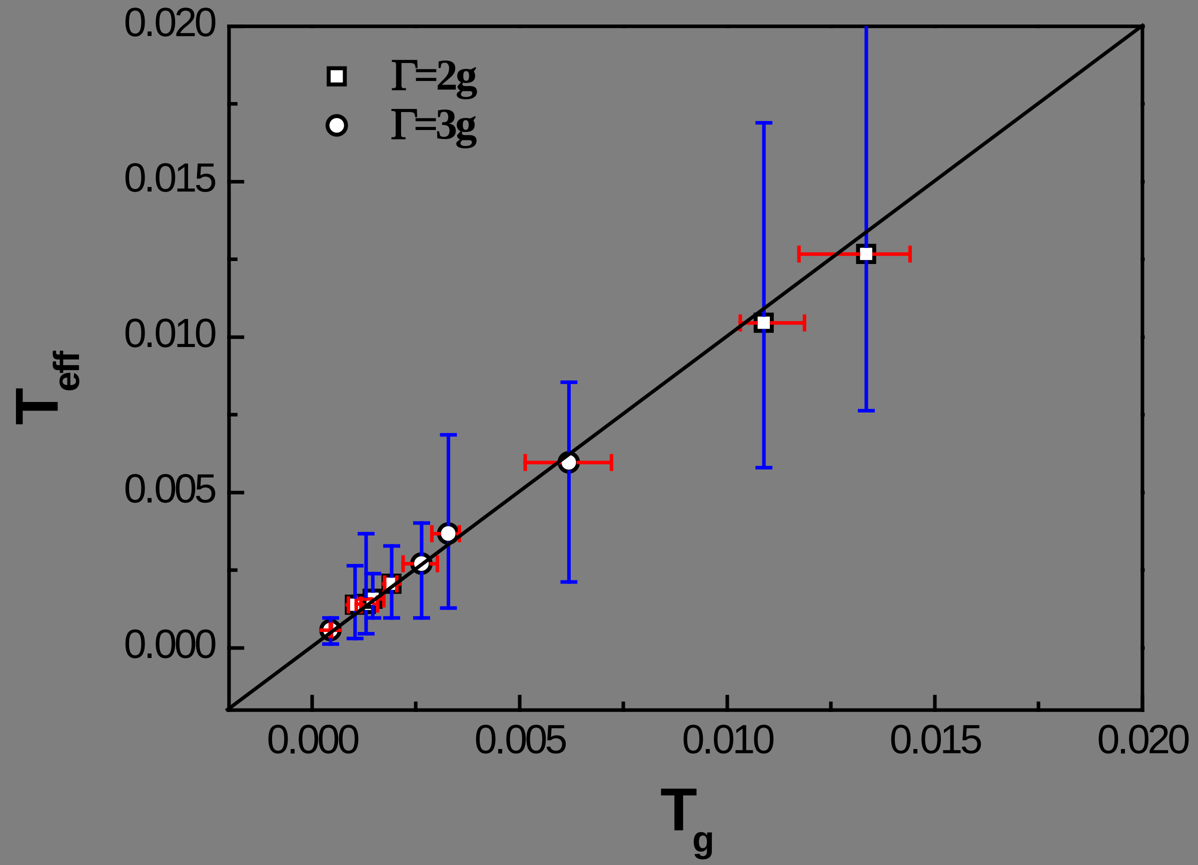

0.020
0.015
0.010
0.005
0.000
Γ=2g
Γ=3g
T_eff
0.000
0.005
0.010
0.015
0.020
T_g

小　结

1 位移、瞬时速度和加速度均满足高斯分布

2 体系满足涨落耗散关系或细致平衡条件

3 有效温度和颗粒温度近似相等

颗粒平衡态体系?

颗粒固体

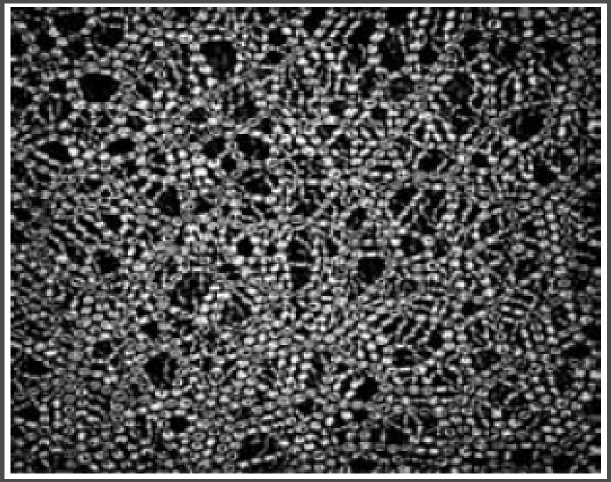

颗粒固体

表相重量

Vanel, Duran, '97

cylinder radius (mm) 20
bead diameter (mm): 1.5, 2, 3

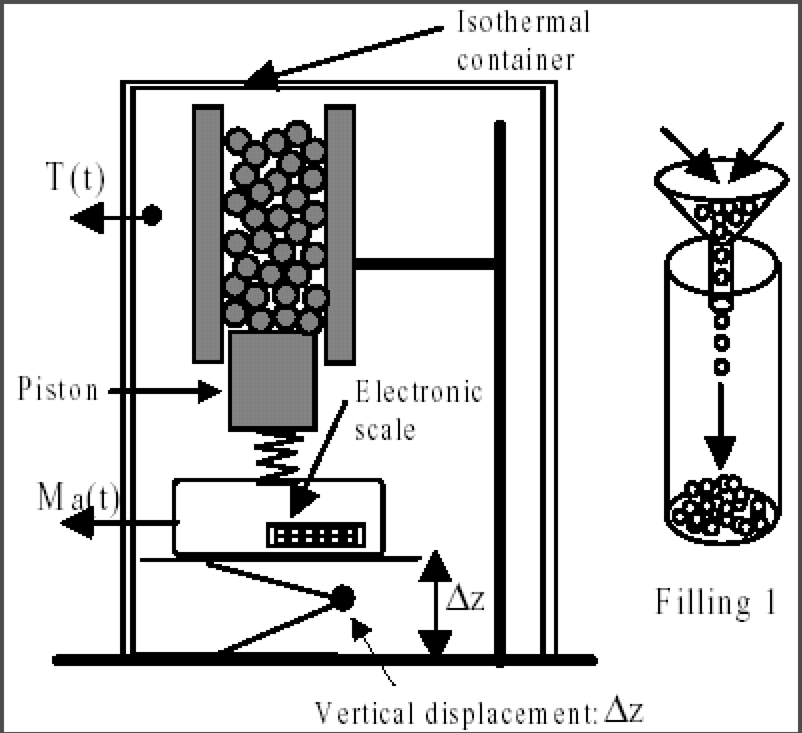

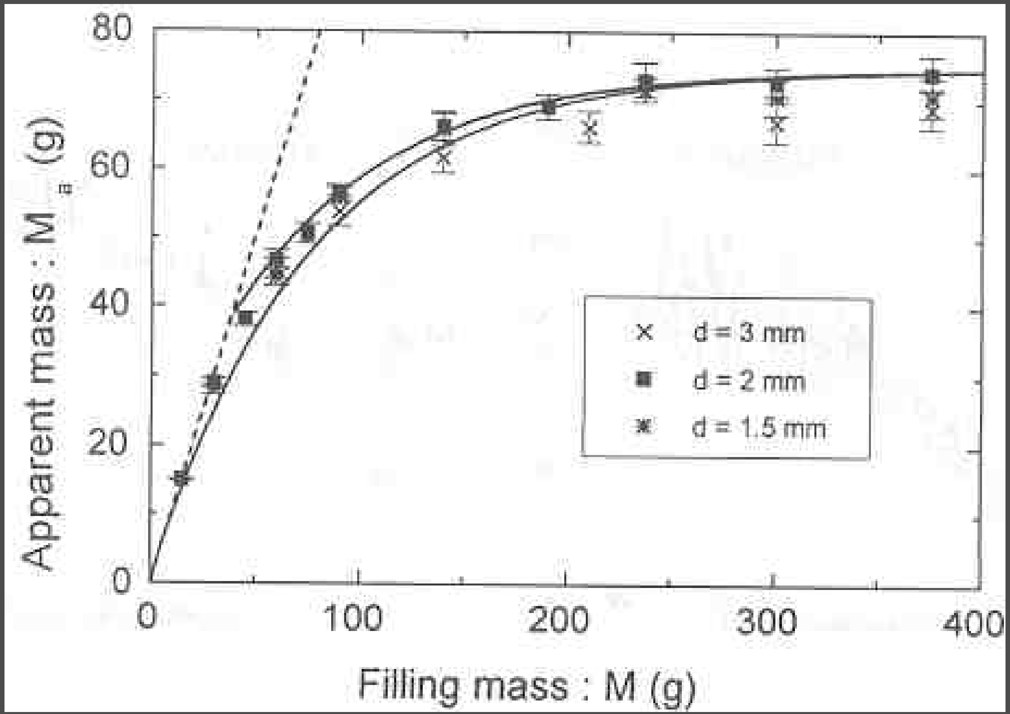

Where has the missing weight gone?

沙堆底面的力分布

Vanel et. al., PRE 60, R5040, 1999

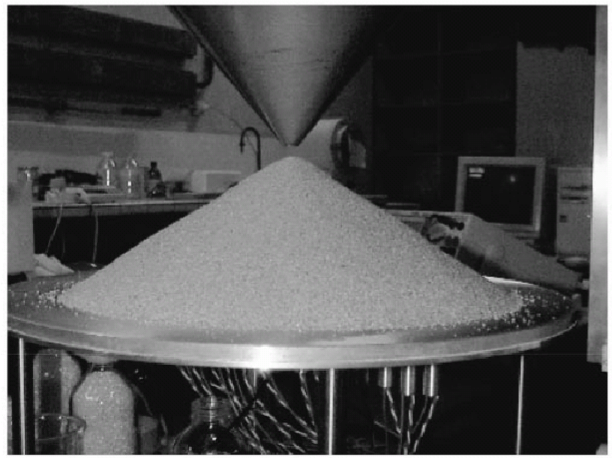

pile of sand
1.2 mm diameter
8 cm high
33^o repose angle

localized deposition

uniform deposition

颗粒固体

力链及拱的形成

Travers, Bideau, et. al. Europhys. Lett. 4, 329, 1987.

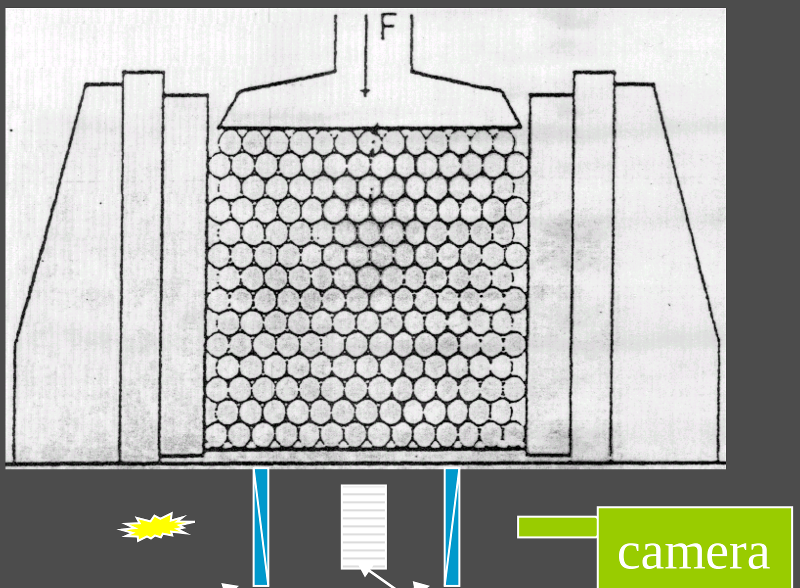

polarizers

Plexiglass cylinder
25 mm long
4~6 mm diameter

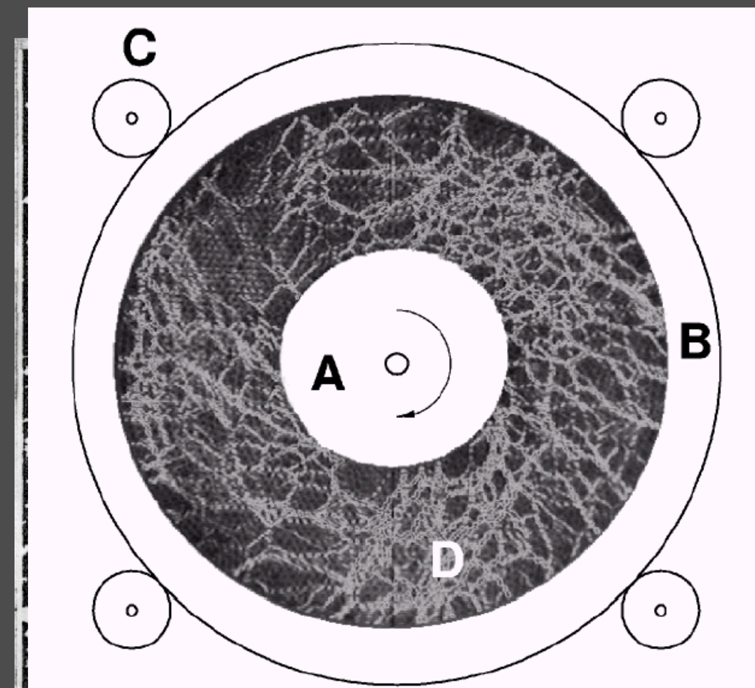

D. Howel, et. al., PRL 82, 5241, 1999

Highly inhomogeneous
Arching, force chains transmit loading to walls

Sound probing in sheared granular solid

颗粒固体

Background

Effectives Coherent Modes

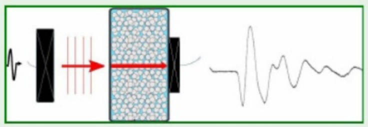

Waves Propagation

- Disordered Media
- Nonlinear Behaviour

Multiple Scattering of Elastic Waves

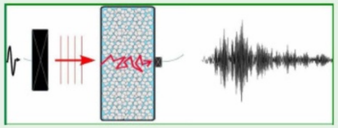

Acoustics

- Granular Media
- Heterogeneous Media

Porous & Geological Media

Grains & Powders

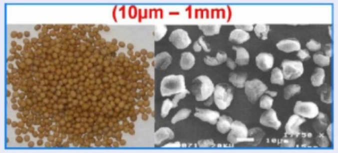

Pastes & Non Colloidal Suspensions

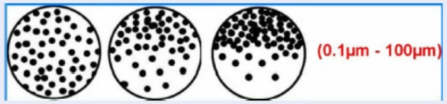

颗粒固体

Linear sound propagation in dry granular media

Jia, Caroli & Velicky, PRL 82 (1999)

♦ $\lambda_E \geq 10\ d$: coherent waves (*E*)

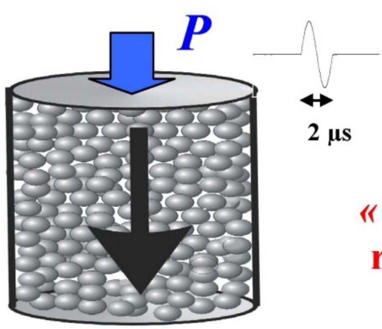

« *E* » signal is reproducible

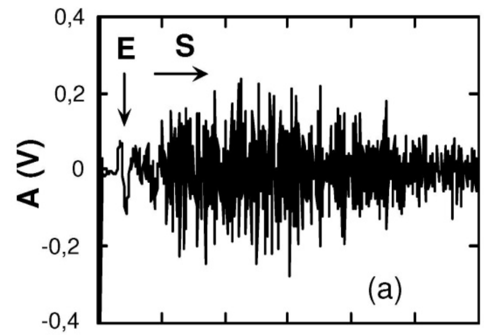

♦ $\lambda_S \sim d$: multiply scattered waves (*S*)

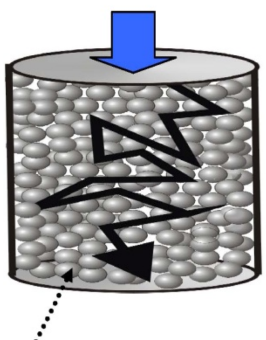

« *S* » signal is configuration specific

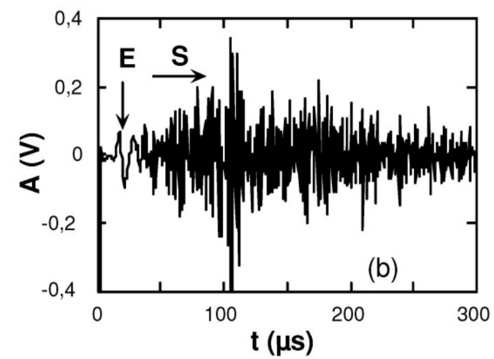

glass beads *d*: 600-800 µm

颗粒固体

Motivation

Granular Matter

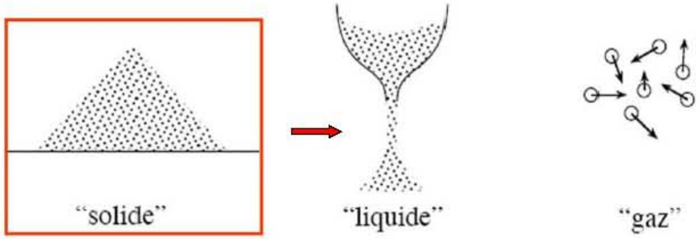

⇨ *Statics & Dynamics (dense flow): Contact force networks*

under load
(Dantu, 1957)

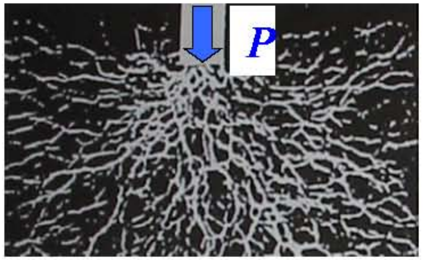

ξ: 5-10 d
(d: grain size)

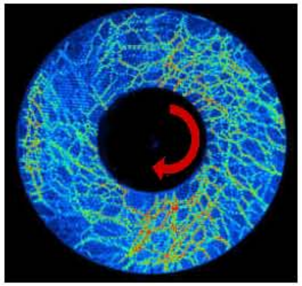

under shear
(Howell et al, 1999)

♦ Non invasive acoustic probing: statics (viscoelasticity) and dynamics (dense flow) (reversible sound-matter interaction: $u < 10^{-9}$ m)

♦ « Perturbating » the granular medium by sound (irreversible sound-matter interaction: $u \sim 10^{-9} - 10^{-7}$ m): effective granular temperature

vs weakly shaking / shearing ($u > 10^{-4}$ m), leading to the solid-liquid transition

Gas – liquid – solid transitions in Granular Matter

颗粒固体

Jamming-unjamming transition

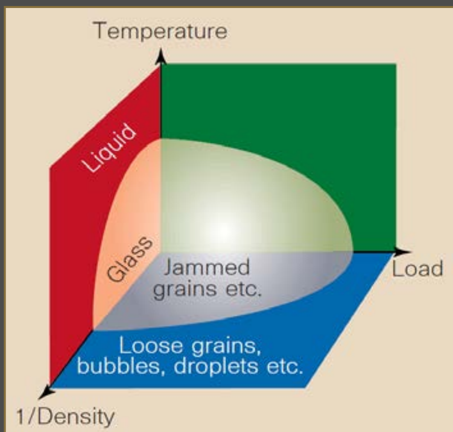

A. J. Liu *et. al.*, Nature **396**, 21 (1998)

K. To et. al. PRL **86**,71 (2001)

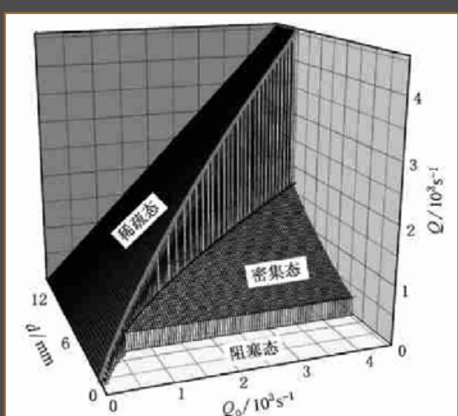

Dilute-dense flow transition

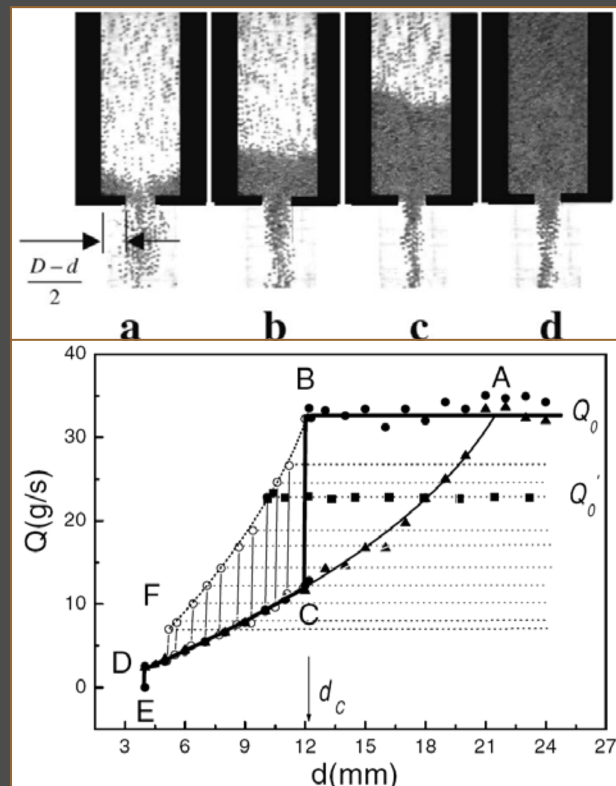

M. Hou *et. al.* PRL **91**,204301(2003)

Granular gas-liquid transition

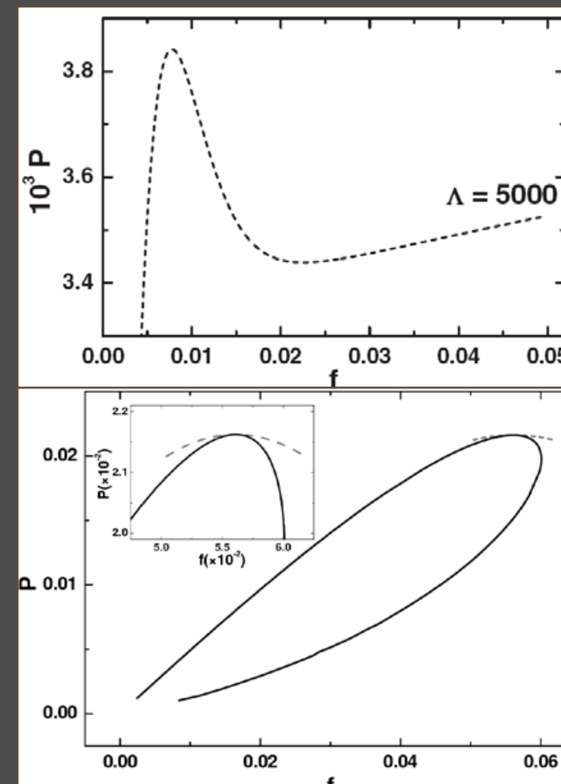

R. Liu *et. al.* Phys. Rev. E **75,** 079705 (2007)

颗粒固体

Experimental setup

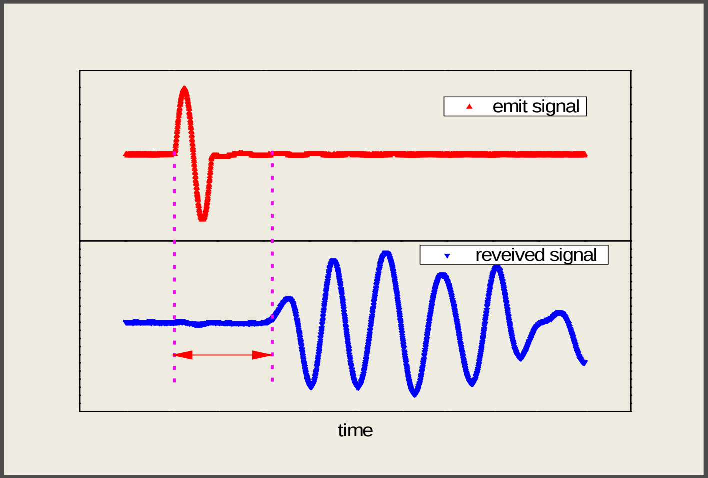

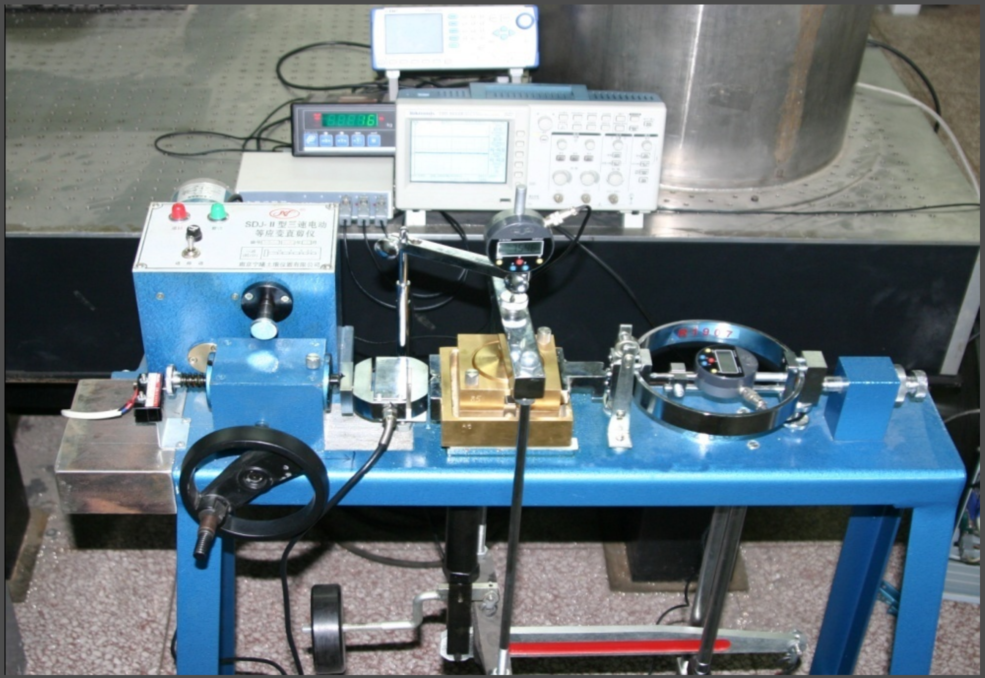

$$V = \frac{L}{T_{tof}}$$

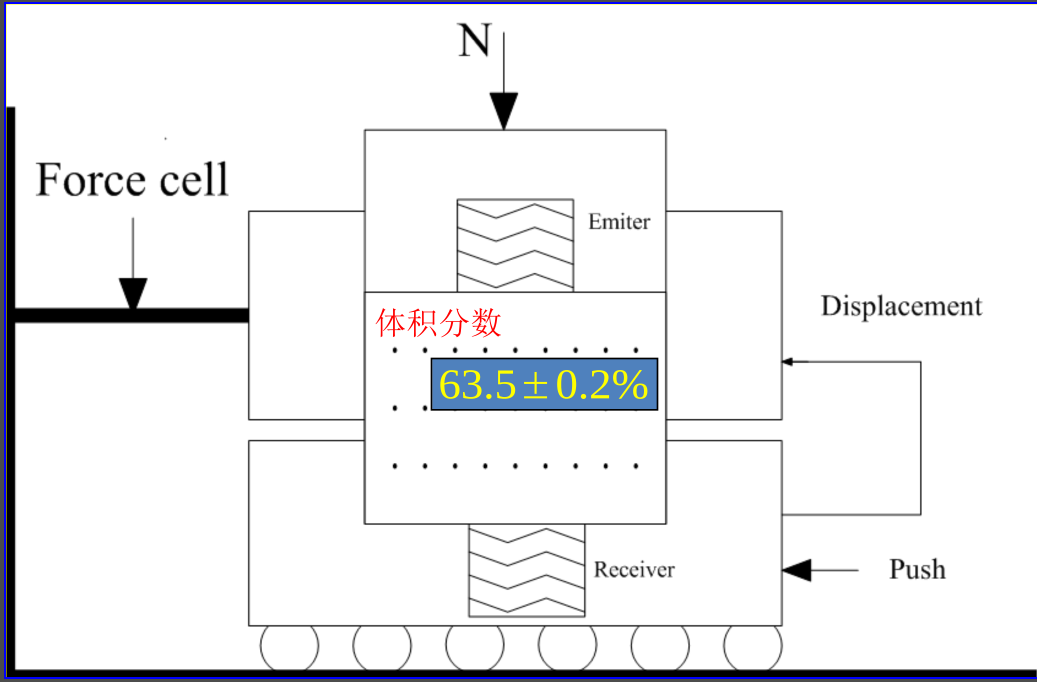

Sound speed and yield stress in simple sheared dense granular solid (longitudinal wave)

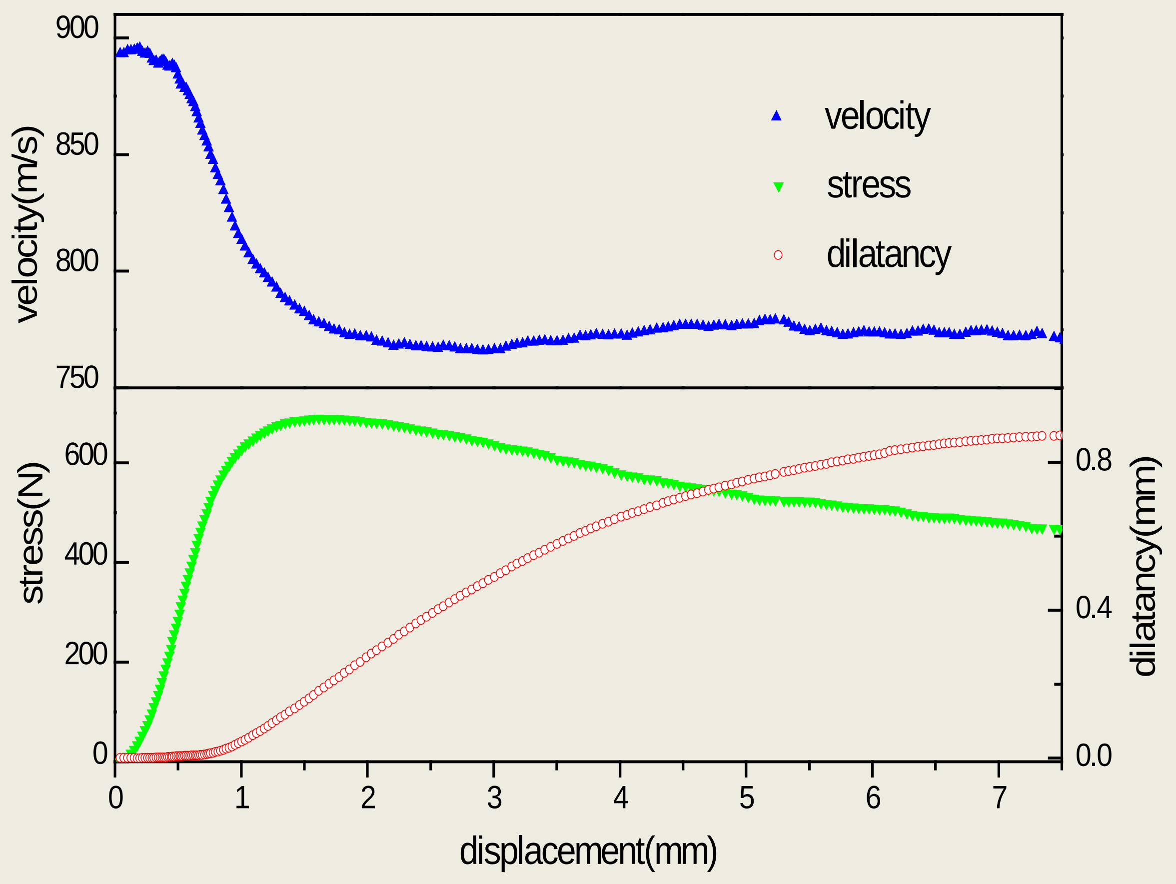

Sound speed (shear wave) and yield stress in simple sheared dense granular solid

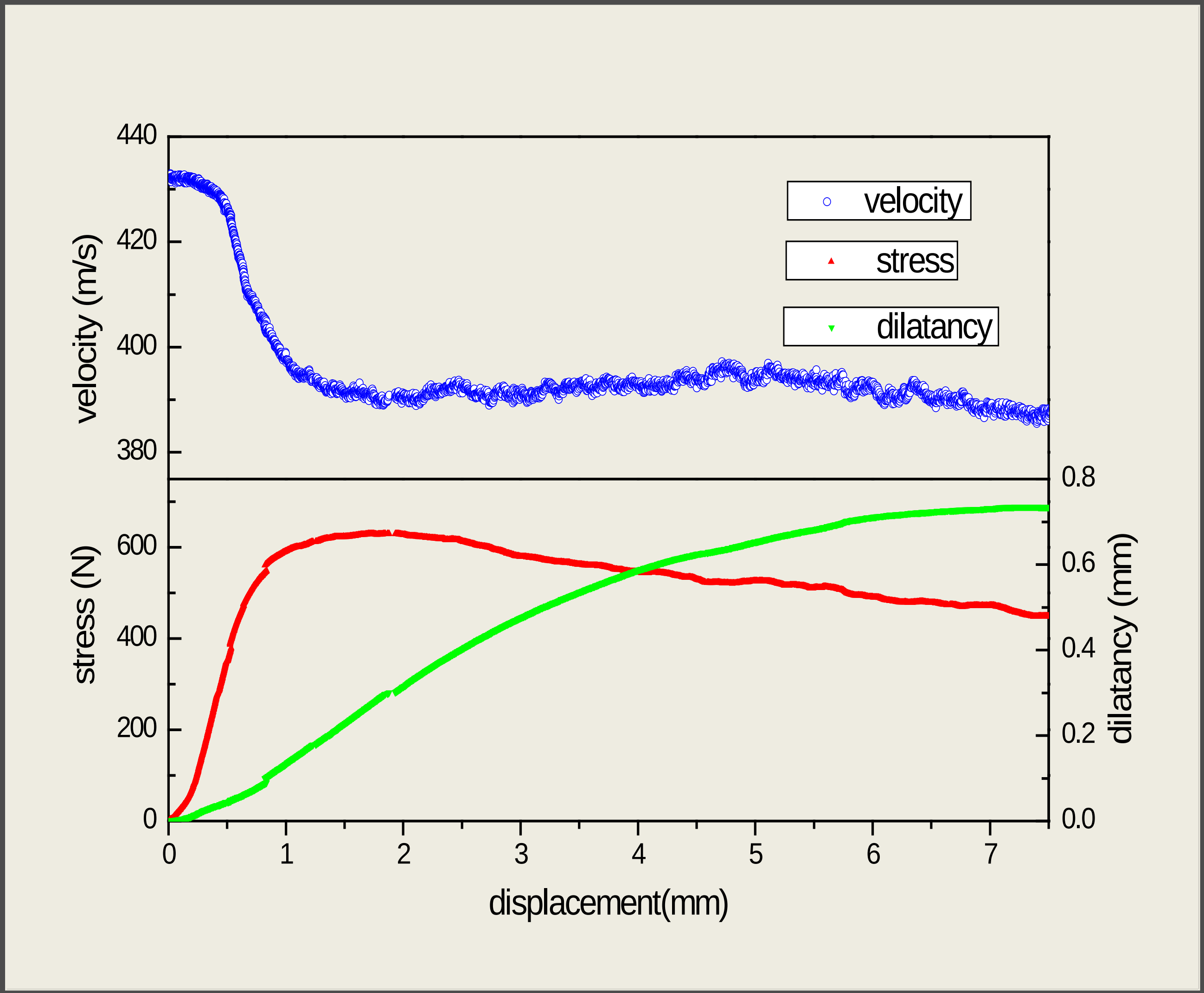

颗粒固体

red： main stress coordinations

blue： shear stress coordination：

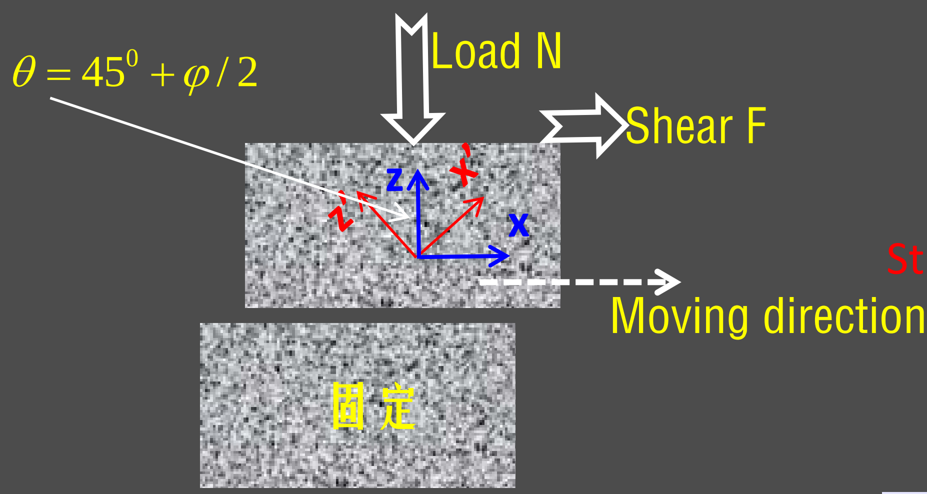

$$\theta = 45^0 + \varphi / 2$$

Internal friction angle

Stress under red coordinates

$$\begin{pmatrix} \sigma_1 & 0 & 0 \\ 0 & \sigma_1 & 0 \\ 0 & 0 & \sigma_3 \end{pmatrix}$$

Then in blue coordinates, stress is

$$\sigma_{ij} = \begin{pmatrix} N + \alpha F & 0 & -F \\ 0 & N - F\cot\theta & 0 \\ -F & 0 & N \end{pmatrix}$$

$$\alpha = \tan\theta \sin^2\theta - \cot\theta \cos^2\theta$$

$$\sigma_1 = N - F\cot\theta$$

$$\sigma_3 = N + F\tan\theta$$

Take friction angle as 27°

Y. Jiang and Mario Liu

颗粒固体

Sound speed

Based on the elastic theory, sound speed

$$S_{ij} = \rho^{-1} M_{imnj} \hat{k}_m \hat{k}_n$$

$$M_{imnj} = \frac{\partial \sigma_{im}}{\partial u_{nj}} = -\frac{\partial^2 w}{\partial u_{im} \partial u_{nj}}$$ Stiffness tensor

$$\hat{k}_n = k_n / k$$ Wave vector

sound speed is obtained by the root square
Of the three eigenvalues。

从弹性势能函数$w(\rho, u_{ij})$出发
得刚度$M_{imnj}(\rho, u_{ij})$,
将应变u_{ij}转换成应力σ_{ij},
得$S_{ij}(\rho, \sigma_{ij})$,计算其本征值,
有：$c_{1,2,3}(\rho, \sigma_{ij})$

Consider the sound wave propagates along z direction, the speed of sound is a function of number density and the stress

$$c_{1,2,3}(\rho, \sigma_{ij})$$

颗粒固体

Internal energy

$$w\left(\rho, u_{ij}\right)$$

$$w = B_0\left(-\frac{\rho_1 - \rho/\rho_{rcp}}{1-\rho/\rho_{rcp}}\right)^{0.15}\sqrt{\Delta}\left(\frac{2}{5}\Delta^2 + \frac{1}{\xi}u_s^2\right)$$

We take：

$$B_0 = 12.2GPa$$

$$\xi = 5/3$$

$$\rho_1 = 0.74$$

$$\rho_{rcp} = 1585(1588.2)kg/m^3$$ RCP

颗粒固体

Comparison of the calculation with the experimental results

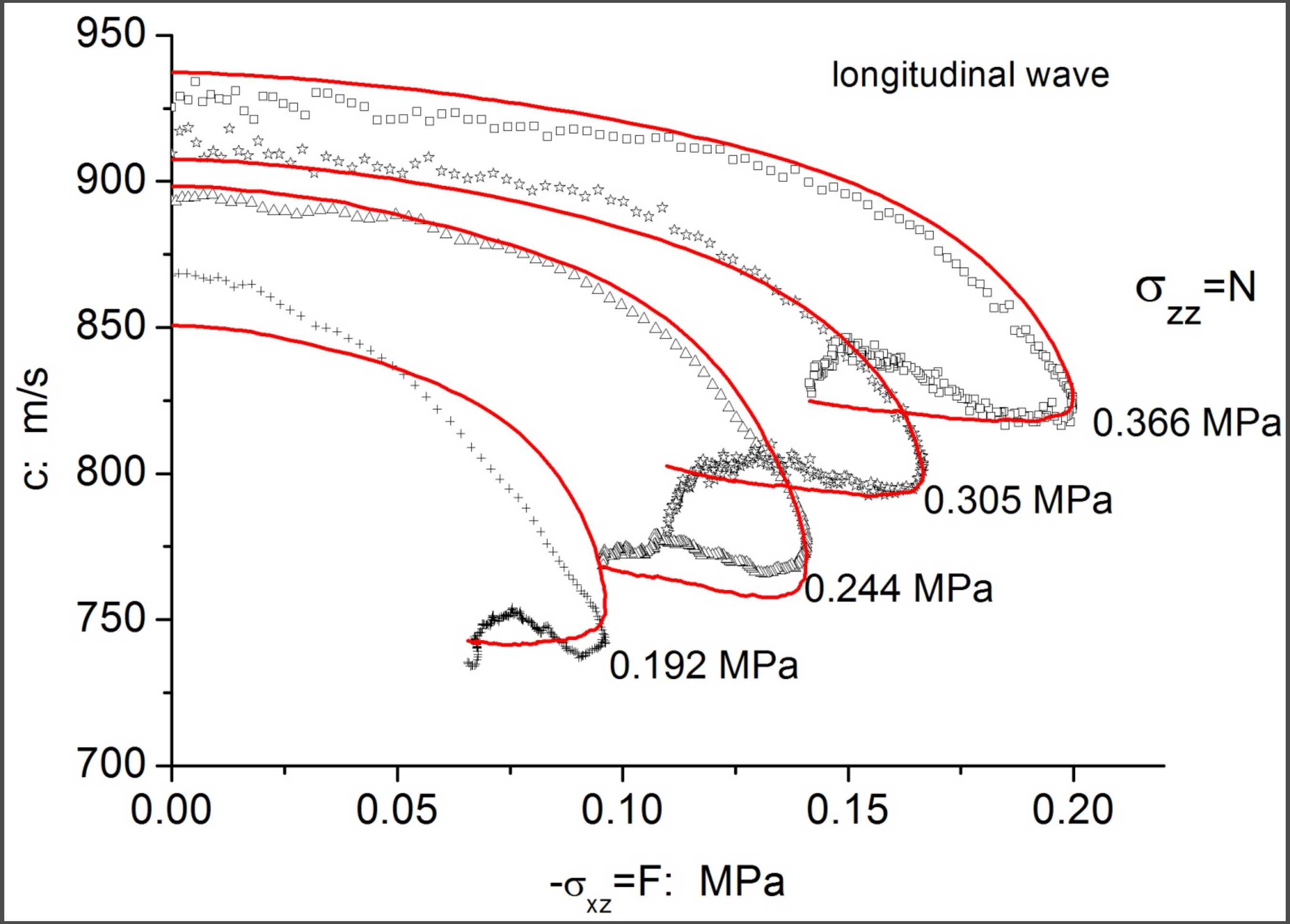

Under different load, density and shear force we measured

$$c=c(\rho,N,F)$$

Using these ρ,N,F values sound speed is calculated and compared with the experimental results as shown above

小 结

声波在颗粒固体中的传播速度和振幅的变化是一种很好的探测颗粒介质结构与力链分布变化的方法。本节介绍了获取剪切颗粒体系中用飞行时间法获取声速的实验与理论计算方法。